UNITED NATIONS EDUCATIONAL, SCIENTIFIC AND CULTURAL ORGANIZATION
INTERNATIONAL ATOMIC ENERGY AGENCY
INTERNATIONAL CENTRE FOR THEORETICAL PHYSICS

SMR/917 - 22

# SECOND WORKSHOP ON SCIENCE AND TECHNOLOGY OF THIN FILMS

**( 11 - 29 March 1996 )**

---

" The physics and fabrication of coupled electron gas structures. "

presented by:

**G.A.C. JONES**
University of Cambridge
Cavendish Laboratory
Semiconductor Physics Research
Madingley Road
CB3 OHE Cambridge
United Kingdom

---

These are preliminary lecture notes, intended only for distribution to participants.

# The Physics and Fabrication of Coupled Electron Gas Structures

*A selection of papers from the Semiconductor Physics Group, Cavendish Laboratory, University of Cambridge, UK.*

# Resonant tunneling between parallel, two-dimensional electron gases: A new approach to device fabrication using *in situ* ion beam lithography and molecular beam epitaxy growth

K. M. Brown, E. H. Linfield, D. A. Ritchie, G. A. C. Jones, M. P. Grimshaw, and M. Pepper
*University of Cambridge, Cavendish Laboratory, Madingley Road, Cambridge CB3 OHE, United Kingdom*

(Received 15 November 1993; accepted for publication 13 January 1994)

Using the techniques of *in situ* focused ion beam lithography and molecular beam epitaxy regrowth high quality, patterned back gate, double quantum well devices have been fabricated. Independent ohmic contacts were made to the two two-dimensional electron gases (2DEGs) using a "selective depletion" scheme, and using further gates the carrier densities in each well were controlled. Resonant tunneling between the two electron gases was observed as a function of carrier density in each 2DEG, and as a function of the bias applied between the two wells. Extremely large peak-to-valley ratios were observed, resulting from removal of unwanted parallel tunneling paths.

There has recently been considerable interest in the physical properties of closely spaced (<20 nm) two-dimensional electron gases (2DEGs) however, experimental work in these systems is somewhat limited due to the difficulties involved in sample fabrication. Two groups have independently overcome these problems, using first shallow ohmic contacts[1] and second, a "selective depletion" technique[2] with front and back Schottky gates, the backgates being deposited on the rear of a wafer which had previously been thinned to ~50 $\mu$m.

In this letter we describe a novel approach to this fabrication problem using *in situ* focused ion beam (FIB) lithography and molecular beam epitaxy (MBE) regrowth.[4] Again a selective depletion scheme is used, however in our case the back gates are grown into the wafer (~0.3 $\mu$m from the lower 2DEG) and patterned *in situ* with a Ga focused ion beam.[5] This results in the formation of a highly flexible, robust device in which not only can independent contacts be achieved to the two layers,[6] but both 2DEG carrier concentrations can be modified with front- and back gates. We have observed resonant tunneling between the 2DEGs as the carrier densities in each well are varied, and as a function of the dc bias applied between the two layers. In contrast to previous work,[1,3] very low background tunneling was observed when off resonance resulting in very large peak-to-valley ratios.

A detailed description of the *in situ* fabrication technique is given in Refs. 4–6, and outlined here. First, 65 nm of $n^+$-GaAs was grown by MBE. The wafer was then transferred to an ion beam implantation chamber via ultrahigh vacuum chambers. Using 30 keV $Ga^+$ ions, selective areas were implanted at a dose of $8\times10^{12}$ ions/cm$^2$, thus rendering the exposed $n^+$-GaAs insulating.[5] Ions were implanted in regions, above which ohmic contacts to the 2DEGs would later be made, thereby avoiding problems with leakage between 2DEG and back gate. In addition, the ion beam was used to divide the back gate into separate conducting regions [Fig. 1(a)]. Following implantation the wafer was transferred back into the MBE growth chamber, again under UHV conditions, where the remainder of the structure was grown. The 2DEGs were confined in two, 19.5 nm GaAs quantum wells, separated by a 13 nm $Al_{0.33}Ga_{0.67}As$ barrier.

After growth standard photolithographic and wet etching techniques were used to define a Hall bar mesa. Annealed AuNiGe was used to make ohmic contacts to both the 2DEGs and the various back gate regions. Finally, NiCr:Au surface Schottky gates were deposited across the full width of the mesa [Fig. 1(a)].

The electrical properties of the individual layers were characterized using low temperature magnetoresistance measurements. Without application of any gate voltages the top 2DEG had a carrier density of $3.4\times10^{11}$ cm$^{-2}$ and a mobility of $6\times10^5$ cm$^2$ (Vs)$^{-1}$, whereas the bottom 2DEG had a carrier density of $2.4\times10^{11}$ cm$^{-2}$ and a mobility of $1.5\times10^5$ cm$^2$ (V s)$^{-1}$.

Independent contacts to the two layers were then obtained by biasing front gate $A$ to $-0.5$ V and back gate $B$ to $-1.3$ V [Fig. 1(a)]. These gate voltages are sufficient to fully deplete one 2DEG but leave the other unaffected.[2] The device is now made up of two, independently contacted, overlapping strips of 2DEG, with the area overlap being 120 $\mu$m$\times$80 $\mu$m. Front- and back gates were used to alter the carrier densities in the upper and lower 2DEGs, respectively, over the entire tunneling area.

Figure 2(b) shows the conductance between the two layers as a function of front-gate voltage ($V_{fg}$), and hence the carrier density in the upper well. The conductance between the two layers is low, except at the particular front-gate voltage that produces equal carrier densities in the two wells, where an extremely sharp peak is seen. In contrast to 3D–2D tunneling, conservation of in-plane momentum ($k_\parallel$) allows 2D–2D tunneling only when the bottoms of the 2D subbands are closely aligned. In the equilibrium tunneling case, this condition is satisfied when there are equal carrier densities in the two wells, i.e., $\mu_1=\mu_2$ {where $\mu$=the chemical potential in each well [see Fig. 1(b)]}. In addition the width of the tunneling peak is 1.4 meV, which is much less than the Fermi energy of ~15 meV, as expected due to $k_\parallel$ conservation in this resonant tunneling process. At front gate voltages of less than $-0.35$ V the electrons in the upper 2DEG are fully

 0003-6951/94/64(14)/1827/3/$6.00 © 1994 American Institute of Physics 

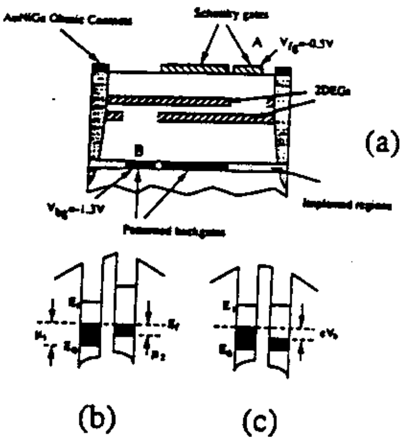


FIG. 1. (a) Schematic diagram showing the device structure indicating the positions of front and back gates. The wafer consists of a 65 nm $n^+$-GaAs backgate, a 325 nm $Al_{0.33}Ga_{0.67}As$ barrier, a 26 nm, $7\times10^{17}$ $cm^{-3}$ Si doped $Al_{0.33}Ga_{0.67}As$ layer to supply carriers to the lower quantum well, followed by a 52 nm undoped AlGaAs spacer layer. The 2DEGs are then confined in two, 19.5 nm GaAs quantum wells, separated by a 13 nm $Al_{0.33}Ga_{0.67}As$ barrier. Above this is grown a standard high mobility 2DEG structure of 26 nm $Al_{0.33}Ga_{0.67}As$ spacer, 52 nm $n^+$-$Al_{0.33}Ga_{0.67}As$ and a 13 nm GaAs capping layer, (b) diagram showing the conduction band profile when the gates are unbiased, (c) diagram showing the conduction band profile when the device is on resonance by applying a dc bias ($V_b$) between the two 2DEGs.

depleted and the interlayer conductance approaches zero. In contrast to previous work[3] on this topic, we have complete control over the area where the tunneling occurs and therefore the parallel contribution to the tunneling current from uncontrolled regions of the sample can be reduced to extremely low levels. This enables much higher peak-to-background ratios to be obtained (>50:1).

The inset of Fig. 2 shows the variation of the conductance peak position with both front- and back gates. The solid line represents the combination of front- and back gate voltages that produce equal carrier densities in the two wells. This fits the experimental data well until the two 2DEGs are very close to pinch-off and are of very low mobility. Furthermore, there is little variation of peak width over the full range of backgate voltages.

Figure 3 shows the current-voltage characteristics obtained by measuring the tunnel current when a dc voltage ($V_b$) is applied between the two 2DEGs ($V_{fg}=-0.2$ V). In this case the resonance condition is achieved by applying an offset, $eV_b=(\mu_1-\mu_2)$, between the Fermi energies in each well to align the bottoms of the 2D subbands [Fig. 1(c)]. Two peaks are observed at bias voltages of $V_b=4$ mV and $V_b=-38$ mV. The peak at $V_b=4$ mV is due to resonant tunneling from the ground state of the top well into the ground state of the bottom well ($E_0-E_0$). The peak at $V_b=-38$ mV is due to resonant tunneling from the ground state of the bottom well into the first excited state in the top well ($E_0-E_1$). The bias between the two layers is dropped entirely across the barrier, therefore bias positions of these peaks measures the relative subband energy spacing directly. A self-consistent solution of the Schrödinger equation for

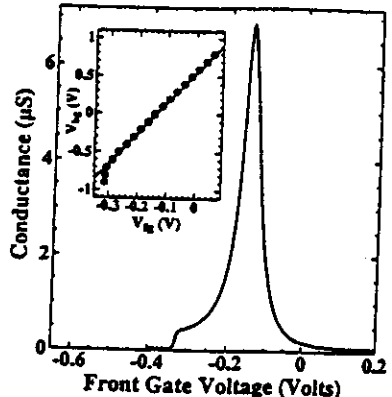


FIG. 2. Graph showing the conductance between the two 2DEGs as a function of front gate voltage. The inset shows the effect of back gate voltage on the conductance peak position. The solid line represents the combination of front- and backgate voltages that produce equal carrier densities in each well. This was found from the magnetoresistance characterization data, and the structural parameters of the device.

finite wells predicts an energy difference of 39 meV between the two lowest 2D subbands, and this agrees well with the measured subband spacing of 42 meV.

The inset of Fig. 3 shows the effect of a back gate voltage on the bias position of the ($E_0-E_0$) tunneling peak. The solid line represents the difference in the carrier densities of the two wells (and hence Fermi energy), as a function of back gate voltage. A third resonant peak was also observed (not shown), arising from tunneling from $E_0$ in the top well into $E_1$ in the bottom well. The peak-to-valley ratios of these features is very large (up to 12:1), due to the reduction of background tunneling to low levels.

These results illustrate the success of our fabrication technique, which has some notable advantages over the pre-

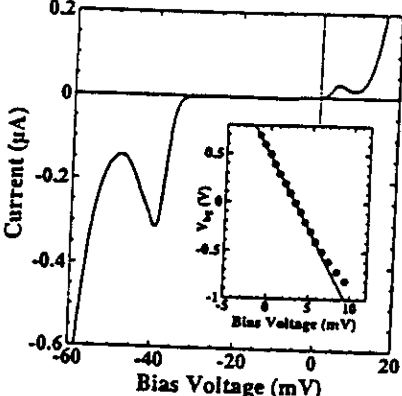


FIG. 3. Graph showing the current-voltage characteristics between the layers ($V_{fg}=-0.2$ V). The inset shows how the ($E_0-E_0$) tunneling peak position moves with back gate voltage. The solid line represents the difference in chemical potential between the two wells as a function of back gate voltage. This relationship is known from both magnetoresistance and structural data.



4

vious methods.[1,2] First, the samples are fairly straightforward to fabricate, avoiding difficult processes such as sample thinning[2,3] and shallow contacts,[1] therefore a very high yield of devices is obtained (approaching 100%). These points are particularly important for the study of tunneling in systems of lower dimension (i.e., tunneling into quantum wires and quantum boxes), defined using further, lower yield, lithographic processes. Second, due to the close proximity of the backgate layer, we are able to accurately define the area where the tunneling occurs as well as the carrier density in the tunneling region. This enables the background tunneling to be reduced to extremely low levels, resulting in very high peak-to-valley ratios, a feature crucial for the operation of mesoscopic structures based on vertical transport.[7] Finally the device can be operated with gate voltages of $<-2$ V, thus removing many of the practical problems of dealing with the high gate voltages ($>200$ V) used in Refs. 1–3.

The drawbacks of this technology are first the overhead associated with construction of the *in situ* implantation system. Second, once grown, the backgate pattern cannot be changed (in contrast to Refs. 2 and 3), although this is a small price to pay when the total sample fabrication and assessment time is only a few days.

In conclusion, we have developed a novel technique of *in situ* ion beam lithography allowing independent contacts to be made to two, 2DEG layers separated by 13 nm. Control of both upper and lower carrier densities can be achieved with front- and backgates, allowing detailed study of the tunneling between the 2DEGs as a function of carrier density. A very low background tunneling current was obtained, resulting in higher peak-to-valley ratios than seen in previous work.[1,3]

We would like to thank A. R. Hamilton for interesting discussions on this work. We should also like to thank D. Heftel for technical support. This work has been supported by SERC. D. A. R. wishes to acknowledge funding from the Toshiba Cambridge Research Centre.

[1] See, for example, W. Demmerle, J. Smoliner, G. Berthold, E. Gornik, G. Weimann, and W. Schlapp, Phys. Rev. B 44, 3090 (1991), and references therein.
[2] J. P. Eisenstein, L. N. Pfeiffer, and K. West, Appl. Phys. Lett. 57, 2324 (1990).
[3] J. P. Eisenstein, L. N. Pfeiffer, and K. West, Appl. Phys. Lett. 58, 1497 (1991).
[4] E. H. Linfield, G. A. C. Jones, D. A. Ritchie, and J. H. Thompson, Semicond. Sci. Technol. 8, 415 (1993).
[5] K. Brown, E. H. Linfield, G. A. C. Jones, D. A. Ritchie, and J. H. Thompson, J. Vac. Sci. Technol. B (in press).
[6] K. M. Brown, E. H. Linfield, D. A. Ritchie, G. A. C. Jones, M. P. Grimshaw, and A. C. Churchill, J. Vac. Sci. Technol. (to be published).
[7] See, for example, S. Datta *et al.*, Phys. Rev. Lett. 21, 2344 (1985); M. Okuda, K. Fujii, and A. Shimizu, Appl. Phys. Lett. 57, 2232 (1990).

# Tunneling between two-dimensional electron gases in a strong magnetic field

K. M. Brown, N. Turner, J. T. Nicholls, E. H. Linfield, M. Pepper, D. A. Ritchie, and G. A. C. Jones
*Cavendish Laboratory, Madingley Road, Cambridge CB3 0HE, England*
(Received 19 July 1994; revised manuscript received 8 September 1994)

We have measured the tunneling between two two-dimensional electron gases at high magnetic fields $B$, when the carrier densities of the two electron layers are matched. For filling factors $\nu<1$, there is a gap in the current-voltage characteristics centered about $V=0$, followed by a tunneling peak at $\sim6$ mV. Both features have been observed before and have been attributed to electron-electron interactions within a layer. We have measured high field tunneling peak positions and fitted gap parameters that are proportional to $B$, and independent of the carrier densities of the two layers. This suggests a different origin for the gap to that proposed by current theories, which predict a $\sqrt{B}$ dependence.

Following recent experimental work[1-3] there has been much theoretical interest in the tunneling of electrons out of a two-dimensional electron gas (2DEG) in a strong magnetic field.[4-9] Following on from experiments of Demmerle *et al.*,[2] Eisenstein *et al.*[3,10] measured the tunneling from one 2DEG to a similar parallel 2DEG, the two being separated by a 175 Å barrier. In zero magnetic field there is resonant tunneling between the two 2DEGs when their carrier densities are equal. In a strong magnetic field, however, the current-voltage ($I$-$V$) characteristics between the two layers exhibit a gap when the filling factor $\nu$ is less than unity. This suppression of tunneling has been interpreted as evidence for electron-electron interactions within a 2DEG, and the resulting gap was labeled a "Coulomb gap." It was also suggested[3] that, at high magnetic fields, electron-electron interactions are responsible for lowering the effective mass of electrons in the lowest Landau level (LL).

In this paper we present tunneling results obtained on similar double 2DEG samples based on GaAs. We observe a gap in the $I$-$V$ characteristics, but we shall show that the gap and the associated tunneling peak do not follow the $\sqrt{B}$ behavior predicted by current theories. Instead we observe a high field gap and a tunneling peak that are both linear in $B$ and independent of filling factor.

Double quantum wells and buried patterned back gates were fabricated by *in situ* ion beam lithography and molecular beam epitaxy regrowth. These techniques allow patterned back gates to be grown into the wafer structure, the details of which have been published elsewhere.[11-13] Subsequent optical lithography was used to define a Hall bar mesa, and to deposit Au Schottky gates aligned with the back gates. The device was put into the tunneling configuration (as shown in the left hand inset of Fig. 1) by applying negative voltages to side front and back gates (not shown). The two electron gases then overlap in a 100 $\mu$m × 150 $\mu$m area. The carrier densities of the top ($n_1$) and bottom ($n_2$) 2DEGs in the tunneling area were controlled by voltages applied to the top ($V_{g1}$) and bottom ($V_{g2}$) gates, respectively.

We present results obtained from one particular wafer (C751), which consists of two modulation-doped 180 Å GaAs quantum wells separated by a 125 Å $Al_{0.33}Ga_{0.67}As$ barrier. The upper 2DEG has an as-grown carrier density of $n_1=3.1\times10^{11}$ cm$^{-2}$ and a mobility of $8\times10^5$ cm$^2$/V s; the corresponding quantities for the lower 2DEG are $n_2=1.8\times10^{11}$ cm$^{-2}$ and $2\times10^5$ cm$^2$/V s. The surface gates were evaporated 800 Å above the top 2DEG, whereas the buried gates were fabricated 3500 Å below the bottom 2DEG.

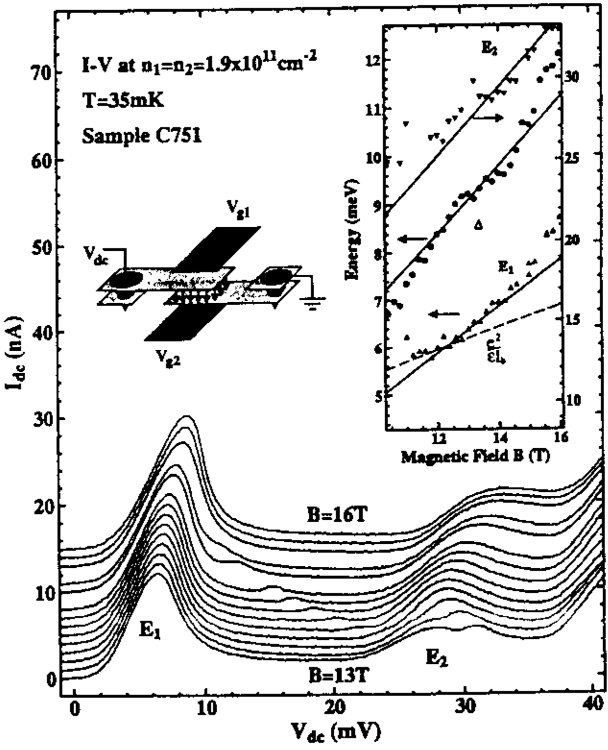


FIG. 1. Low temperature $I$-$V$ characteristics when $n_1=n_2=1.9\times10^{11}$ cm$^{-2}$. Sweeps (vertically offset up the figure) were measured at 0.2 T intervals, and those at 15.4 T and 14.8 T are missing. Left hand inset: the device in the tunneling configuration. Right hand inset: fitted gap $\Delta$ and peak positions $E_1$ and $E_2$ as a function of magnetic field $B$. The solid lines are the fits $E_1=0.30\hbar\omega_c$, $E_2=1.3\hbar\omega_c$, and $\Delta=0.42\hbar\omega_c$. The dashed line shows the Coulomb energy $0.4e^2/\epsilon l_B$.

 © 1994 The American Physical Society

Figure 1 shows the *I-V* characteristics of sample C751 measured at 35 mK from 13 to 16 T, when the carrier densities in the tunneling region were set to $n_1 = n_2 = 1.9\times 10^{11}$ cm$^{-2}$. In contrast to the resonant tunneling that occurs at zero magnetic field, there is a strong suppression of the tunneling around $V=0$ at high magnetic fields. A suppression of the zero bias tunneling (though not enough to form a gap) has also been observed at filling factors as high as $\nu=8$, but we only show data for $\nu<1$. Our samples have a lower mobility than those used in previous studies,[3] but the features that we observe are the same, though not as well defined. One advantage of the lower mobility samples is that the high field measurements ($\nu<1$) were not affected by fractional quantum Hall states.

The data in Fig. 1 show a gap centered at $V=0$ which gives way to a tunneling peak (labeled $E_1$) at ~5–7 mV, and a higher peak at ~30 mV (labeled $E_2$). The additional splitting of the $E_2$ peak around 13 T is due to a peak that moves to lower voltage as the magnetic field is increased. This extra peak is due to inter-LL transitions originating from the first excited 2D subband of the quantum wells; we shall concentrate on results only within the lowest 2D subband. In the right hand inset of Fig. 1 we have plotted the $E_1$ and $E_2$ peak positions between 9 and 16 T. The two sets of data points have been fitted with straight lines forced through the origin, with slopes of $E_1 = (0.30\pm 0.04)\hbar\omega_c$ and $E_2 = (1.3 \pm 0.1)\hbar\omega_c$, where the cyclotron energy is $\hbar\omega_c = 1.67$ meV/T for GaAs.

Additional information about the gap can be obtained from the functional form of the *I-V* characteristics. He *et al.*[6] predict that the tunneling current at $\nu=1/2$ will have the form $I=I_0\exp(-\Delta/V)$, where the gap parameter $\Delta = 2\pi e^2/\epsilon l_B$, and $l_B=\sqrt{\hbar/eB}$ is the magnetic length. In another description of this system, Ashoori *et al.*[14] assumed a linear variation of the density of states about $E_F$, and argued that the tunneling current should have the form $I\sim V^3$. Johansson and Kinaret[7] predict a similar form, but of a higher power.

Experimentally, we cannot fit the low voltage tunneling current with any polynomial. Instead, we find that the function $I=I_0\exp(-\Delta/V)$ fits the tunneling data best in the high bias regime, a surprising result given that the theory[6] should only be applicable in the low energy limit, $V\rightarrow 0$. The inset to Fig. 2 shows an *I-V* characteristic at 16 T and $\nu=1/2$ plotted as $\ln|I|$ vs $1/V$; equally good fits were obtained over a wide range of filling factors $0.2<\nu<2$. The values of $\Delta$ extracted from the *I-V* sweeps in Fig. 1 are plotted along with $E_1$ and $E_2$ in the figure inset. The gap parameter $\Delta$ is best fit by the function $\Delta = 0.44\hbar\omega_c$.

Theoretical descriptions of the gap and the $E_1$ tunneling peak can be subdivided into those that ignore interlayer correlations[4–7] and those that incorporate interlayer interactions.[8,9] Quantum mechanical calculations[5,6] of the former type predict that, for the compressible state at $\nu=1/2$, the tunneling peak occurs at the energy $0.4e^2/\epsilon l_B \sim \sqrt{B}$. The Coulomb energy $0.4e^2/\epsilon l_B$ (shown as a dashed line in the Fig. 1 inset) is comparable to the energy of the $E_1$ peak position. Our data shows, however, that the $E_1$ peak position is better fit by a linear, rather than a square root, function of magnetic field $B$.

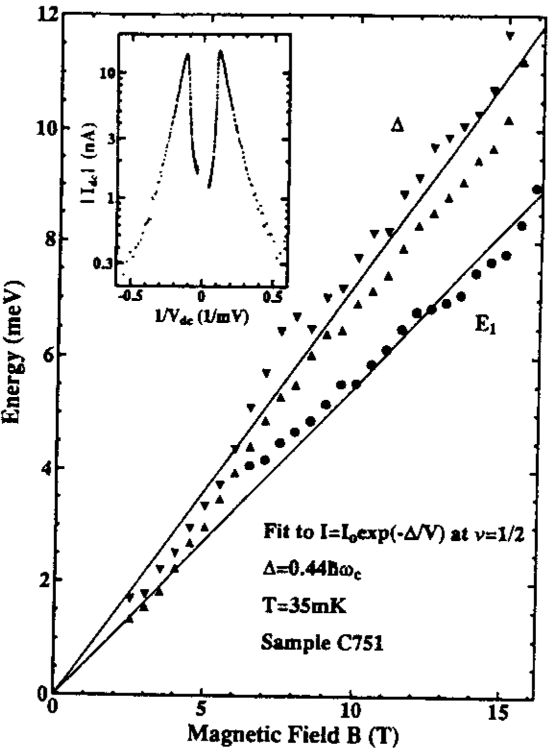


FIG. 2. The peak position $E_1$ (circles) and the fitted gap parameter $\Delta$ (up and down triangles for positive and negative bias directions) measured at $\nu=1/2$ as a function of magnetic field. The lines are least-squares fits forced through the origin with slopes of $0.44\hbar\omega_c$ and $0.33\hbar\omega_c$. Inset: $\ln|I|$ vs $1/V$ for $n_1=n_2=1.94\times 10^{11}$ cm$^{-2}$ at $B=16$ T, showing the range of fit to the function $I=I_0\exp(-\Delta/V)$.

To test theoretical predictions[6] at $\nu=1/2$, we performed a series of experiments at magnetic fields and carrier densities ($n_1=n_2$), such that the lowest LL in each layer was always half-filled. At filling factor $\nu=1/2$, the two 2DEGs in the tunneling region are Fermi liquids,[15] and complications due to the current flowing along the edges of the tunneling region are avoided. We have investigated this filling factor over a wide range of magnetic fields, and Fig. 2 shows the value of the gap parameter $\Delta$ measured at $\nu=1/2$ from 3 to 16 T. The up and down triangles show the fitted values of $\Delta$ in the two bias directions. Not only is the magnitude of $\Delta$ much smaller than theoretically predicted ($2\pi e^2/\epsilon l_B = 85$ meV at 10 T), but the average value of $\Delta$ is best fit by the function $\Delta = (0.44\pm 0.02)\hbar\omega_c$, which is proportional to $B$ rather than $\sqrt{B}$. The position of the $E_1$ peak was also measured at $\nu=1/2$, the least-squares fit forced through the origin gives $E_1 = 0.33\hbar\omega_c$. Whether $n$ or $\nu$ is held fixed the gap parameter as a function of magnetic field has the same slope of $0.44\hbar\omega_c$. Similar results for $\Delta$ and $E_1$ were obtained at filling factors $\nu=0.4$ and 0.6, showing that the choice of $\nu=1/2$ is not special.

Johansson and Kinaret[7] modeled the electron liquids in each of the two layers as Wigner crystals. The energy of the tunneling peak is predicted to be proportional to the intralayer Coulomb energy $E_C = e^2/\epsilon a$, where $a$ is the lattice

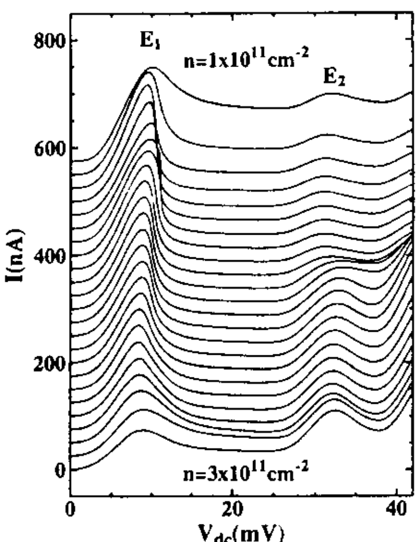


FIG. 3. $I$-$V$ characteristics measured at $B=16$ T, as the filling factor $\nu$ was varied from 0.26 to 0.77. Successive sweeps have been displaced up the figure.

parameter of the Wigner crystal determined by the 2D electron density $n$. $E_C$ is comparable to $E_1$, but the model predicts that the energy of the peak maximum depends only on the carrier densities $n_1$ and $n_2$. Figure 3 shows the $I$-$V$ characteristics measured when the magnetic field was fixed at $B=16$ T, while the carrier densities $n=n_1=n_2$ were varied over the range $(1-3)\times 10^{11}$ cm$^{-2}$. The $E_1$ and $E_2$ peak positions remained constant as the filling factor was changed by a factor of 3. A similar independence of the gap with electron density has also been observed by Ashoori *et al.*[1,14] The $E_1$ peak occurs at $0.3\hbar\omega_c$ and the $E_2$ peak remains at approximately $1.3\hbar\omega_c$, the same values that were obtained when the carrier densities were fixed and the magnetic field was varied (see Fig. 1). The fitted gap parameter $\Delta$ remained constant at $0.44\hbar\omega_c$. We find no evidence that the $E_1$ peak position scales with carrier density as $E_1\sim\sqrt{n}$, as predicted by Johansson and Kinaret.[7] In a model that also incorporates interlayer electron correlations, Varma *et al.*[9] have also predicted that the gap will be a strong function of the interelectron distance within a layer; the results in Fig. 3 show this not to be the case.

In previous experiments[2] at 4.2 K, the position of the maxima in $dI/dV$ were used to identify inter-LL transitions that occur when the bias energy $eV=\pm\hbar\omega_c, \pm 2\hbar\omega_c$. There is a maximum when there is tunneling from the $N=0$ LL in one 2DEG to the $N=1,2$ LL in the other 2DEG. There was no indication of a suppression of tunneling at zero bias in these experiments, possibly due to the high measuring temperature. In experiments[3] that extended this earlier work to lower temperatures and higher magnetic fields, a gap was measured. The $E_2$ tunneling peak was interpreted as an inter-LL transition, occurring at $1.3\hbar\omega_c$ rather than at the usual cyclotron energy $\hbar\omega_c$. It was suggested that the increased cyclotron energy was due to a decrease of the effective mass resulting from intralayer Coulomb interactions.[16]

We have investigated other samples with different mobilities and $Al_xGa_{1-x}As$ barrier widths, and have obtained similar tunneling results to those shown in Figs. 1–3. For barrier widths where tunneling is important (100–200 Å), we observe linear magnetic field dependent behavior for $E_1$, $E_2$, and $\Delta$. The energies $E_1$ and $E_2$ have roughly the same values as in C751, but the fitted values of $\Delta$ are larger in more disordered samples. In all cases, by whatever criterion we choose to describe the $E_1$ tunneling peak (for example, by an onset voltage or a peak position), we always obtain a linear magnetic field dependence for the quantity chosen. These results suggest that the $E_1$ tunneling peak, like the $E_2$ peak, could be related to the Landau level structure within each 2DEG. There is, however, no obvious LL structure that would give rise to a peak at $0.3\hbar\omega_c$. If spin splitting is taken into account, then a spin-flip transition of $2g\mu_BSB = 0.3\hbar\omega_c$ would suggest a $g$ value of 4.5; such a large $g$ value that is independent of $\nu$ is not expected in GaAs. Moreover, spin splitting cannot account for the suppression of tunneling about zero bias.

Theoretical descriptions of electron-electron interactions in a strong magnetic field (for example, the fractional quantum Hall effect) work within the lowest Landau level approximation $\hbar\omega_c \gg e^2/\epsilon l_B$. The energy gap for a fractional state (for example, $\nu=1/3$) is expected to be proportional to the energy $e^2/\epsilon l_B$. Various calculations have included the effect of higher LLs and have predicted a departure from $\sqrt{B}$ towards linear behavior for the fractional gap. We could be observing an analogous effect for the tunneling gap between two 2DEGs, though as we suggest in the following paragraphs the explanation could be more mundane.

We have been able to follow[17] the $E_1\approx 0.3\hbar\omega_c$ tunneling peak down to low magnetic fields ($B=1$ T, $\nu=8$). It would be suprising if we could detect intralayer electron correlations at such high filling factors, and a classical description of the system may be more appropriate. In a classical theory put forward by Efros and Pikus,[8] the Coulomb gap arises due to correlations both between and within the electron layers. The classical theory predicts[8] that, for fixed carrier densities $n_1=n_2$, the gap $\Delta$ is linear in $\nu$ for $0.3<\nu<0.9$; our data in Fig. 1 show that $\Delta$ is linear in $B$. The classical theory also predicts that, for a given filling factor, the gap $\Delta$ scales with $\sqrt{B}$; the data at $\nu=1/2$ in Fig. 2 show that this is not the case.

The available theories do not describe our data; at constant carrier densities they predict a gap that is either proportional to $\sqrt{B}$ or to $\nu$. Our data shows that the gap only depends on $B$. In further experiments[18] we have measured the $I$-$V$ characteristics when the lower 2DEG was fixed at $n_2=3.1\times 10^{11}$ cm$^{-2}$ at $B=16$ T. The $E_1$ and $E_2$ tunneling peaks and the fitted gap $\Delta$ remained constant as $n_1$ was varied from $3.1\times 10^{11}$ cm$^{-2}$ to $1.1\times 10^{11}$ cm$^{-2}$. This result, as well as those presented in Figs. 1–3, strongly suggest a classical origin for the gap. If this is the case then the $E_2$ peak can be explained as being the usual inter-LL transition at $\hbar\omega_c$ which has been displaced by $0.3\hbar\omega_c$ to $1.3\hbar\omega_c$.

In conclusion, we have observed a suppression of tunneling between two partially filled LLs. With our samples we have been able to extend tunneling measurements over a wide range of carrier densities and filling factors. Providing that the sample does not freeze out at high magnetic field.

our results show that the gap solely depends on the magnetic field $B$, and is independent of mobility and carrier densities of the two layers. We show that the $E_1$ peak energy is not proportional to the electron-electron interaction energies $e^2/\epsilon l_B$ or $e^2/\epsilon a$.

We wish to thank the Engineering and Physical Sciences Research Council (U.K.) for supporting this work. J.T.N. acknowledges support from the Isaac Newton Trust and D.A.R. acknowledges support from Toshiba Cambridge Research Centre.

[1] R. C. Ashoori, J. A. Lebens, N. P. Bigelow, and R. H. Silsbee, Phys. Rev. Lett. **64**, 681 (1990).
[2] W. Demmerle *et al.*, Phys. Rev. B **44**, 3090 (1991).
[3] J. P. Eisenstein, L. N. Pfeiffer, and K. W. West, Phys. Rev. Lett. **69**, 3804 (1992).
[4] S.-R. E. Yang and A. H. MacDonald, Phys. Rev. Lett. **70**, 4110 (1993).
[5] Y. Hatsugai, P.-A. Bares, and X. G. Wen, Phys. Rev. Lett. **71**, 424 (1993).
[6] S. He, P. M. Platzman, and B. I. Halperin, Phys. Rev. Lett. **71**, 777 (1993).
[7] P. Johansson and J. M. Kinaret, Phys. Rev. Lett. **71**, 1435 (1993).
[8] A. L. Efros and F. G. Pikus, Phys. Rev. B **48**, 14 694 (1993).
[9] C. M. Varma, A. I. Larkin, and E. Abrahams, Phys. Rev. B **49**, 13 999 (1994).
[10] J. P. Eisenstein, L. N. Pfeiffer, and K. W. West, Surf. Sci. **305**, 393 (1994).
[11] E. H. Linfield, G. A. C. Jones, D. A. Ritchie, and J. H. Thompson, Semiconduc. Sci. Technol. **9**, 415 (1993).
[12] K. M. Brown *et al.*, Appl. Phys. Lett. **64**, 1827 (1994).
[13] K. M. Brown *et al.*, J. Vac. Sci. Technol. B **12**, 1293 (1994).
[14] R. C. Ashoori, J. A. Lebens, N. P. Bigelow, and R. H. Silsbee, Phys. Rev. B **48**, 4616 (1993).
[15] B. I. Halperin, P. A. Lee, and N. Read, Phys. Rev. B **47**, 7312 (1993).
[16] A. P. Smith, A. H. MacDonald, and G. Gumbs, Phys. Rev. B **45**, 8829 (1992).
[17] K. M. Brown *et al.* (unpublished).
[18] K. M. Brown *et al.*, Physica (to be published).

Temperature Studies of the Tunnelling Between Parallel Two-Dimensional Electron Gases

N. Turner, J. T. Nicholls, E. H. Linfield, K. M. Brown, M. Pepper, D. A. Ritchie and G. A. C. Jones

*Cavendish Laboratory, Madingley Road, Cambridge CB3 0HE, UK*

(28 April 1995)

## Abstract

We have measured the temperature dependence of the tunnelling conductance $G = dI/dV_{\mathrm{sd}}$ between two parallel two-dimensional electron gases in perpendicular magnetic fields, supplementing earlier measurements as a function of applied dc bias. For filling factors below $\nu = 10$ there is a suppression of the conductance near $V_{\mathrm{sd}} = 0$, which develops into a strong gap when $\nu < 1$. We have studied the activation of the conductance minimum at $V_{\mathrm{sd}} = 0$, and the temperature dependence of the shape of the conductance peaks on either side. We find that the activation energy of the minimum is approximately an order of magnitude smaller than the full width of the energy gap measured in bias, but has the same linear magnetic field dependence. Temperature divides the tunnelling characteristics $G(V_{\mathrm{sd}})$ into three regions around $V_{\mathrm{sd}} = 0$: a central region where $dG/dT > 0$, sandwiched between two regions where $dG/dT < 0$.

The resonant tunnelling characteristics between parallel two-dimensional electron gases (2DEGs) in high perpendicular magnetic fields, where the Landau level (LL) filling factor $\nu < 1$, are dominated by the "Coulomb gap." Low temperature measurements of the tunnelling conductance $G = dI/dV_{sd}$, as a function of the dc voltage $V_{sd}$ applied between two parallel 2DEGs with matched carrier densities, reveal a deep minimum centred around zero-bias $V_{sd} = 0$. Such a minimum in the conductance characteristic $G(V_{sd})$ in Figure 1 can be ascribed to a gap tied to the Fermi energy in the tunnelling density of states. The width of the gap can be characterised by the separation $\Delta$ of the peaks in $G(V_{sd})$, and is equivalent to the gap parameter $\Delta$ defined in the expression for the tunnelling current $I = I_0 \exp(-\Delta/V_{sd})$ predicted by the theoretical model of He *et al.* [1] From our earlier investigations [2-4] of the Coulomb gap measured at low temperatures we concluded that, irrespective of whether measurements are made at fixed carrier density or fixed filling factor, $\Delta$ depends linearly on magnetic field $B$ ($\Delta \approx 0.45\hbar\omega_c$, where $\hbar\omega_c$ is the cyclotron energy $\hbar eB/m^* = 1.67$ meV/T in GaAs) and is independent of carrier density $n$ over a wide range of filling factors $0.3 < \nu < 10$. Many-body theories [1,5-9] of the Coulomb gap applicable for $\nu < 1$ predict a gap which is proportional to either $e^2/\epsilon l_B$ (where $l_B = \sqrt{h/eB}$ is the magnetic length) or $e^2/\epsilon a$ (where $a \propto n^{1/2}$ is the average in-plane separation of electrons). Other experimental studies [10] of the high field $\nu < 1$ regime report a gap following a modified square-root field dependence. There is a partial suppression of the zero-bias tunnelling at higher filling factors; we have observed [4] traces of a gap at filling factors as high as $\nu = 10$. The measured width of the incomplete gap follows the same magnetic field dependence as that at high fields. Here we present further data taken over a range of magnetic fields showing the temperature dependence of the zero-bias tunnelling conductance $G(V_{sd} = 0)$. The conductance is thermally activated at low temperatures with an activation energy $E_a$ which is proportional to the applied magnetic field.

The sample, identical to those used previously [2,4], consists of two GaAs quantum well 2DEGs which are 180 Å wide, and separated by a 125 Å $Al_{0.33}Ga_{0.67}As$ barrier. The as-grown carrier densities and mobilities of the upper and lower layers are $n_1 = 3.2 \times 10^{11}$ cm$^{-2}$,

$\mu_1 = 8 \times 10^5$ cm$^2$/Vs and $n_2 = 1.8 \times 10^{11}$ cm$^{-2}$, $\mu_2 = 2 \times 10^5$ cm$^2$/Vs respectively. Surface gates evaporated 800 Å above the upper 2DEG and buried backgates patterned 3500 Å below the lower 2DEG are used to make independent contacts to the two layers, isolating a 100 $\mu$m $\times$ 150 $\mu$m tunnelling area where the two gases overlap. The Fig. 1 inset shows the device in the tunnelling configuration. Additional gates control the carrier densities in the tunnelling area; the proximity of the backgate to the lower 2DEG, compared with a backgate evaporated onto a thinned sample, allows accurate control of $n_2$ with small voltages and ensures a uniform electron density over the whole tunnelling region. References [11–13] contain further information on the design and fabrication of these devices.

It is posssible to precisely match the carrier densities $n_1$ and $n_2$ in the tunnelling region by maximising the symmetry of the resonant tunnelling peak $G(V_{sd})$ at $B = 0$, and all the measurements reported in this paper were carried out under this condition. Once matched, the tunnelling characteristics remain highly symmetrical at all magnetic fields; Figure 1 shows a typical characteristic at $B = 8$ T with $n_1 = n_2 = 1.6 \times 10^{11}$ cm$^{-2}$. The zero-bias suppression separates two conductance peaks of nearly equal magnitude, flanked by regions of negative differential conductance. The separation $\Delta$ of the two peaks directly measures the width of the gap in the tunnelling density of states. Figure 2 shows how these tunnelling characteristics evolve as the temperature is raised from 1.5 K to 6 K. As the temperature is increased, both the suppression of tunnelling at $V_{sd} = 0$ and the height of the surrounding peaks are reduced, however, the peak-to-peak separation characterised by $\Delta$ changes very little as the zero-bias suppression is removed. There are certain values of $V_{sd}$ at which the $G(V_{sd})$ characteristic is unaffected by the changing temperature, dividing the characteristics into regions of positive and negative $dG/dT$.

Plots of $\log G(V_{sd} = 0)$ *vs.* $1/T$ at $B = 6.5$ T and $B = 8$ T in Fig. 3 show clear linear behaviour at low temperatures, indicating activated transport. Above 4 K the data points fall below the projection of the low temperature linear fit. When the temperature rises above 10 K the tunnelling conductance no longer increases with increasing temperature. The activation energy measured from the 8 T data is $E_a = 0.349 \pm 0.007$ meV, an order

of magnitude smaller than $\Delta = 6.88 \pm 0.2$ meV, measured from $G(V_{sd})$ characteristics at the same magnetic field. By varying $n_1 = n_2$, the matched carrier concentrations, we have measured $E_a$ at $\nu = 1/2$ over the magnetic field range $6 \leq B \leq 8$ T. In Figure 4 the ratio $r = E_a/\Delta$ is shown to be roughly independent of magnetic field.

Previously, in similar experiments, Eisenstein *et al.* [14] have measured the activation of the tunnelling conductance at high magnetic fields, also finding an activation energy which is roughly proportional to their measured gap parameter. The magnitude of our activation energy is roughly a factor of two smaller than these measurements; however, we have not been able to directly compare data at the same carrier densities and filling factors. The most significant difference between the sample described here and that of Eisenstein is the mobility; the thicknesses and compositions of the MBE layers are almost identical, but the low temperature mobility our samples (2–8 $\times$ $10^5$ cm$^2$/Vs) is up to an order of magnitude lower. This reduced mobility could be responsible for producing a less well developed gap with a lower activation temperature. The data of Ashoori *et al.*, [15,16] taken using samples with 2DEGs estimated to have a mobility of around $2 \times 10^5$ cm$^2$/Vs, proves to be a good fit to a model with such a gap, which has a width linear in $B$. It is possible that 2DEG mobility can control the detailed shape, but not the overall width of the Coulomb gap.

At higher filling factors, when the gap has not completely developed, $\Delta$ follows the same magnetic field dependence as for $\nu = 1/2$. [4] However, the temperature dependence of $G(V_{sd} = 0)$ does not exhibit a clear activated regime. In Figure 5 the data for both $\nu = 1.5$ and $\nu = 2.5$ show considerable curvature at low temperatures. The departure from activated behaviour and the fact that $G(V_{sd} = 0)$ does not approach zero at low temperatures are indicative of the presence of states at the Fermi energy; the tunnelling density of states no longer goes to zero at the centre of the gap. In comparison activated behaviour has been reported [14] up to $\nu = 2$ in samples with higher mobility.

To summarise, in our investigation of the temperature dependence of the zero-bias suppression of resonant tunnelling we have observed a gap in the tunnelling density of states with a maximum width which is independent of temperature. In our samples, at tempera-

tures below 4 K and for $\nu = 1/2$, tunnelling conduction is activated across a gap apparently ten times smaller than the low temperature gap parameter $\Delta$. We conclude that in our samples there must be a finite density of states between the centre of the gap and its edge, and the ratio of the activation width to the full width $\Delta$ may be a function of the sample mobility. At higher filling factors the zero-bias conductance is not simply activated, indicating that the gap closes as the filling factor increases. Measurements of the low temperature gap parameter indicate that the high and low field Coulomb gaps have the same physical origin, although they have a different temperature dependence.

We wish to thank the Engineering and Physical Sciences Research Council (UK) for supporting this work. JTN acknowledges support from the Isaac Newton Trust, and DAR acknowledges support from Toshiba Cambridge Research Centre.

## REFERENCES


[1] S. He, P. M. Platzman, and B. I. Halperin, Phys. Rev. Lett. **71**, 777 (1993).

[2] K. M. Brown *et al.*, Phys. Rev. B **50**, 15465 (1994).

[3] K. M. Brown *et al.*, Physica (1995), in press.

[4] N. Turner *et al.*, preprint (1995).

[5] S.-R. E. Yang and A. H. MacDonald, Phys. Rev. Lett. **70**, 4110 (1993).

[6] Y. Hatsugai, P.-A. Bares, and X. G. Wen, Phys. Rev. Lett. **71**, 424 (1993).

[7] P. Johansson and J. M. Kinaret, Phys. Rev. Lett. **71**, 1435 (1993).

[8] A. L. Efros and F. G. Pikus, Phys. Rev. B **48**, 14694 (1993).

[9] C. M. Varma, A. I. Larkin, and E. Abrahams, Phys. Rev. B **49**, 13999 (1994).

[10] J. P. Eisenstein, L. N. Pfeiffer, and K. W. West, Phys. Rev. Lett. **74**, 1419 (1995).

[11] E. H. Linfield, G. A. C. Jones, D. A. Ritchie, and J. H. Thompson, Semiconduc. Sci. Technol. **9**, 415 (1993).

[12] K. M. Brown *et al.*, Appl. Phys. Lett. **64**, 1827 (1994).

[13] K. M. Brown *et al.*, J. Vac. Sci. Technol. B **12**, 1293 (1994).

[14] J. P. Eisenstein, L. N. Pfeiffer, and K. W. West, Phys. Rev. Lett. **69**, 3804 (1992).

[15] R. C. Ashoori, J. A. Lebens, N. P. Bigelow, and R. H. Silsbee, Phys. Rev. Lett. **64**, 681 (1990).

[16] R. C. Ashoori, J. A. Lebens, N. P. Bigelow, and R. H. Silsbee, Phys. Rev. B **48**, 4616 (1993).

# FIGURES

FIG. 1. Typical tunnelling conductance characteristic at high magnetic field, $B = 8$ T, with filling factor $\nu = 0.85$. Tunnelling is suppressed around $V_{sd} = 0$ by a gap in the tunnelling density of states. The separation of the peaks around zero-bias defines $\Delta$, the width of the gap.

FIG. 2. Evolution of tunnelling characteristics at $B = 8$ T and $\nu = 1/2$, as the temperature is increased from 1.5 K to 6 K. Sweeps are plotted for $T = 1.5, 1.9, 2.4, 2.8, 3.5, 4.3, 5.0, 6.0$ K.

FIG. 3. Arrhenius plots of $G(V_{sd} = 0)$ *vs* $1/T$ at $B = 6.5$ T and $B = 8$ T. In both cases the carrier densities are fixed fixed such that $\nu = 1/2$ in both layers. The straight line fits to the activated regions give activation temperatures of $3.10 \pm 0.09$ K at $B = 6.5$ T and $4.05 \pm 0.08$ K at $B = 8$ T.

FIG. 4. The ratio $r$ of the activation energy $E_a$ (determined from Arrhenius plots) to $\Delta$ (measured from $G(V_{sd})$ characteristics), as a function of magnetic field. Within experimental error $r$ is a constant $r = 0.047$, showing that $E_a$ and $\Delta$ share roughly the same linear dependence on magnetic field.

FIG. 5. Arrhenius plots illustrating the lack of activated behaviour in the tunnelling conductance at higher filling factors, $\nu = 1.5$ and $\nu = 2.5$.

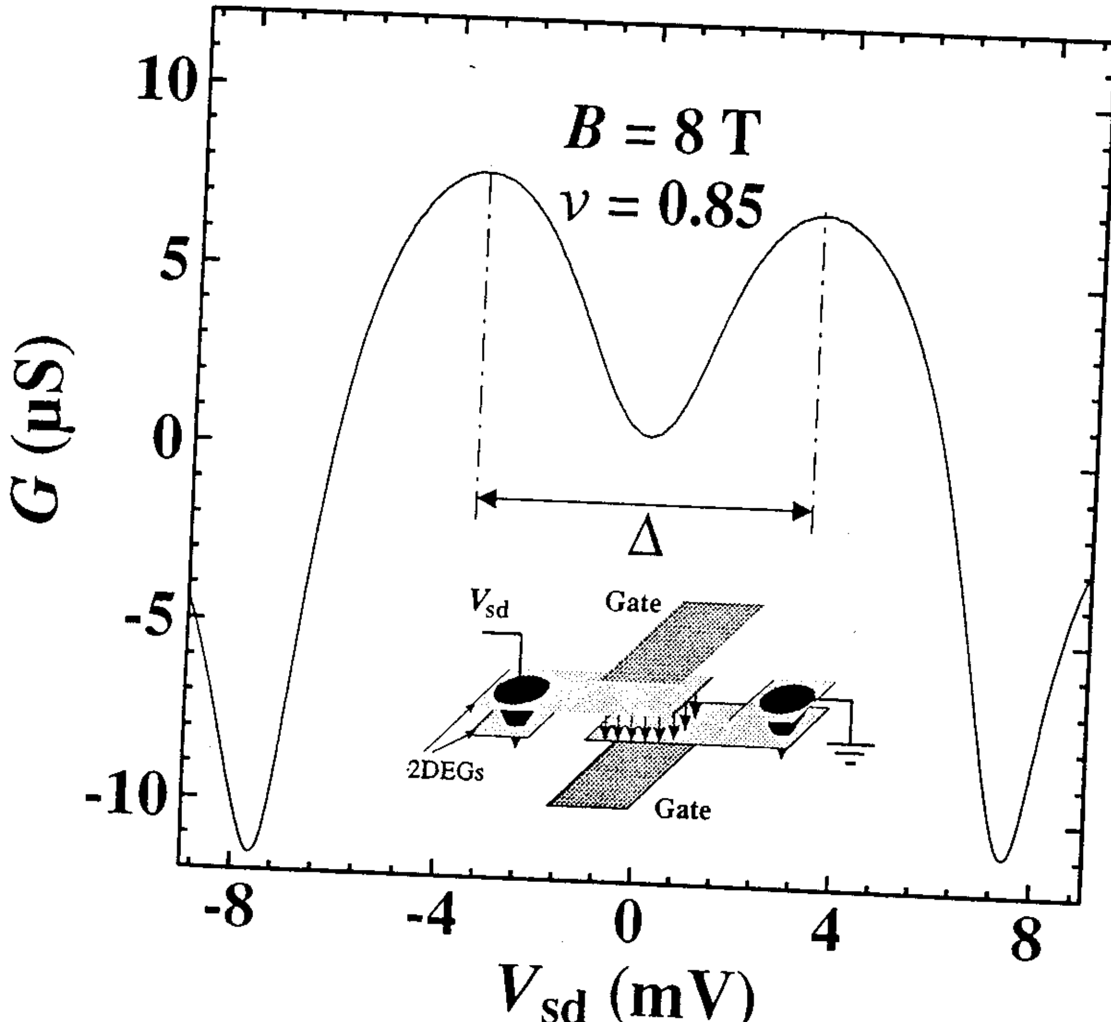

B = 8 T
ν = 0.85
Δ
V sd
Gate
Gate
2DEGs
G (μS)
V sd (mV)
10
5
0
-5
-10
-8
-4
0
4
8

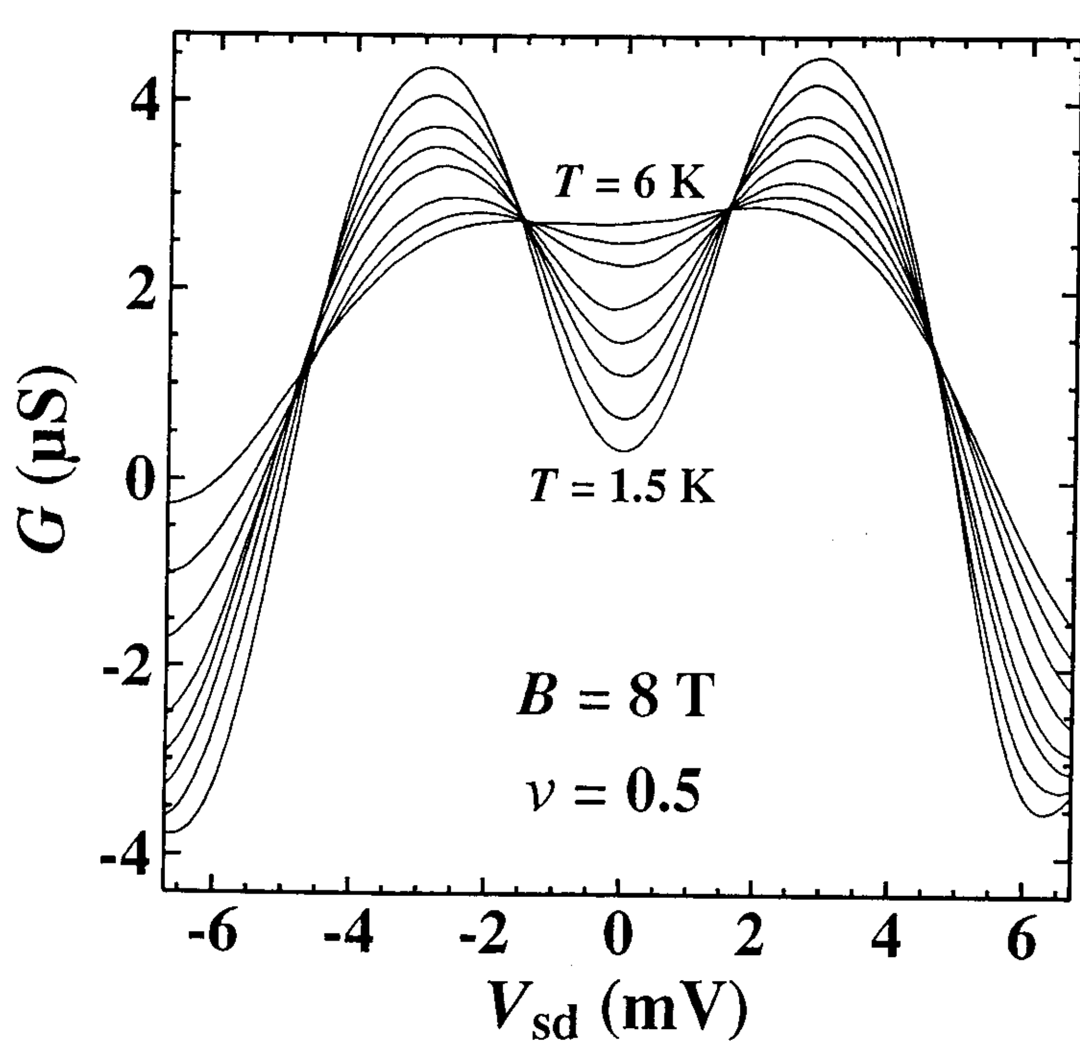

4
2
0
-2
-4
G (µS)
-6
-4
-2
0
2
4
6
V sd (mV)
T = 6 K
T = 1.5 K
B = 8 T
ν = 0.5

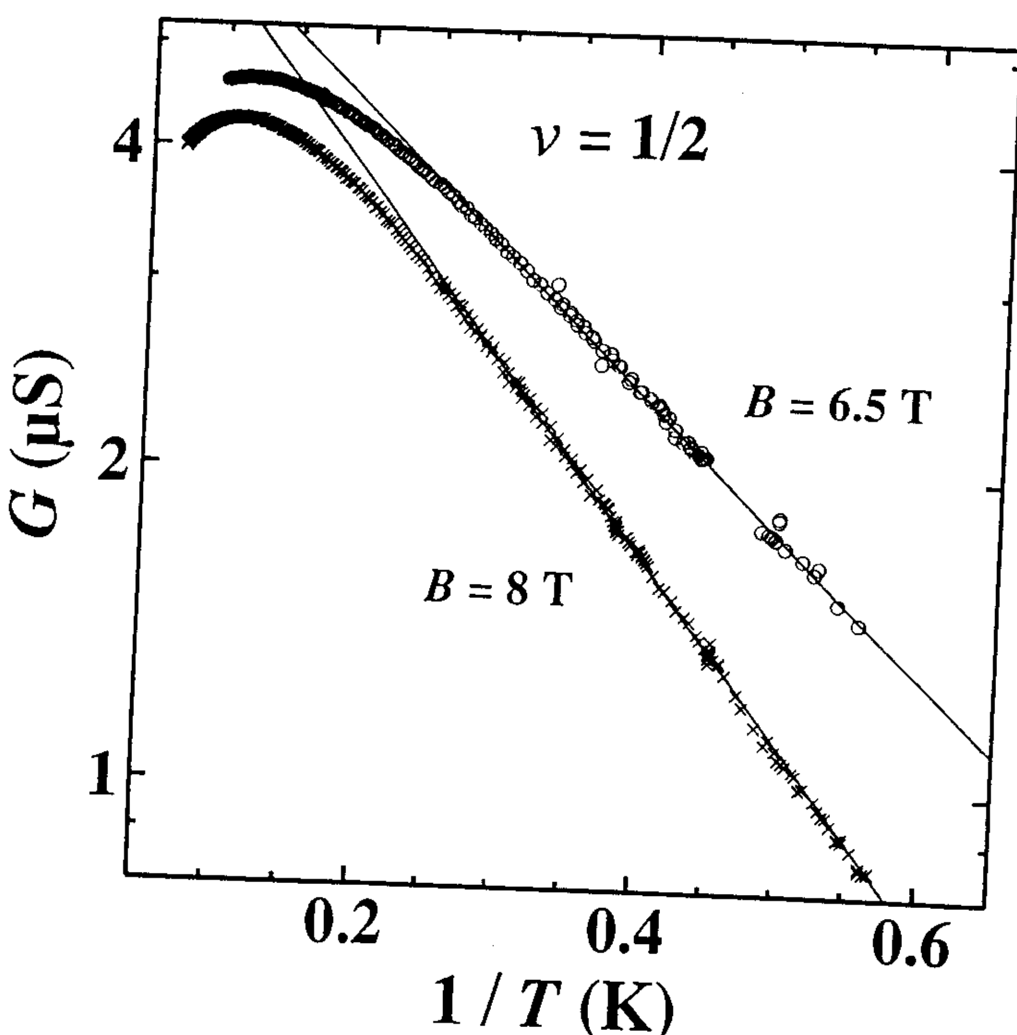
ν = 1/2
B = 6.5 T
B = 8 T
G (μS)
4
2
1
0.2
0.4
0.6
1 / T (K)

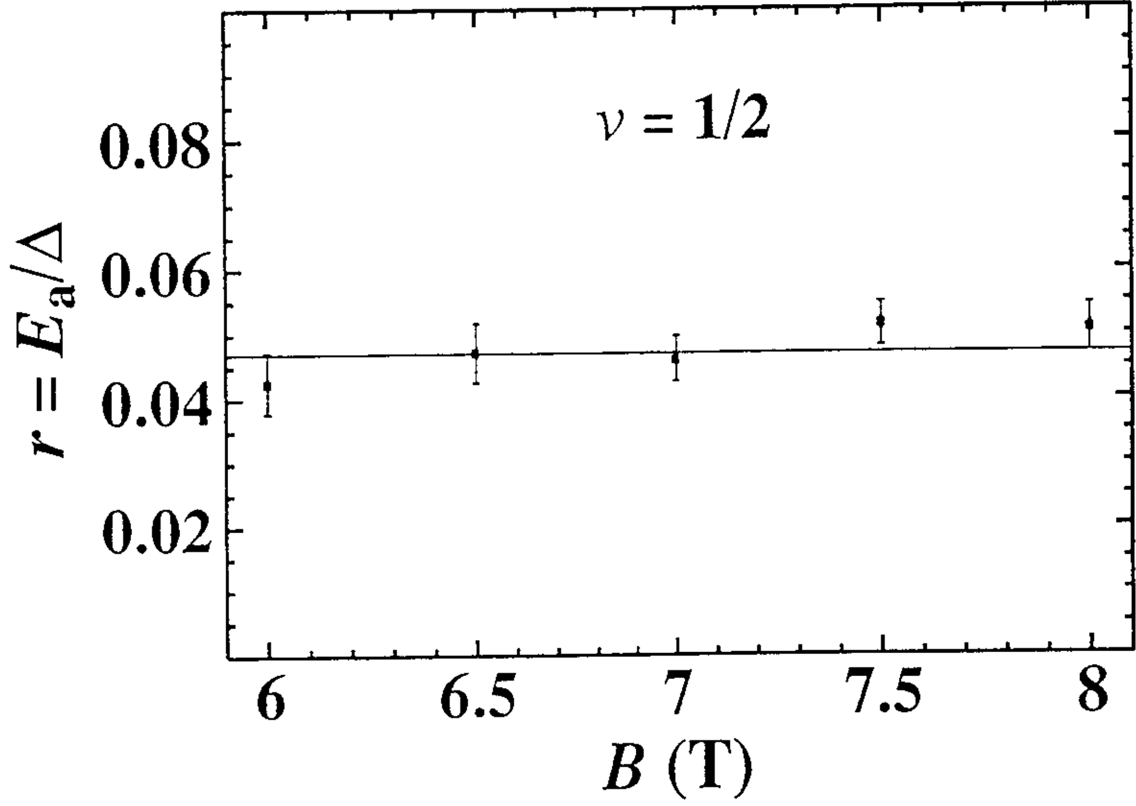

$\nu = 1/2$
0.08
0.06
0.04
0.02
$r = E_a/\Delta$
6
6.5
7
7.5
8
$B$ (T)

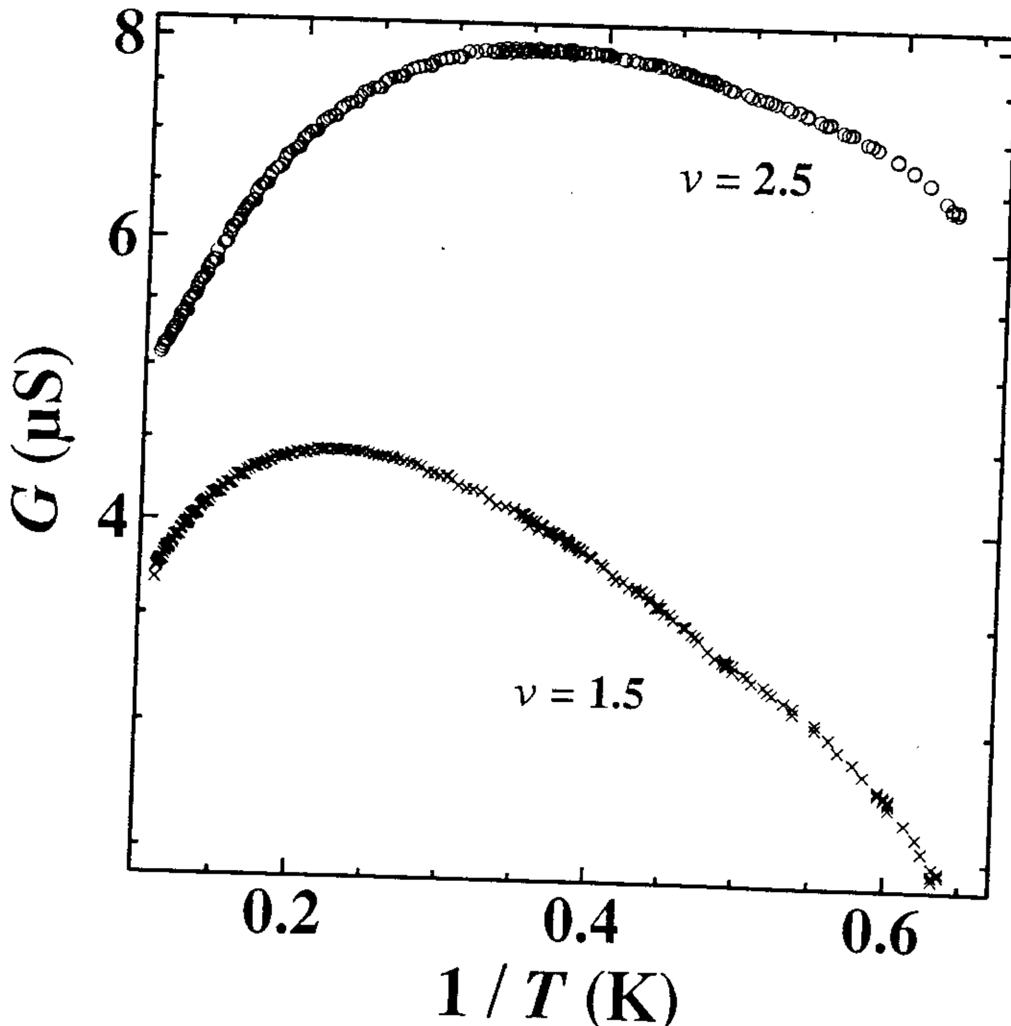
8
6
4
G (μS)
ν = 2.5
ν = 1.5
0.2
0.4
0.6
1 / T (K)

# Resonant resistance enhancement in double-quantum-well GaAs-$Al_xGa_{1-x}As$ heterostructures

A. Kurobe
*Toshiba Cambridge Research Centre, 260 Cambridge Science Park, Milton Road, Cambridge CB4 4WE, United Kingdom*

I. M. Castleton, E. H. Linfield, M. P. Grimshaw, K. M. Brown, D. A. Ritchie, M. Pepper,* and G. A. C. Jones
*Cavendish Laboratory, Madingley Road, Cambridge CB3 0HE, United Kingdom*
(Received 3 March 1994; revised manuscript received 2 May 1994)

We present a study of electron transport in coupled quantum-well structures controlled by both front and back gates. The resonant resistance enhancement is systematically investigated by varying the mobility in each quantum well. We show that a large mobility ratio between the two wells gives a large resonant resistance enhancement only when the level broadening is smaller than the symmetric-antisymmetric gap of the coupled system.

The advent of thin-layer growth of semiconductors has made it possible to design and realize new semiconductor devices based on quantum mechanics. One of the observed phenomena, which is directly related to the wave nature of electrons, is the wave-function coupling between two closely spaced two-dimensional electron gases (2DEG's). This can be obtained in systems such as double-quantum-well (DQW) structures. If the scattering in the double 2DEG system is not symmetric, an increase in resistance, i.e., resistance resonance, arises when the two 2DEG's are resonantly coupled.[1] This is because a higher mobility 2DEG, the wave function of which is localized in one of the two wells, is delocalized over both wells by hybridization at resonance, and thus suffers increased scattering in the lower mobility well. The size of the hybridization is characterized by the energy gap between the hybridized symmetric and antisymmetric states, $\Delta_{SAS}$.

The concept of resistance resonance can be applied to the velocity modulation transistor (VMT) proposed by Sakaki and co-workers.[2,3] In this device the conductance modulation is achieved by changes to the mobility while the carrier density is kept constant. VMT operation has been achieved in single conduction channel structures,[4,5] but is hard to demonstrate in double-channel structures due to the difficulty of fabricating a back gate which can be sufficiently biased to compensate the carrier density change arising from the front-gate voltage variation.

In this paper, we describe the successful fabrication of DQW-VMT structures using the technique of molecular-beam epitaxy (MBE) regrowth on an epilayer patterned by an *in situ* focused ion beam.[6] By comparing the size of the resistance resonance among devices with different values of mobility, we show that a high-mobility ratio is not sufficient for a sizable resistance resonance effect. In addition, the mobility of both 2DEG's must be large enough that the level broadening due to scattering is smaller than $\Delta_{SAS}$.

The modulation-doped DQW structures (Fig. 1) were grown on semi-insulating GaAs substrates by MBE. All samples consisted of two 150-Å-wide quantum wells separated by a 25-Å $Al_{0.33}Ga_{0.67}As$ barrier. Electrons in the 2DEG's were supplied by Si-doped $Al_{0.33}Ga_{0.67}As$ layers placed above and below the DQW. The whole DQW structure was then isolated by a 0.31-$\mu$m $Al_{0.33}Ga_{0.67}As$ barrier from an $n^+$-type GaAs back-gate layer grown underneath. Ohmic contacts to the double 2DEG's were achieved, without contacting to the $n^+$-type GaAs back-gate layer, using MBE regrowth on an *in situ* focused ion-beam patterned epilayer.[6] After growth, devices were processed into a Hall bar geometry with a front Schottky gate as well as the back gate. The leakage current between the back gate and the 2DEG's was less than 1 nA throughout the gate voltage range reported here. The resistance of the samples was measured using a

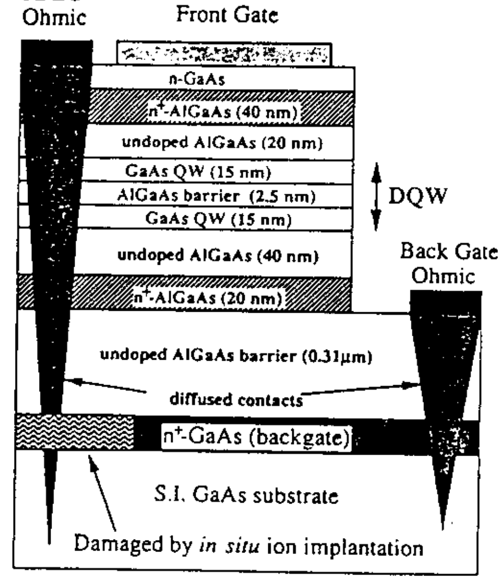


FIG. 1. Schematic cross section of back-gated DQW structure. The doping level of $n^+$-type $Al_{0.33}Ga_{0.67}As$ layers was $1\times10^{18}$ cm$^{-3}$. An MBE regrowth on an *in situ* ion beam patterned epilayer was used to form Ohmic contacts to the 2DEG's without contacting the $n^+$-type GaAs back gate layer.

0163-1829/94/50(11)/8024(4)/$06.00 50  ©1994 The American Physical Society

standard lock-in technique with a relative error ($\delta R/R$) smaller than 0.2%.

In order to achieve a large resistance resonance, a significant difference in the scattering rate between the two wells is desirable. The QW's were not intentionally doped,[3] but a mobility difference between the QW's occurred naturally due to diffusion of dopant from the $n^+$-type $Al_xGa_{1-x}As$ back-doped layer into the back $Al_xGa_{1-x}As$ spacer layer during MBE growth. This diffusion caused enhanced ionized impurity scattering and hence a lower mobility in the back 2DEG. In order to adjust the effect of the diffusion, we varied the growth temperature ($T_g$) of the lower doped layer in three samples: $A$ ($T_g=520\,^\circ$C), $B$ ($T_g=580\,^\circ$C), and $C$ ($T_g=630\,^\circ$C); the growth temperature for all other layers remaining fixed at 630 °C. This gave a systematic change in the mobility of back 2DEG, as diffusion of silicon is strongly temperature dependent.

By means of sequential depopulation of the double 2DEG's by the front-gate voltage, the mobility ratio between the front and back 2DEG at the same carrier concentration, $r=\mu_{\text{front}}/\mu_{\text{back}}$, was determined from the resistance at resonance and that at pinch off of the front 2DEG.[1] The values of $r$ were approximately 2, 14, and 100 for devices $A$, $B$, and $C$, respectively. The symmetric-antisymmetric gap was then determined to be $\Delta_{SAS}=1.2\pm0.1$ meV from Shubnikov–de Haas analysis[7] for sample $A$, which is in good agreement with the value of 1.3 meV calculated self-consistently.

The clearest resonant resistance enhancement was observed as a function of the back-gate voltage in sample $B$ (Fig. 2). The resonance enhancement occurred at more negative back-gate voltages as the front-gate voltage was made more negative. This is expected as at resonance the two wells should possess equal values of carrier concentration. The figure also shows the effect of an in-plane magnetic field $B_{in}$ which was applied perpendicular to the source-drain current. The resonant enhancement is suppressed by $B_{in}$ as low as 1 T, because the in-plane field shifts two parabolic dispersion curves, originating from each well (see the inset of Fig. 3), and the wave functions at the Fermi level are forced to localize within each well even at the resonance condition. Systematic suppression of the resonance resistance similar to that in Fig. 2 was also observed in samples $A$ and $C$. Details of this phenomena are described elsewhere.[8] Therefore, the resistance at $B_{in}=1$ T can be regarded as the background resistance, i.e., an expected resistance when no resistance enhancement occurs. We define the size of the resistance resonance by $\Delta R/R$, where $R$ is the resistance without resonance enhancement at the resonance gate voltage, and $\Delta R$ is the increment of the resistance due to the wave-function hybridization.

Figure 3 compares the resistance resonance as a function of front-gate voltage in three samples at a back-gate voltage of $V_{bg}=+0.6$ V; the values of $\Delta R/R$ were 0.040, 0.22, and 0.071 for devices $A$, $B$, and $C$. The resistance enhancement increased from $A$ to $B$, as the mobility ratio was increased from 1.8 to 14. Note, however, that device $C$, which has the largest mobility ratio of 105, showed a smaller resonance enhancement than that of device $B$. This indicates that the mobility ratio is not the only factor limiting the size of the resistance resonance. It is also to be noted that the "peak," obtained by subtracting the resistance at $B_{in}=1$ T from that at $B_{in}=0$ T, is broadest for the device $C$; the full width at half maximum, $\Delta V_{fg}$, is 0.10, 0.073, and 0.15 V for devices $A$, $B$, and $C$, respectively.

If the scattering rate in the back 2DEG is so large that the level broadening due to the scattering, $\Gamma$, is larger than the coupling energy $\Delta_{SAS}$, it is expected that the symmetric and antisymmetric wave functions would not be well defined. This is because a characteristic time for the hybridization to occur is $\sim\hbar/\Delta_{SAS}$, and the lifetime

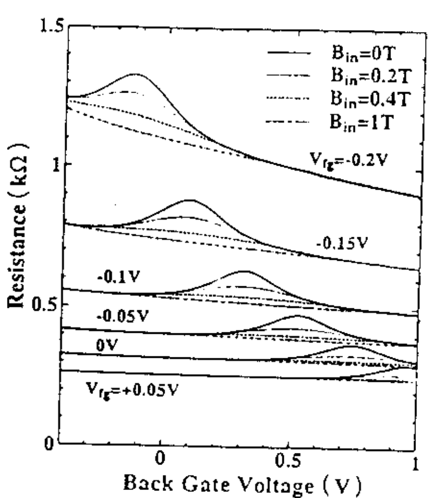


FIG. 2. Resistance as a function of the back-gate voltage at various front-gate voltages for device $B$, $T=4.2$ K. The mobility ratio is $\approx 14$. The resistance resonance is suppressed by an in-plane magnetic field perpendicular to the source-drain current.

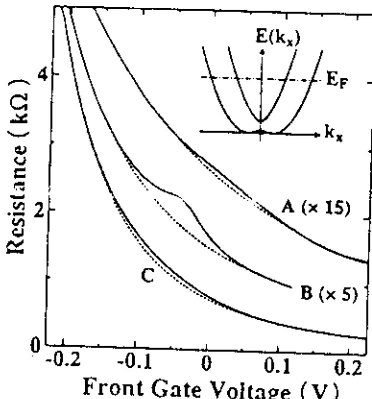


FIG. 3. Comparison of the resistance resonance among samples $A$, $B$, and $C$ at a back-gate voltage of $+0.6$ V, $T=4.2$ K. Solid curves, $B_{in}=0$ T; broken curves, $B_{in}=1$ T. The inset shows dispersion curves (energy vs wave vector) for the DQW in an in-plane magnetic field. Note that wave-function coupling occurs only near $k_x=0$, where two energy levels anticross.

of the state is $\sim\hbar/\Gamma$. If $\Delta_{SAS} < \Gamma$, the hybridization does not take place effectively and the size of the resonance resistance will be decreased. The mobility of the back 2DEG, $\mu_{back}$, was estimated by fully depleting the front 2DEG. For the gate bias condition shown in Fig. 3, the values of $\mu_{back}$ were $3.3\times10^5$, $2.6\times10^4$, and $1.3\times10^3$ for samples $A$, $B$, and $C$, respectively. Assuming for simplicity that the values of transport and quantum lifetimes are the same, $\mu_{back}=7.2\times10^3$ cm$^2$/V s corresponds to a level broadening of $\Gamma=1.2$ meV, which is the value of $\Delta_{SAS}$ of the present device structures. The back 2DEG mobility of device $C$ is smaller than this critical value, which indicates that the level broadening is another factor in determining the size of the resistance resonance.

In a conventional theory of the resonance resistance, in which the scattering rates in the wells are additive,[1] the size of the resistance enhancement is given by a single parameter, i.e., the mobility ratio $r$. The conventional approach fails when $\Delta_{SAS}\approx\Gamma$ as is discussed above. Vasko has developed a quantum transport theory for DQW structures with asymmetric scattering based on a $2\times2$ model Hamiltonian, which is valid even when $\Gamma>\Delta_{SAS}$.[9] He assumed a short-range impurity scattering potential, and thus the transport and quantum lifetimes are identical in this theory. Using the expression given by Vasko, the size of the resistance resonance can be written as

$$[\Delta R/R]/[(r-1)^2/4r]=t^2/(1+t^2)\ , \quad (1)$$

where $t=\Delta_{SAS}\tau/\hbar$, and $\tau^{-1}=(\tau_{front}^{-1}+\tau_{back}^{-1})/2$ is the average impurity scattering rate in the DQW. When the level broadening is small ($\hbar/2\tau \ll \Delta_{SAS}/2$), Eq. (1) reduces to an expression described in Ref. 1, namely, $\Delta R/R=(r-1)^2/4r$.

Figure 4 shows the normalized size of the resistance resonance, i.e., the left-hand side of Eq. (1), for the three samples as a function of the dimensionless parameter $t$, together with the theory by Vasko. Here, $\tau$ for the experimental data was estimated from the mobility, i.e., the transport lifetime. Several data points for each sample arise from the use of different back-gate voltages. The experimental error of the normalized resistance resonance is mainly from the estimate of $r$ ($\delta r/r\approx10\%$). As is seen in the figure when the level broadening is increased ($t$ is reduced) from sample $A$ to $C$, the normalized resistance resonance decreases rapidly, which is consistent with the theory. But the discrepancy in the magnitude between theory and experiment is quite large, an order of magnitude difference for samples $B$ and $C$.

It is to be noted, however, that the direct comparison between the theory and experiment is not possible, because Eq. (1) assumes that the transport and quantum lifetimes are the same. A theory of resonance resistance in which the difference in the lifetimes is incorporated is desired, since it is well known that the quantum lifetime $\tau_q$ is much smaller than transport time $\tau_{tr}$, especially in modulation-doped heterostructures.[10,11] For example, Coleridge, Stoner, and Fletcher[10] reported $\tau_{tr}/\tau_q=3.9$ for a modulation-doped heterostructure with the mobility of $\mu=5.3\times10^4$ cm$^2$/V s, and $\tau_{tr}/\tau_q=8.9$ for a sample with mobility $\mu=2.4\times10^5$ cm$^2$/V s. If we could use $\tau_q$ rather than $t_{tr}$ for the experimental data in Fig. 4, the value of $t$ will be reduced and the comparison will be more favorable. Unfortunately, we could not deduce quantum lifetimes from Shubnikov–de Haas (SdH) oscillation, since the same carrier concentration exists in each well and thus the SdH oscillation consists of contributions from the high- and low-mobility 2DEG's. When the double 2DEG's exist, the contribution from the intersubband scattering will also have to be considered, which will reduce the quantum lifetime compared to that in a single 2DEG.[12,13] Inhomogeneity of the samples may also be responsible for the discrepancy. For example, monolayer fluctuations at the interfaces lead to a fairly large fluctuation of $\Delta_{SAS}$ ($\sim22\%$), when the thickness of the $Al_xGa_{1-x}As$ barrier is 25 Å. This will act as an extra scattering of the hybridized states, and will also reduce the quantum lifetime. This effect will be the same for all the samples, since the DQW's were grown at the identical growth condition. Although quantitative agreement between theory and experiment is an open question, the qualitative agreement in Fig. 4 confirms that the level broadening diminishes the resonance resistance enhancement.

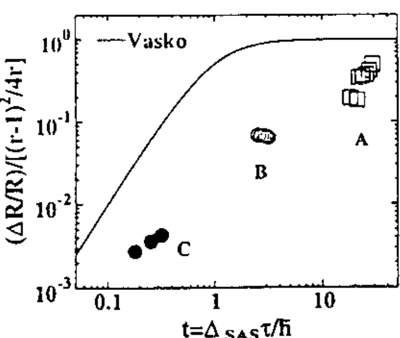


FIG. 4. Normalized size of the resistance resonance as a function of dimensionless lifetime $t=\Delta_{SAS}\tau/\hbar$ for samples $A$, $B$, and $C$ at $T=4.2$ K. The change in $t$ for each sample is caused by variation of the back-gate voltages. Transport lifetime was used for $\tau$ in experimental data. Solid curve was obtained from Vasko's theory (Ref. 9). $\Delta_{SAS}=1.2$ meV.

In conclusion, we have demonstrated that level broadening, as well as the mobility ratio, are key factors in understanding the phenomenon of resistance resonance.

Work at the Cavendish Laboratory was supported by the U.K. Science and Engineering Research Council. D.A.R. acknowledges the support of the Toshiba Cambridge Research Centre.

*Also at Toshiba Cambridge Research Centre, 260 Cambridge Science Park, Milton Road, Cambridge CB4 4WE, United Kingdom.

[1]A. Palevski, F. Beltram, F. Capasso, L. Pfeiffer, and K. W. West, Phys. Rev. Lett. 65, 1929 (1990).
[2]H. Sakaki, Jpn. J. Appl. Phys. 21, L381 (1982).
[3]Y. Ohno, M. Tsuchiya, and H. Sakaki, Appl. Phys. Lett. 62, 1952 (1993).
[4]K. Hirakawa, H. Sakaki, and J. Yoshino, Phys. Rev. Lett. 54, 1279 (1985).
[5]A. Kurobe, J. E. F. Frost, M. P. Grimshaw, D. A. Ritchie, G. A. C. Jones, and M. Pepper, Appl. Phys. Lett. 60, 3268 (1993).
[6]E. H. Linfield, G. A. C. Jones, D. A. Ritchie, and J. H. Thompson, Semicond. Sci. Technol. 8, 415 (1993).
[7]G. S. Boebinger, A. Passner, L. N. Pfeiffer, and K. W. West, Phys. Rev. B 43, 12 673 (1991).
[8]A. Kurobe, I. M. Castleton, E. H. Linfield, M. P. Grimshaw, K. M. Brown, D. A. Ritchie, M. Pepper, and G. A. C. Jones, Phys. Rev. B 50, 4889 (1994).
[9]F. T. Vasko, Phys. Rev. B 47, 2410 (1993).
[10]P. T. Coleridge, R. Stoner, and R. Fletcher, Phys. Rev. B 39, 1120 (1989).
[11]S. Das Sarma and F. Stern, Phys. Rev. B 32, 8442 (1985).
[12]D. R. Leadley, R. J. Nicholas, J. J. Harris, and C. T. Foxon, Semicond. Sci. Technol. 5, 1081 (1990).
[13]P. T. Coleridge, Semicond. Sci. Technol. 5, 961 (1990).

PHYSICAL REVIEW B VOLUME 50, NUMBER 7 15 AUGUST 1994-I

# Wave functions and Fermi surfaces of strongly coupled two-dimensional electron gases investigated by in-plane magnetoresistance

A. Kurobe
*Toshiba Cambridge Research Centre, 260 Cambridge Science Park, Milton Road, Cambridge CB4 4WE, United Kingdom*

I. M. Castleton, E. H. Linfield, M. P. Grimshaw, K. M. Brown, and D. A. Ritchie
*Cavendish Laboratory, Madingley Road, Cambridge CB3 0HE, United Kingdom*

M. Pepper
*Toshiba Cambridge Research Centre, 260 Cambridge Science Park, Milton Road, Cambridge CB4 4WE, United Kingdom and Cavendish Laboratory, Madingley Road, Cambridge CB3 0HE, United Kingdom*

G. A. C. Jones
*Cavendish Laboratory, Madingley Road, Cambridge CB3 0HE, United Kingdom*
(Received 11 April 1994)

We have studied the in-plane magnetoresistance of coupled double-quantum-well structures, in which each well has a different mobility and where the values of carrier concentration can be varied independently. Resistance resonances, observed at zero magnetic field, were suppressed with an in-plane magnetic field of 1 T, provided the field was perpendicular to the current. The magnetoresistance showed structure which changed systematically with front-gate and back-gate voltages, and was due to the deformation of both wave functions and Fermi surfaces in the in-plane magnetic field.

In recent years there has been much interest in closely separated double two-dimensional electron-gas (2DEG) systems with several effects being observed, such as resonant tunneling between parallel 2DEG's,[1,2] which has been measured in devices where each 2DEG was independently contacted.[3] The Coulomb barrier to tunneling in a high transverse magnetic field has also been reported.[4] If the coupling between the two electron gases becomes large enough, the system at resonance can be described by symmetric and antisymmetric states, which are responsible for lateral transport. When the two 2DEG's possess different values of mobility, an increase in resistance at resonance is then observed.[5,6] This is because a higher mobility 2DEG, which is localized in one of the two wells, extends into both 2DEG's by hybridization at resonance, and thus suffers increased scattering. The symmetric-antisymmetric gap, however, can be destroyed in a strong transverse magnetic field by electron correlation.[7–10]

The requirements of conservation of energy and transverse momentum mean that tunneling between parallel 2DEG's is possible only when the dispersion curves for the two 2DEG's overlap, i.e., only at resonance in the absence of a magnetic field. However, application of an in-plane magnetic field $B_{in}$ shifts the transverse momentum by an amount proportional to $B_{in}$, and tunneling is only allowed at points where two Fermi circles intersect each other.[11–13] The distortion of the Fermi surfaces in coupled 2DEG's due to in-plane magnetic fields has been measured from Shubnikov–de Haas oscillations,[14] but the in-plane magnetoresistance was not discussed. In this Brief Report we present electron transport results in strongly coupled 2DEG structures in an in-plane magnetic field. The measured lateral transport is due to symmetric and antisymmetric states, which is in sharp contrast to the tunnel resistance measurements reported in Ref. 11. We show that the resonance resistance is suppressed by an in-plane magnetic field of about 1 T, and the degree of the suppression depends on the direction of the in-plane field relative to the current. We also found structure at a high magnetic field, which moved with front- and back-gate voltages. These effects are discussed as being associated with the deformation of wave functions and the Fermi surfaces in the in-plane magnetic field.

The sample employed here is a modulation-doped double-quantum-well (DQW) structure grown on a semi-insulating GaAs substrate by molecular-beam epitaxy (MBE). The DQW consists of two 150-Å-wide quantum wells separated by a 25-Å $Al_{0.33}Ga_{0.67}As$ barrier. Electrons in the 2DEG's were supplied by Si-doped $Al_{0.33}Ga_{0.67}As$ layers (200 Å wide, $1\times10^{18}$ cm$^{-3}$) placed above and below the DQW structure; for the lower layer a 400-Å $Al_{0.33}Ga_{0.67}As$ spacer separated the doped $Al_{0.33}Ga_{0.67}As$ from the DQW, while for the top layer a 200-Å spacer was used. The whole of the DQW structure was isolated by a 0.31-$\mu$m $Al_{0.33}Ga_{0.67}As$ barrier from an $n^+$ GaAs back-gate layer grown underneath. The growth temperature $T_g$ was 630° except at the back $n^+$ $Al_{0.33}Ga_{0.67}As$ layer, where $T_g$ was lowered to 520 °C. Ohmic contacts to the double 2DEG's were, however, required without contacting to the $n^+$ GaAs back-gate layer, and this was achieved using MBE regrowth on an *in situ* focused ion beam patterned epilayer.[15] After growth, devices were processed with a Hall bar geometry with a front Schottky gate as well as a back gate. The mobility of the front 2DEG at $T=1.5$ K was $2.0\times10^5$ cm$^2$/V s at

0163-1829/94/50(7)/4889(4)/$06.00 50 4889 ©1994 The American Physical Society

the carrier concentration of $1.2\times10^{11}$ cm$^{-2}$, while that of the back 2DEG was $1.1\times10^{5}$ cm$^2$/V s at the same carrier concentration; this was obtained by fully depleting one of the 2DEG's. The somewhat lower mobility in the back 2DEG was due to diffusion of dopant from the doped $Al_{0.33}Ga_{0.67}As$ layer into the back $Al_{0.33}Ga_{0.67}As$ spacer during growth.

The resistance as a function of front-gate voltage ($V_{fg}$) at various back-gate voltages ($V_{bg}$) is shown by solid curves in Fig. 1. Arrows indicate the position of the resonance, which was determined from the beating of the Shubnikov–de Haas (SdH) oscillations at $T=1.5$ K.[14] The symmetric-antisymmetric energy gap of $\Delta_{SAS}=1.2\pm0.1$ meV, which is in agreement with a theoretical value of 1.3 meV, was also obtained from SdH oscillations. A resonant increase in resistance, i.e., resistance resonance, can be seen in Fig. 1(a) at the right-hand side of the actual resonance voltage, because the resistance peak is distorted due to the change of the front 2DEG mobility with the front-gate voltage. A mobility ratio estimated from the size of the resistance resonance[5] was 2, which is comparable to 1.8, the value derived from the mobility measurements.

We applied a magnetic field parallel (to within 0.2°) to the 2DEG's. When the in-plane magnetic field $B_{in}$ was applied perpendicular to the source-drain current $j$, the resistance resonance was suppressed at a magnetic field as low as 1 T [broken curves in Fig. 1(a)]. We also observed anisotropy in the effect of an in-plane field [Fig. 1(b)], as an in-plane magnetic field parallel to the current also diminished the peak, not by the suppression of the resistance resonance but by enhancement of the resistance away from the resonance.

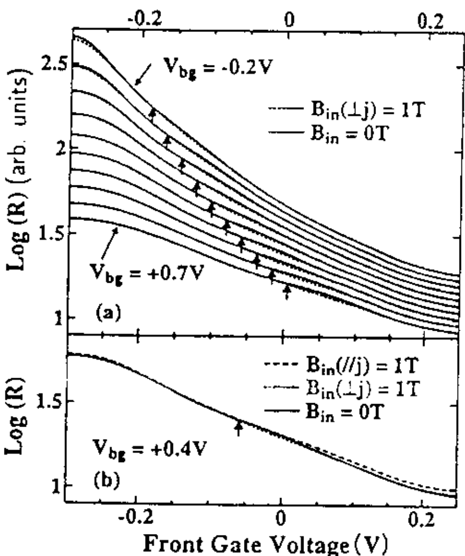


FIG. 1. Resistance resonance as a function of front-gate voltage with and without an in-plane magnetic field at $T=4.2$ K. Arrows indicate resonance front-gate voltage. (a) $B_{in}\perp j$. Back-gate voltage $V_{bg}$ was changed from $-0.2$ to $+0.7$ V with a step of 0.1 V. Curves are shifted for clarity. The systematic change in the front-gate voltage required for resonance as a function of back-gate voltage confirms that the carrier concentration in each well is well controlled by the gates. (b) Anisotropy of the in-plane magnetoresistance. $V_{bg}=+0.4$ V.

The suppression of the resistance resonance by an in-plane magnetic field was observed more clearly in a different sample, in which the mobility ratio was increased to $\approx 14$, the mobility of the back 2DEG being $\approx 2\times10^4$ cm$^2$/V s. For this device the back $n^+$ $Al_{0.33}Ga_{0.67}As$ layer was grown at a higher temperature of 580 °C to enhance diffusion of the dopant. The resistance as a function of the back-gate voltage, in this case, is plotted in Fig. 2 for $V_{fg}=-0.15$ V at various in-plane magnetic fields. When the in-plane magnetic field was applied perpendicular to the current, the resistance resonance was fully suppressed at the field of 1 T. On the other hand, the suppression was not complete if the field was parallel to the current.

These experimental results can be understood from the shape of the wave function in an in-plane magnetic field. Let us consider a DQW Hamiltonian in a magnetic field $\mathbf{B}=(0,B_{in},0)$ in the $xy$ plane.[14,16,17] Taking a Landau gauge, $\mathbf{A}=(zB_{in},0,0)$, the Hamiltonian reads

$$H=\frac{\hbar^2}{2m}\left[k_x+\frac{eB_{in}z}{\hbar}\right]^2+\frac{\hbar^2k_y^2}{2m}-\frac{\hbar^2}{2m}\frac{\partial^2}{\partial z^2}+V(z)\ , \quad (1)$$

where $V(z)$ is the DQW confining potential, and $k_x$ and $k_y$ are wave vectors in the $x$ and $y$ directions, respectively. At $B_{in}=0$ an interwell coupling lifts degeneracy at resonance, and symmetric $|\varphi_S\rangle$ and antisymmetric states $|\varphi_{AS}\rangle$ are formed. Those low mobility delocalized states show parabolic $k_x$ dispersions (each minimum at $k_x=0$), and the shape of the wave functions in the $z$ direction is independent of $k_x$. Once $B_{in}$ is finite, however, the first term in Eq. (1) shifts the parabolic $k_x$ dispersions for states localized in each well by an amount $\Delta k_x=\pm ez_{SAS}B_{in}/\hbar$, where $z_{SAS}=\langle\varphi_{AS}|z|\varphi_S\rangle$. This is illustrated in the right inset of Fig. 2 for $k_y=0$. The interwell coupling, in this case, hybridizes localized QW or-

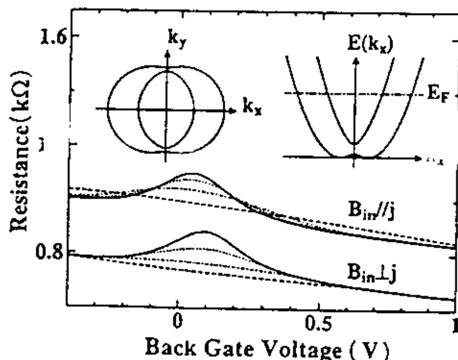


FIG. 2. Suppression of resistance resonance by in-plane magnetic fields for a device with a mobility ratio $\approx 14$. $T=4.2$ K. Data for $B_{in}\parallel j$ are shifted for clarity. $B_{in}=0$ T (solid curves), 0.2 T (dotted curves), 0.4 T (broken dotted curves), and 1 T (broken curves). Insets show dispersion curves (right) and Fermi surfaces (left) for a coupled DQW structure in an in-plane magnetic field.

bits only near $k_x=0$, where the two shifted parabolic dispersions cross each other. Therefore, if $B_{in}$ is large enough, the wave functions at the Fermi level are decoupled and localized by the in-plane magnetic field. This can lead to the suppression of the resistance resonance.

The anisotropy of the in-plane magnetoresistance is explained by the hybridization of wave functions on the Fermi surfaces. As is shown in the left inset of Fig. 2, the Fermi surfaces arise from two shifted Fermi circles originating from quantum wells. But they are distorted where the two circles overlap each other, and the interwell coupling hybridizes wave functions to form delocalized states. When the current is driven perpendicularly to the magnetic field, i.e., in the $x$ direction, contributions to the conductivity come mainly from the Fermi surfaces near the $k_x$ axis.[18] Since these states are easily decoupled and localized by the in-plane magnetic field, the resistance resonance is suppressed. On the other hand, if the current is applied along the $y$ axis, i.e., parallel to the magnetic field, the contribution from those near the $k_y$ axis will be larger. This leads to less suppression of the resistance resonance, since states in those regions of the Fermi surfaces are hybridized even in the presence of an in-plane magnetic field.

Further experimental investigations were made for the device with a lower mobility ratio, because both of the 2DEG's showed large mobility, and the carrier concentration in each well was determined from the SdH oscillation. Figure 3 shows the negative magnetoresistance ($B_{in}\perp j$) due to the suppression of the resistance resonance at $V_{bg}=0$ V when the front-gate voltage was adjusted to resonance (solid curve) and was away from the resonance (broken curve). We defined a decay magnetic field $B_{decay}$, at which the in-plane magnetoresistance at resonance condition falls off by half, and measured $B_{decay}$ at various back-gate voltages, i.e., different carrier concentrations. $B_{decay}$ was found to decrease almost linearly with the Fermi wave vector $k_F$ (inset of Fig. 3). Here $k_F(=\sqrt{2\pi n_s})$ was calculated using the carrier concentration $n_s$ in each well at resonance. As a lower Fermi level implies a smaller wave vector (see the right inset of Fig. 2), the hybridization is stronger and the suppression of the resistance resonance occurs at a larger magnetic field. It is further noted that the hybridization away from the resonance is not maximized at $B_{in}=0$ T, resulting in an increase in hybridization by an in-plane magnetic field at one side of the Fermi surfaces (see top left inset of Fig. 4). This explains why the decay magnetic field is minimized at the resonance.

The in-plane magnetoresistance measurements were extended to higher fields to probe the distortion of the Fermi surfaces. Figure 4 shows the results at $V_{bg}=+0.4$ V for a range of front-gate voltages. The carrier concentration in the back well was $3.02\times10^{11}$ cm$^{-2}$, the resonance front-gate voltage was $-0.06$ V, and the in-plane magnetic field was parallel to the current. A steplike increase in the resistance was observed below 2 T, the field at which this occurred increased as the front-gate voltage moved away from the resonance. Increasing the field resulted in a dip followed by an increase. The location of the dip decreased in magnetic field as the front-gate voltage was made more negative. Similar behavior was also observed when $B_{in}$ was perpendicular to the current.

An in-plane magnetic field $B_0$, at which one of the Fermi circles is inscribed by the other, was calculated from the carrier densities in the front and back wells, and is shown in Fig. 4 for each front-gate voltage. The position of $B_0$ coincides with that of the steplike increase of the resistance at a lower magnetic field, and suggests that it is due to increased hybridization at one side of the Fermi surfaces ("in-plane magnetic-field-induced resistance resonance").

In order to understand the dip in Fig. 4, we calculated the shape of the Fermi surfaces as a function of $B_{in}$. We first solved Schrödinger and Poisson equations self-consistently to reproduce observed carrier concentrations, and obtained wave functions numerically at $B_{in}=0$ T. Using these as basis functions, the Hamiltonian (1)

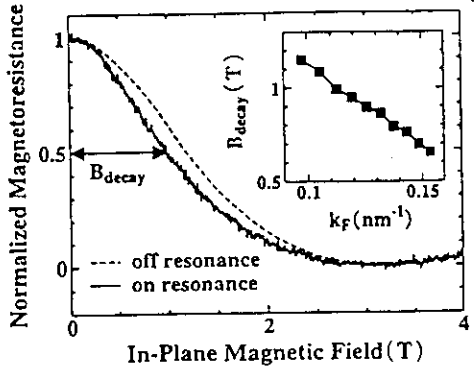


FIG. 3. Negative in-plane magnetoresistance ($B_{in}\perp j$) at and away from the resonance front-gate voltage. $V_{bg}=0$ V, $T=4.2$ K. Solid curve: $V_{fg}=-0.12$ V. Broken curve: $V_{fg}=-0.04$ V. Definition of $B_{decay}$ is also shown. Inset shows $B_{decay}$ as a function of the Fermi wave vector.

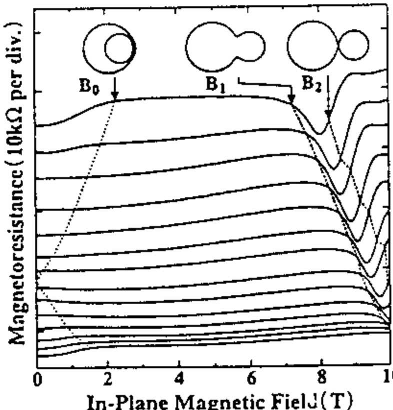


FIG. 4. In-plane magnetoresistance ($B_{in}\parallel j$) at various front-gate voltages. $V_{bg}=+0.4$ V, $T=4.2$ K. $V_{fg}$ was changed from $-0.225$ V (top curve) to $+0.1$ V (bottom curve) with a step of 25 mV. Curves are shifted for clarity. Broken lines connect calculated in-plane fields $B_0$, $B_1$, and $B_2$ at each front-gate voltage, corresponding Fermi surfaces being illustrated in insets.

was diagonalized, and magnetic fields $B_1$ and $B_2$ in Fig. 4 were obtained at each front-gate voltage. If the in-plane field is large enough, the two Fermi circles separate from each other at $B_2$. Before this, however, at a magnetic field $B_1$, the upper dispersion branch in Fig. 2 is depopulated, i.e., the inner Fermi surface in Fig. 2 disappears. As is shown in Fig. 4, the resistance dip always resides between $B_1$ and $B_2$, i.e., the resistance decreases when the Fermi level lies between the gap created by the interwell coupling. This strongly suggests that the origin of the dip is the suppression of the intersubband scattering between the lower and upper dispersion branches. Unlike the case of multisubbands in a single channel,[19,20] the resistance increases again, because two enclosed Fermi surfaces are restored due to the double-well shape of the lower dispersion branch.

In conclusion, we have demonstrated that the in-plane magnetoresistance characterizes wave-function coupling and Fermi-surface distortion in strongly coupled 2DEG systems.

Work at the Cavendish Laboratory was supported by the U.K. Science and Engineering Research Council. D.A.R. acknowledges the support of the Toshiba Cambridge Research Centre.

[1]J. P. Eisenstein, L. N. Pfeiffer, and K. W. West, Appl. Phys. Lett. 58, 1497 (1991).

[2]W. Demmerle, J. Smoliner, G. Berthold, E. Gornik, G. Weimann, and W. Schlapp, Phys. Rev. B 44, 3090 (1991).

[3]J. P. Eisenstein, L. N. Pfeiffer, and K. W. West, Appl. Phys. Lett. 57, 2324 (1990).

[4]J. P. Eisenstein, L. N. Pfeiffer, and K. W. West, Phys. Rev. Lett. 69, 3804 (1992).

[5]A. Palevski, F. Beltram, F. Capasso, L. Pfeiffer, and K. W. West, Phys. Rev. Lett. 65, 1929 (1990).

[6]Y. Ohno, M. Tsuchiya, and H. Sakaki, Appl. Phys. Lett. 62, 1952 (1993).

[7]G. S. Boebinger, H. W. Jiang, L. N. Pfeiffer, and K. W. West, Phys. Rev. Lett. 64, 1793 (1990).

[8]Y. W. Suen, J. Jo, M. B. Santos, L. W. Engel, S. W. Hwang, and M. Shayegan, Phys. Rev. B 44, 5947 (1991).

[9]G. S. Boebinger, L. N. Pfeiffer, and K. W. West, Phys. Rev. B 45, 11 391 (1992).

[10]A. H. MacDonald, P. M. Platzman, and G. S. Boebinger, Phys. Rev. Lett. 65, 775 (1990).

[11]J. P. Eisenstein, T. J. Gramila, L. N. Pfeiffer, and K. W. West, Phys. Rev. B 44, 6511 (1991).

[12]J. A. Simmons, S. K. Lyo, J. F. Klem, M. E. Sherwin, and J. R. Wendth, Phys. Rev. B 47, 15 741 (1993).

[13]L. Zheng and A. H. MacDonald, Phys. Rev. B 47, 10 619 (1993).

[14]G. S. Boebinger, A. Passner, L. N. Pfeiffer, and K. W. West, Phys. Rev. B 43, 12 673 (1991).

[15]E. H. Linfield, G. A. C. Jones, D. A. Ritchie, and J. H. Thompson, Semicond. Sci. Technol. 8, 415 (1993).

[16]J. M. Heisz and E. Zarembra, Semicond. Sci. Technol. 8, 575 (1993).

[17]T. Jungwirth and L. Smrcka, J. Phys. Condens. Matter 5, L217 (1993).

[18]Note that if a wave vector $\mathbf{k}$ is on the Fermi surface, the velocity of an electron $v(\mathbf{k})=\hbar^{-1}(\partial E/\partial \mathbf{k})$ is normal to the Fermi surface. Since the $x$ component of the velocity contributes to the conduction in the $x$ direction, the conductivity can be evaluated mainly from the Fermi surface near the $k_x$ axis in the left inset of Fig. 2.

[19]T. Englert, J. C. Maan, D. C. Tsui, and A. C. Gossard, Solid State Commun. 45, 989 (1983).

[20]S. Mori and T. Ando, J. Phys. Soc. Jpn. 48, 865 (1980).

Semicond. Sci. Technol. 9 (1994) 1744–1747. Printed in the UK

LETTER TO THE EDITOR

# Transport properties of a wide-quantum-well velocity modulation transistor structure

**A Kurobe†, I M Castleton‡, E H Linfield‡, M P Grimshaw‡, K M Brown‡, D A Ritchie‡, G A C Jones‡ and M Pepper†‡**

† Toshiba Cambridge Research Centre, 260 Cambridge Science Park, Milton Road, Cambridge CB4 4WE, UK
‡ Cavendish Laboratory, Madingley Road, Cambridge CB3 0HE, UK

Received 26 May 1994, accepted for publication 7 July 1994

**Abstract.** Results are presented on electron transport in a wide-quantum-well dual-channel velocity modulation transistor, where both front and back gates modulate the resistance through variation of the mobility, whilst maintaining a constant carrier concentration. A mobility modulation ratio of over 100 is achieved at a carrier concentration of $2 \times 10^{11}$ cm$^{-2}$ by transferring electrons between the two conducting channels which are 100 nm apart. Mobility modulation due to deformation of the wavefunctions is also observed when one of the channels is fully depleted.

Progress in thin layer growth technologies such as molecular beam epitaxy (MBE) has resulted in a wide variety of heterostructures and devices based on a two-dimensional electron gas (2DEG) being proposed and investigated [1]. One example is the velocity modulation transistor (VMT), suggested by Sakaki as the basis for a new family of field effect transistors [2]. In the VMT, the conductance is modulated not by change in the carrier density but by the change in the mobility. The mobility modulation can be achieved in various ways, i.e. the deformation of wavefunction in a single 2DEG channels [3, 4], the transfer of electrons between high- and low-mobility channels [5], and the enhancement of resonance resistance in coupled double quantum well structures [6]. In order to keep the carrier concentration constant, however, a back gate as well as a front gate must be fabricated. VMT operation has been achieved in single-conducting-channel devices [3, 4], but only partially demonstrated in wide-quantum-well dual-channel structures, as originally proposed [5]. A particular difficulty in this case is fabricating reliable 2DEG ohmic contacts with only a small leakage current to the back gate over a large working voltage range.

In this letter we present results for wide-quantum-well VMT structures fabricated using MBE regrowth on an *in situ* ion-beam-patterned epilayer. This technique considerably reduces leakage current and enables application of a large back-gate voltage. A mobility modulation ratio of over 100 is demonstrated by transferring electrons from front to back interfaces. We have also observed a further mobility modulation due to wavefunction deformation when one of the 2DEGs is fully depleted.

The structure consisted of a 100 nm wide quantum well (figure 1), which can accommodate electrons at the front (normal) and back (inverted) heterointerfaces. The electrons at the front interface were obtained by modulation doping and had a high mobility, whilst the electrons at the back interface were achieved by $\delta$-doping and had a low mobility. The wavefunction at the back interface was further disrupted by an AlGaAs spike (2 nm thick) inserted 8 nm away from the back interface [7]. The whole structure was isolated from an $n^+$-GaAs back-gate layer by an undoped AlGaAs back barrier layer (0.1 $\mu$m). Ohmic contacts to the 2DEGs, which do not make electrical contact to the back-gate layer, were then achieved using the technique of MBE regrowth on an *in situ* ion-beam-patterned epilayer [8].

Figure 2 shows the Hall carrier concentration ($n_H$), evaluated at $B = 0.4$ T, as a function of front-gate voltage ($V_{fg}$) for various back-gate voltages ranging from $-1.2$ V to $+0.7$ V. The measurements were performed at $T = 4.2$ K using a standard lock-in technique. The leakage current between the back gate and the 2DEGs throughout was less than 1 nA, over the whole range of data presented. When $V_{fg}$ was made too negative, the ohmic contacts failed, and the data in this voltage range are not shown in the figure. There are two important aspects of figure 2 in the region where the two 2DEGs coexist:

0268-1242/94/091744+04$19.50 © 1994 IOP Publishing Ltd

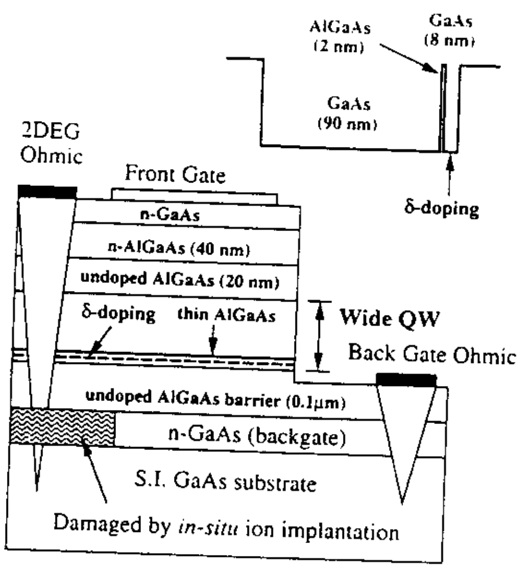


**Figure 1.** Schematic cross section of a wide-quantum-well dual-channel VMT structure. The doping levels of the $n^+$-AlGaAs layer and δ-doped layer were $1 \times 10^{18}$ cm$^{-3}$ and $2.5 \times 10^{11}$ cm$^{-2}$ respectively. MBE regrowth on an *in situ* ion-beam-patterned epilayer was used to form ohmic contacts to the 2DEGs without contacting the $n^+$-GaAs back-gate layer. The inset shows the structure of the wide quantum well.

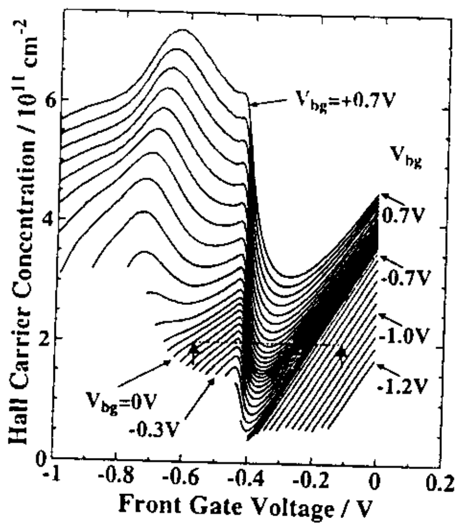


**Figure 2.** Hall carrier concentration ($n_H$) as a function of front-gate voltage at various back-gate voltages. $T = 4.2$ K. The front 2DEG is fully depleted at $V_{fg} = -0.44$ V, whilst the back 2DEG is fully depleted at $V_{bg} = -0.65$ V. Two vertical arrows show an example of VMT operation.

(i) The measured $n_H$ represents the true carrier concentration only when a single 2DEG is present. It can be shown from a classical transport theory for double 2DEG systems [9] that the measured $n_H$ is written as

$$n_H = (n_f\mu_f + n_b\mu_b)^2/(n_f\mu_f^2 + n_b\mu_b^2) \qquad (1)$$

in the low-field limit where $\mu_f B \ll 1$ and $\mu_b B \ll 1$. Here $n_{f(b)}$ and $\mu_{f(b)}$ are the carrier concentration and mobility of the front (back) 2DEG, respectively. It is noted that, when both 2DEGs are present, $n_H \approx n_f$ if $\mu_f \gg \mu_b$.

(ii) The front gate depopulates only the front 2DEG when both of the 2DEGs are present, and then the back 2DEG if the front 2DEG is fully depeleted (sequential depopulation). This is because the system is similar to a capacitor in which two parallel charge sheets are present.

In figure 2, the front 2DEG is totally pinched-off at $V_{fp} = -0.44$ V. When the back-gate voltage is large ($V_{bg} > -0.65$ V), the curves are 'N'-shaped, showing a minimum near $V_{fg} = -0.4$ V. This is easily understood from equation (1): the measured $n_H$ is dominated by the high-mobility front carrier concentration when both of the 2DEGs are present ($V_{fg} > -0.44$ V), and $n_H$ represents the carrier density of the low-mobility back 2DEG only when the front 2DEG is fully depleted ($V_{fg} < -0.44$ V). The slope, $\Delta n_H/\Delta V_{fg}$, at $V_{bg} = -0.65$ V ($V_{fg} > -0.44$ V) was $8.6 \times 10^{11}$ cm$^{-2}$ V$^{-1}$, and an insulator thickness of $\approx 77$ nm is calculated assuming a simple capacitance argument. This is consistent with the distance of 70 nm between the front heterointerface and the front gate. When the front 2DEG is absent ($V_{fg} < -0.44$ V), $n_H$ for $V_{bg} \leqslant 0$ V decreases linearly with $V_{fg}$, i.e. the back 2DEG is depleted by the front gate. Here, the slope, $\Delta n_H/\Delta V_{fg}$, is $4.1 \times 10^{11}$ cm$^{-2}$ V$^{-1}$ at $V_{bg} = 0$ V, an estimated insulator thickness being $\approx 0.16$ μm. This value is consistent with the structural distance between the front gate and the back heterointerface (0.17 μm), confirming that the measured $n_H$ represents the carrier concentration of the back 2DEG in this gate voltage range ($V_{fg} < -0.44$ V and $V_{bg} < 0$ V).

The curves in figure 2 for $V_{fg} < -0.44$ V are also 'N'-shaped, when the back-gate voltage is made more positive ($V_{bg} > 0$ V), showing a peak near $V_{fg} = -0.65$ V. This is due to the population of the higher subband, as was simulated in self-consistent calculations [10]. The calculations indicate that the higher subband state extends throughout the wide quantum well and will be of lower mobility than the front 2DEG because of its significant wavefunction amplitude near the δ-doped layer. In this case the measured $n_H$ is a function of the carrier densities and mobilities of both of the subbands. Equation (1) suggests that the depopulation of the higher subband by the front gate will lead to the 'N'-shaped curve, if the mobility of the higher subband is larger than that of the ground subband (back 2DEG).

When the back-gate voltage is made sufficiently negative, the back 2DEG can be completely depleted. This is seen in figure 2, for $V_{bg} < -0.65$ V, since there is a linear change of $n_H$ with the front-gate voltage. The pinch-off voltage for the front 2DEG becomes more positive as the back-gate voltage is made more negative. This is a substrate bias effect by the back-gate voltage in the front 2DEG, and is seen more clearly in the Shubnikov–de Haas (SdH) oscillations shown in figure 3, where $V_{bg}$ was changed from $-0.1$ V to $-1.1$ V at a fixed $V_{fg}$ of $-0.1$ V. Here the SdH oscillation arises mainly from the front 2DEG, since the

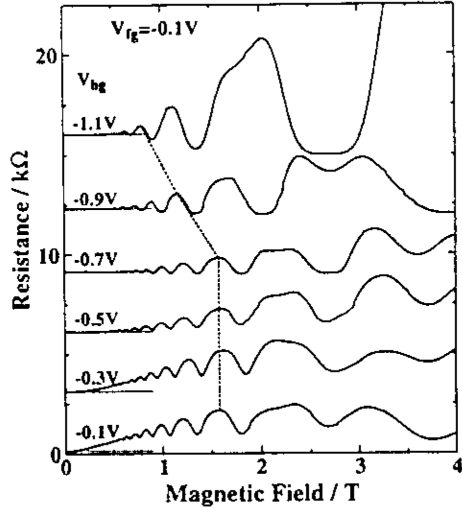


**Figure 3.** Shubnikov–de Haas oscillations at $V_{fg} = -0.1$ V at various back-gate voltages. $T = 1.2$ K. The broken line is a guide to the eye, showing peaks of the same Landau index. The dotted lines are zeros in magnetoresistance, illustrating parallel conduction for $V_{bg} \geqslant -0.5$ V. The curves are offset for clarity.

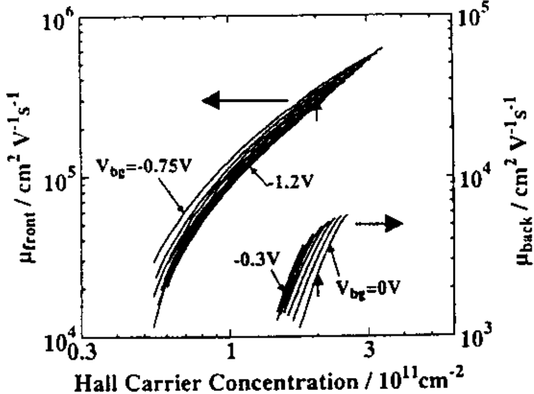


**Figure 4.** Mobilities of front and back 2DEGs as a function of carrier concentration. $T = 4.2$ K. The carrier concentration was changed by the front-gate voltage, whilst maintaining a single 2DEG. Data are taken for the gate voltage ranges of $V_{bg} \leqslant -0.75$ V for the front 2DEG, and of $V_{fg} < -0.44$ V and $V_{bg} < 0$ V for the back 2DEG. Vertical arrows correspond to the example of VMT operation shown in figure 2.

mobility of the back electrons is quite low. When $V_{bg} \geqslant -0.7$ V, the oscillation period stays the same with only small modification due to the back 2DEG. In this case both 2DEGs are present and the back gate cannot affect the front electrons. Also note that a positive magnetoresistance at low fields becomes more noticeable when $V_{bg}$ is made more positive and there is an increase in the number of back electrons. On the other hand, once the back 2DEG is removed ($V_{bg} < -0.65$ V), the back gate can be used to deplete carriers in the front channel, and the SdH period changes accordingly.

Mobilities of the front and back 2DEGs were determined by fully depleting the back or front electrons respectively, i.e. in the gate voltage range where only a single 2DEG is present. Figure 4 shows the results at various back-gate voltages with the carrier concentration being changed by the front-gate voltage. The mobility of the back 2DEG was two orders of magnitude smaller than that of the front 2DEG. It is interesting to note that the mobility of each 2DEG changes at different values of $V_{bg}$. For example, at a carrier concentration of $2 \times 10^{11}$ cm$^{-2}$ the mobility of the front 2DEG at $V_{bg} = -0.75$ V decreased by 9% as $V_{bg}$ decreased by 0.1 V, and that of the back 2DEG at $V_{bg} = 0$ V increased by 51% as $V_{bg}$ decreased by the same amount.

We reported previously a similar mobility modulation for a front 2DEG in an identical wide-quantum-well structure [4, 11], where the back 2DEG was depleted by the acceptor charge in a thick (0.5 $\mu$m) p$^-$-type AlGaAs back barrier rather than the back-gate voltage. The mobility modulation for the single 2DEG was ascribed to the squeezing of the wavefunction by the back gate. This also explains the mobility modulation shown in figure 4: for front electrons, the mobility decreased as the back-gate voltage was made more negative, since the wavefunction was pushed towards the front interface, and the scattering due to ionized impurities in the n$^+$-AlGaAs layer, or residual impurities in the AlGaAs spacer layer, increased. On the other hand, the mobility of the back 2DEG increased as $V_{bg}$ was made more negative, since the wavefunction of back electrons moved away from the back interface, and the scattering due to the $\delta$-doped layer was reduced. The strong carrier concentration dependence of the mobility of the back 2DEG could be due to localization effects [12]. We note that the mobility modulation of each 2DEG by the back-gate voltage confirms VMT operation for a single channel.

Dual-channel VMT operation, where the mobility is modulated due to the transfer of electrons between front and back channels, is also possible in the present device. The vertical arrows in figure 2 provide an example. By changing gate voltages from ($V_{fg}$, $V_{bg}$) = (−0.11 V, −0.9 V) to (−0.57 V, 0 V), electrons are transferred from the high-mobility front channel to the low-mobility back channel without changing the carrier concentration of $2 \times 10^{11}$ cm$^{-2}$. The corresponding mobility change is shown in figure 4, from which it can be ascertained that the mobility ratio of 125 was achieved.

In conclusion, we have demonstrated VMT operation in a wide-quantum-well double-channel structure for the first time. A conductance modulation ratio of more than 100 has been achieved by transferring electrons between two conducting channels which are 100 nm apart. The mobility modulation for a single channel has also been observed by the deformation of the shape of the wavefunction.

We acknowledge useful discussions with J E F Frost. Work at the Cavendish Laboratory was supported by the UK Science and Engineering Resarch Council. DAR acknowledges the support of the Toshiba Cambridge Research Centre.

## References

[1] Weisbuch C and Vinter B 1991 *Quantum Semiconductor Structures* (London: Academic)
[2] Sakaki H 1982 *Japan. J. Appl. Phys.* **21** L381
[3] Hirakawa K, Sakaki H and Yoshino J 1985 *Phys. Rev. Lett.* **54** 1279
[4] Kurobe A, Frost J E F, Grimshaw M P, Ritchie D A, Jones G A C and Pepper M 1993 *Appl. Phys. Lett.* **60** 3268
[5] Kurobe A, Frost J E F, Ritchie D A, Jones G A C and Pepper M 1992 *Appl. Phys. Lett.* **60** 3268
[6] Ohno Y, Tsuchiya M and Sakaki H 1993 *Appl. Phys. Lett.* **62** 1952
[7] Owen P M and Pepper M 1993 *Semicond. Sci. Technol.* **8** 123
[8] Linfield E H, Jones G A C, Ritchie D A and Thompson J H 1993 *Semicond. Sci. Technol.* **8** 415
[9] Reed M A, Kirk W P and Kobiela P S 1986 *IEEE J. Quantum Electron.* **22** 1753
[10] Owen P and Pepper M 1993 *Appl. Phys. Lett.* **62** 1274
[11] Kurobe A 1993 *Semicond. Sci. Technol.* **8** 742
[12] Foxon C T, Harris J J, Wheeler R G and Lacklison D E 1986 *J. Vac. Sci. Technol.* B **4** 511

# Large transconductances observed in an independently contacted coupled double quantum well

N. K. Patel
*Toshiba Cambridge Research Centre, 260 Cambridge Science Park, Milton Road, Cambridge CB4 4WE, United Kingdom*

E. H. Linfield, K. M. Brown, M. P. Grimshaw, D. A. Ritchie, and G. A. C. Jones
*Cavendish Laboratory, Madingley Road, Cambridge CB3 0HE, United Kingdom*

M. Pepper
*Toshiba Cambridge Research Centre, 260 Cambridge Science Park, Milton Road, Cambridge CB4 4WE, United Kingdom and Cavendish Laboratory, Madingley Road, Cambridge CB3 0HE, United Kingdom*

(Received 4 January 1994; accepted for publication 10 March 1994)

Lateral transport in a coupled double quantum well has been studied in a system where each layer can be measured independently. Front and back gates were used to vary the carrier densities in the two wells and hence control the degree of electron coupling. When the carrier densities in the two 2DEGs were matched, the coupling was found to be strongest and resulted in a decrease in the resistance of the measured 2DEG. By using a structure with a low mobility 2DEG in parallel with a high mobility one, we demonstrate a device that displays large resistance changes and a correspondingly high transconductance.

A number of studies have been conducted on coupled double quantum wells (CDQWs) in the past, but only recently has the technology become available to measure each layer of the system separately. Various techniques, including ion implantation,[1] back gate fabrication on thinned substrates,[2] regrowth, and shallow ohmic contacts[3] have all been successfully employed to achieve the separate contacts. The measurements on these CDQW systems can be divided into two main categories, those where the tunneling current transverse to the 2DEGs is measured and those where the lateral transport properties of the 2DEGs are measured. In the tunneling experiments, a bias voltage between the layers is applied, which varies the relative positions of the subbands in the two 2DEGs and hence provides direct information on the 2D to 2D tunneling process. Studies performed by Smoliner *et al.*[3] and more recently by Eisenstein *et al.*[4] have demonstrated that resonant tunneling is the dominant process with the tunnel current reaching a maximum when the subband edges of the 2DEGs are aligned. In the studies of the lateral conductivity of a double quantum well system the effects of coupling between the 2DEGs have also been observed.[5,6] In these experiments both layers were measured simultaneously with a significant resistance increase occurring only when both the coupling and mobility difference between the two layers are large. This phenomenon, first observed by Palevski *et al.*,[5] has been referred to as the "resistance resonance."

In this letter we present a study of the lateral conductivity of a CDQW system. The devices contain both front and back gates that are used to vary the carrier density in each of the quantum wells, hence the degree of coupling between the 2DEGs can be controlled. Furthermore, independent contact to each of the 2DEGs has been achieved, allowing the conductivity of each layer to be measured separately. In previous studies[5,6] the layers have always been measured together, whereas here we are able to report the effect of coupling on each of the individual layers. The measured resistance of the individual layers was found to be very sensitive to the degree of coupling, even when the coupling energies of the system were very small (symmetric-antisymmetric energy gap, $\Delta_{SAS}=0.02$ meV for this structure). These results were found to be consistent with a simple resistor network model based on resonant tunneling between the layers.[7] In addition, by using a sample with a high mobility layer in parallel with a low mobility one, the resistance of the low mobility 2DEG was found to be very sensitive to the degree of coupling. Large resistance changes are produced leading to the prospect of a high transconductance device suitable for high speed switching applications.

Measurements were conducted on MBE grown GaAs/AlGaAs CDQWs that consisted of 20 nm GaAs quantum wells separated by a 7 nm $Al_{0.33}Ga_{0.67}As$ barrier. The full details of the structure are given in Fig. 1(a). This structure resulted in a top 2DEG with a carrier density of $3.5\times10^{11}$ $cm^{-2}$ and a mobility of $4.4\times10^5$ $cm^2\,V^{-1}\,s^{-1}$, whereas the bottom 2DEG had $1.5\times10^{11}$ $cm^{-2}$ carriers and a lower mobility of only $2.8\times10^4$ $cm^2\,V^{-1}\,s^{-1}$. This large difference in the mobilities was a result of the relatively high temperature, 630 °C as measured with an optical pyrometer, used during the molecular beam epitaxial growth of the sample. The high temperature enhanced upward diffusion of the Si dopant atoms, resulting in increased scattering in the lower quantum well and hence a reduced mobility in the lower 2DEG. A buried $n^+$ layer was also incorporated into the structure which was used as a back gate. After the growth of this $n^+$ layer, the growth sequence was interrupted to allow an *in situ* focused ion implantation process to be performed. The $n^+$ layer could thus be patterned into regions that were then used as separate back gates for the CDQW structure subsequently grown on top. Full details of the technique are given by Linfield *et al.*[8] The back gate was patterned into three regions: a full gate (BG) to lie under the main portion of the


0003-6951/94/64(22)/3018/3/$6.00
© 1994 American Institute of Physics

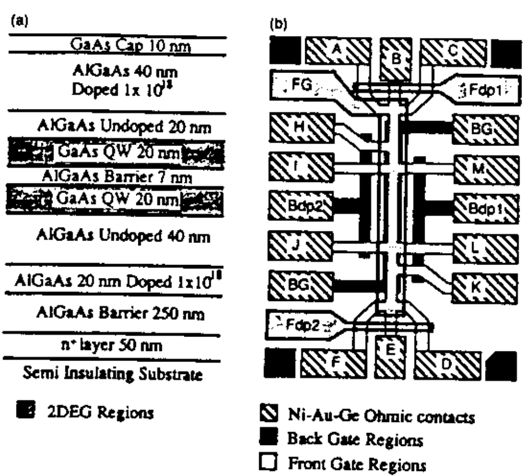


FIG. 1. The cross sectional diagram (a) details the different layers and doping levels for the CDQW structure with the plan view (b) showing the layout of the device including the various gates and contacts. The front depleting gates (Fdp1 and Fdp2) cover the arms connecting the end ohmic contacts to the mesa. Hence, by applying a negative voltage and depleting the top 2DEG, contacts A–F can be used to measure the bottom 2DEG along. Similarly, the side voltage probes have underlying back depleting gates (Bdp1 and Bdp2) and hence these can be used for measuring the top 2DEG alone using contacts H–M. Full front (FG) and back gates (BG) are also present that are used to vary the carrier concentration in each of the 2DEGs.

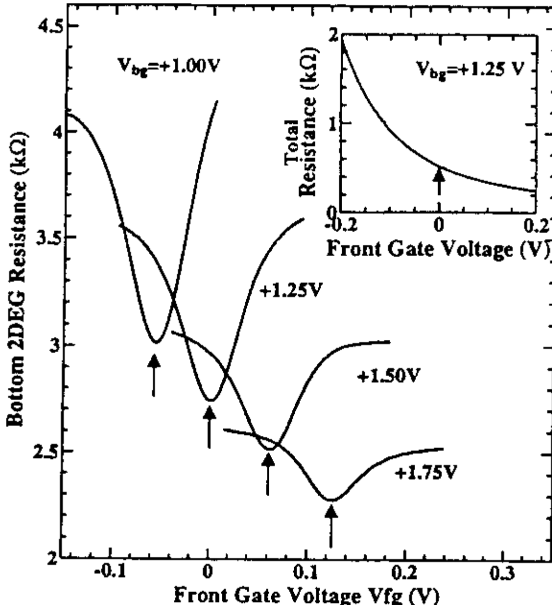


FIG. 2. The resistance of the device as a function of the front gate voltage is shown in the experimental configuration where the current is injected and probed through the bottom 2DEG. A large decrea.e in the bottom 2DEG resistance occurs when the carrier densities in the two layers are matched (indicated by arrows). The inset shows the measured resistance when the two 2DEGs are shorted together at the source and drain, note that no feature is observed when the carrier densities are matched (indicated by the arrow).

mesa and two depleting gates (Bdp1 and Bdp2) which lie under the arms of the side voltage probes. Corresponding Schottky gates were also made on the surface of the device to cover the main portion of the mesa (FG) and to cover the arms of the end voltage probes (Fdp1 and Fdp2) [see Fig. 1(b)]. Using the patterned front and back gates we were then able to conduct independent measurements on the two 2DEGs by employing a selective depletion technique.[1,2] The front depleting gates were used to selectively deplete the top 2DEG, allowing electrical contact to be made only to the bottom 2DEG (using contacts A–F), whereas the back depleting gates were used to selectively deplete the bottom 2DEG allowing contact to the top 2DEG alone to be possible (using contacts H to M).

Figure 2 shows the resistance of the device, as a function of front gate voltage for various values of back gate voltage, when the current is injected and measured through the lower 2DEG. In this experimental configuration, we would expect that if the screening provided by the upper 2DEG is perfect, then the bottom 2DEG should be unaffected by the varying front gate voltage and hence the measured resistance should remain constant. However, the bottom 2DEG resistance shows a pronounced dip at a certain value of the front gate voltage, this value being dependent on the back gate voltage. Similarly, measurements were performed with the current injected and measured through the top 2DEG, shown in Fig. 3. In this case the back gate voltage was swept with the front gate voltage fixed. In this case the measured layer, the top 2DEG, should be unaffected by the varying back gate voltage and the resistance remain constant. However, dips in the resistance are again observed, although the magnitude is

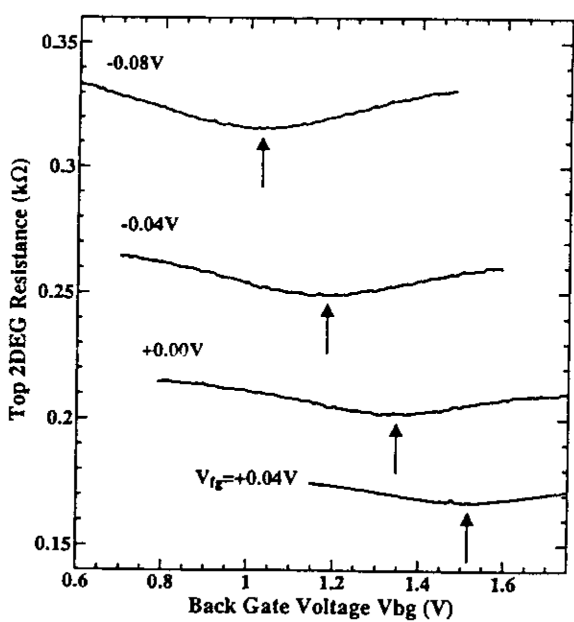


FIG. 3. The resistance of the devices as a function of the back gate voltage is shown in the configuration where the current is injected and probed through the top 2DEG. A small decrease in the top 2DEG resistance is observed when the carrier densities are matched in the two layers.

greatly reduced when compared to the previous measurements.

Magnetoresistance studies of the sample were performed in order to determine the carrier densities of the two 2DEGs, for a given front and back gate voltage. These results confirmed that the resistance dips occur whenever the carrier densities in the two layers are matched. As seen in Fig. 2, as the carrier density in the bottom 2DEG is reduced, by lowering the back gate voltage, the resistance dip appears at a correspondingly lower front gate voltage, at which point the carrier densities in the two 2DEGs are again equal. The resistance change is thus directly related to the coupling of the two 2DEGs, with the amplitude dependent on whether the high mobility or low mobility layer is directly measured.

At this point, we should return to the results of Palevski *et al.*[5] In their studies, the two 2DEGs were measured in parallel and an *increase* in the total resistance was observed whenever the carrier densities in the layers were matched. This was a result of the strong coupling between the layers in their samples that causes the electron wave functions in the quantum wells to become delocalized. Bonding and antibonding states are formed which extend across both quantum wells. This change in the spatial extent of the electron wavefunctions directly affects the sample mobility which leads to the observed increase in the total resistance. In our samples, identical measurements were performed with both layers shorted together at the contacts, the corresponding front gate voltage characteristics are shown in the inset to Fig. 2. A rising resistance is seen due to the depletion of carriers, but no additional structure is observed when the carrier densities are matched (an arrow marks the point when the carrier densities in the two layers are equal). The increase in resistance associated with the "resonant resistance" effect is clearly not observed in these measurements. This result is consistent with the fact that our samples contain a relatively thick barrier and wide quantum wells, both of which decrease the degree of wave function overlap. The coupling energy is only $\Delta_{SAS}=0.02$ meV which is more than an order of magnitude smaller than in the other studies.[5,6] Nevertheless, even with such a small coupling energy we are able to observe coupling effects when the layers are probed individually, as seen in Figs. 2 and 3. The small coupling energies in our samples cause the electron wave functions to remain localized to each of the wells and hence the mobilities in the layers are not significantly altered even at resonance. However, we are able to see large resistance changes due to the fact that the coupling is large enough that resonant tunneling between the layers is still significant. Electrons are therefore able to tunnel from the layer in which they are injected to the adjacent layer while conserving energy and momentum. The observed resistance dips are thus solely due to the extra current path provided by the adjacent layer, which is coupled by way of a resonant tunneling process. The size of this resistance change is then directly related to the ratio of the mobilities of the two layers. A simple transmission line model, as used by Simmons *et al.*,[7] can be used to describe the changes observed in our device. Using this model we find that the relative changes in the resistance are consistent with the ratio of mobilities in the two 2DEGs in our structure.

In summary, the lateral transport in a coupled double quantum well system has been studied. By using samples where independent contact to each layer is possible, we are able to observe for the first time large changes in the sample resistance even when the coupling between the layers is weak. The mechanism for the resistance change is the coupling of adjacent layers by way of resonant tunneling of electrons. This tunneling process can be switched on and off by tuning with either the front or the back gates, thus producing a device that displays large positive and negative transconductances that may be used for high speed switching applications.


[1] K. M. Brown, E. H. Linfield, D. A. Ritchie, G. A. C. Jones, M. P. Grimshaw, and A. C. Churchill, J. Vac. Sci. Technol. (to be published).

[2] J. P. Eisenstein, L. N. Pfeiffer, and K. W. West, Appl. Phys. Lett. 57, 2324 (1990).

[3] J. Smoliner, E. Gornik, and G. Weimann, Phys. Rev. B 39, 12937 (1989).

[4] J. P. Eisenstein, L. N. Pfeiffer, and K. W. West, Phys. Rev. Lett. 69, 3804 (1992).

[5] A. Palevski, F. Beltram, F. Capasso, L. Pfeiffer, and K. W. West, Phys. Rev. Lett. 65, 1929 (1990).

[6] Y. Ohno, M. Tsuchiya, and H. Sakaki, Appl. Phys. Lett. 62, 1952 (1993).

[7] J. A. Simmons, S. K. Lyo, J. F. Klem, M. E. Sherwin, and J. R. Wendt, Phys. Rev. B 47, 15741 (1993).

[8] E. H. Linfield, G. A. C. Jones, D. A. Ritchie, and J. H. Thompson, Semicond. Sci. Technol. 8, 415 (1993).

Resonant Coupling Effects Observed in Independently Contacted Triple Quantum Well Structures

N. K. Patel[†], I. S. Millard[§], E. H. Linfield[§], P. D. Rose[§], D. A. Ritchie[§], G. A. C. Jones[§] and M. Pepper[†§]

[†]Toshiba Cambridge Research Centre, 260 Cambridge Science Park, Milton Road, Cambridge CB4 4WE, United Kingdom
[§]University of Cambridge, Cavendish Laboratory, Madingley Road, Cambridge CB3 0HE, United Kingdom

**Abstract.** Independent contacts have been produced to all three two-dimensional electron gases (2DEGs) in a triple quantum well structure. This has been achieved by using *in-situ* focused ion beam implantation followed by molecular beam epitaxial regrowth. Lateral transport studies of the individual layers have demonstrated resonant coupling between the high mobility 2DEGs. Large resistance changes are observed due to coupling between the layers and these can be enhanced by having all three 2DEGs on resonance. A versatile device can thus be fabricated for studying electron interactions and for designing new multi-layer devices.

PACS:- 73.20.Dx, 72.80.Ey, 73.40.Gk

In the last few years there has been a rapid increase in the study of closely spaced electron gases. In particular, there have been many investigations of double quantum wells (DQWs) [1,2] in which the interactions of the two conducting layers can be probed. The high mobilities obtainable by molecular beam epitaxy (MBE), in combination with the precision of growth, have enabled a systematic study of a number of effects. These have included studies related to interlayer wavefunction coupling [3] and Coulomb interactions [4]. An important ingredient for developing the studies of DQW structures has been the ability to contact independently the two conducting layers, thereby enabling measurements of the layers separately [5] as well as direct tunnelling between the layers [6]. This has led to the observations of a Coulomb gap [7,8] in the tunnelling in a magnetic field, Coulomb drag between layers [9] and incompressibility phenomena [10].

These DQW structures have also exhibited properties that may lead to the fabrication of quantum effect devices. The lateral transport of the individual layers is found to show regions of positive and negative transconductance, which are a direct result of the interlayer tunnelling [5]. The short times associated with this tunnelling process means that the devices can be driven at high speed and thus may be used for generation of harmonics at high frequency [11]. In addition, the tunnelling can be used to transfer current between the layers, which may lead to the development of a high speed current switch. Finally, measurement of the direct tunnelling process reveals regions of negative differential resistance (NDR) [6] which are similar to those seen in double barrier resonant tunnelling diodes (DBRTDs). One major difference between our structures and more conventional DBRTDs, is that the carrier densities in the emitter and collector regions can be continuously changed, with front and back gates, so altering the threshold voltage for the NDR region.

The natural extension of this work is the inclusion of a third quantum well to produce three two-dimensional electron gases (2DEGs) in a Triple Quantum Well (TQW) structure. This adds a further degree of freedom for designing devices, which can be used to enhance the device performance. Alternatively, this provides a further parameter for investigating the interlayer interactions [12]. In this letter, we present the first results from such a structure, demonstrating independent contacting of each 2DEG. An *in-situ* focused ion beam implantation process [13] is used to define a patterned back gate which, in combination with front gates, is used to produce the independent contacts to the different layers. A versatile device car thus be fabricated where the carrier densities in the top and bottom 2DEGs can be controlled by front and back gates respectively. In addition, all voltage probes can independently contact

## References

[1]C. Delalande, G. Bastard, J. Orgonasi, J. A. Brum, H. W. Liu and M. Voos, Phys. Rev. Lett. **59**, 2690 (1987).

[2]For a review see The Quantum Hall Effect, edited by R. E. Prange and S. M. Girvin (Springer-Verlag, New York 1987).

[3]G. S. Boebinger, H. W. Jiang, L. N. Pfeiffer and K. W. West, Phys. Rev. Lett. **64**, 1793 (1990).

[4]K. M. Brown, N. Turner, J. T. Nicholls, E. H. Linfield, M. Pepper, D. A. Ritchie and G. A. C. Jones, Phys. Rev. B **50**, 15465 (1994).

[5]P. P. Ruden and Z. Wu, Appl. Phys. Lett. **59**, 2165 (1991).

[6]H. Sakaki, Jpn. J. Appl. Phys. **21**, L381 (1982).

[7]E. H. Linfield, G. A. C. Jones, D. A. Ritchie and J. H. Thompson, Semicond. Sci. Technol. **8**, 415 (1993).

[8]K. M. Brown, E. H. Linfield, D. A. Ritchie, G. A. C. Jones, M. P. Grimshaw and M. Pepper, Appl. Phys. Lett. **64**, 1827 (1994).

[9]N. K. Patel, I. S. Millard, E. H. Linfield, P. D. Rose, D. A. Ritchie, G. A. C. Jones and M. Pepper, submitted to J. Phys. C.

[10]N. K. Patel, E. H. Linfield, K. M. Brown, M. P. Grimshaw, D. A. Ritchie, G. A. C. Jones and M. Pepper. Appl. Phys. Lett. **64**, 3018 (1994).

[11]L. Hedin and B. I. Lundqvist **4**, 2064 (1971).

[12]J. P. Eisenstein, L. N. Pfeiffer and K. W. West, Phys. Rev. Lett. **68**, 674 (1992).

[13]S. Luryi, Appl. Phys. Lett. **52**, 501 (1988).

**Figure Captions**

FIG. 1 The tunnel conductance is measured between the middle and top 2DEGs as a function of the front gate voltage ($V_{fg}$). Successive traces are taken at 40 mV increments of the back gate voltage, and have been offset vertically for clarity. In the inset, the front gate voltage position of the tunnel peak is plotted as a function of the back gate voltage, this front gate voltage has also been converted to a 2DEG carrier density.

FIG. 2 The Shubnikov-de Haas oscillations for the top 2DEG are shown. Successive traces are taken at 20 mV increments of the back gate voltage, and have been offset vertically for clarity. Lines have been drawn to show the movement of the peaks in the oscillations. Analysis of the period of the oscillations is used to determine the carrier density as a function of the back gate voltage, which is plotted in the inset.

FIG. 3 (a) The two-terminal conductance is measured for (1) the middle and top 2DEG together, (2) the top 2DEG alone and (3) the middle 2DEG alone, as a function of the back gate voltage. The vertical arrow marks the enhancement of the conductance due to resonant tunnelling to the bottom 2DEG. (b) An expanded view of the top 2DEG conductance is also shown, which reaches a maximum just before the middle 2DEG is depleted.

FIG. 4 Simulation data for the carrier densities in the middle and bottom 2DEGs are plotted as a function of the front gate voltage, (a) when the exchange and correlation term has been omitted and (b) when it is included. The experimental data is also shown in (b) as a dashed line.

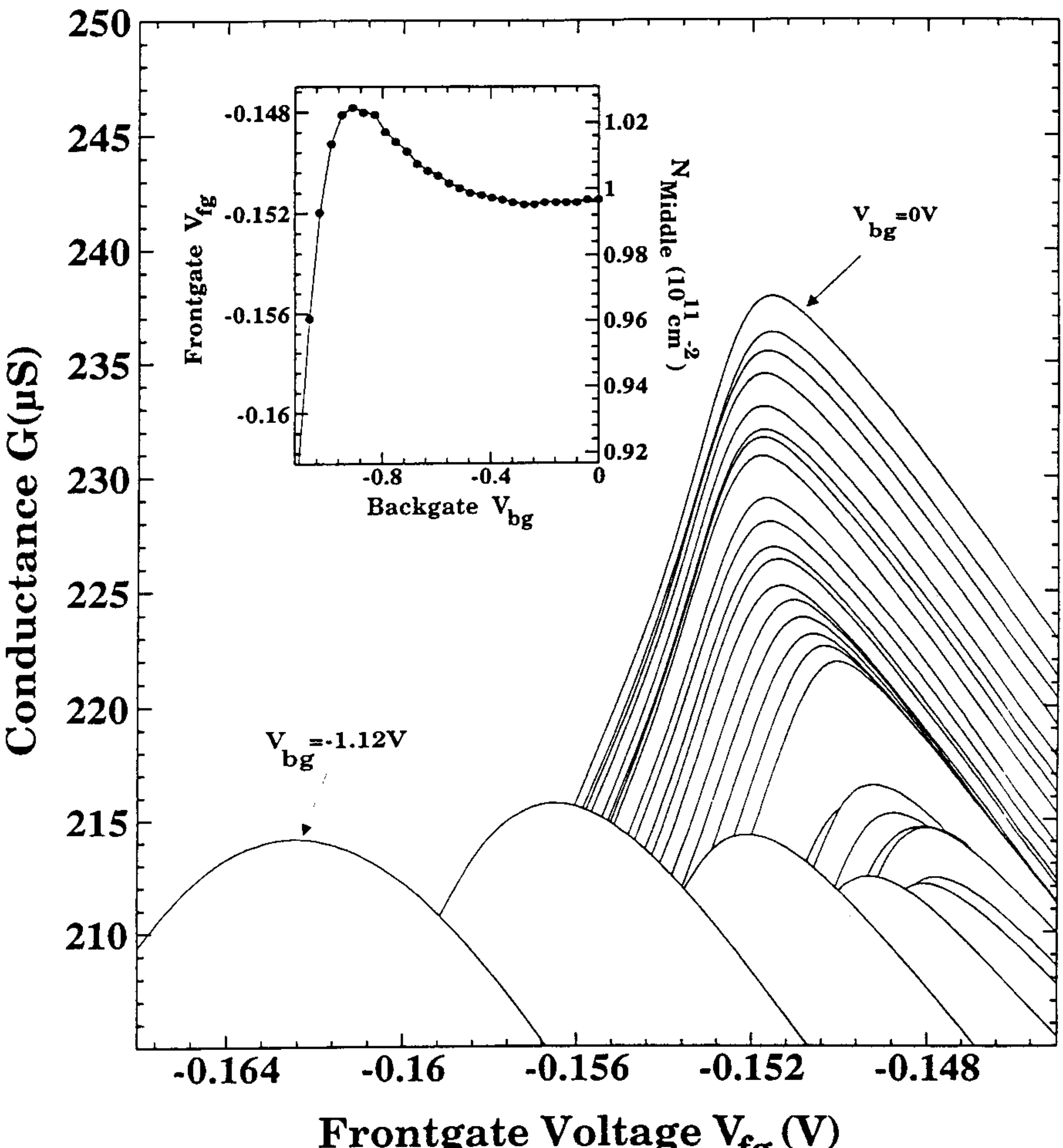


Fig 1

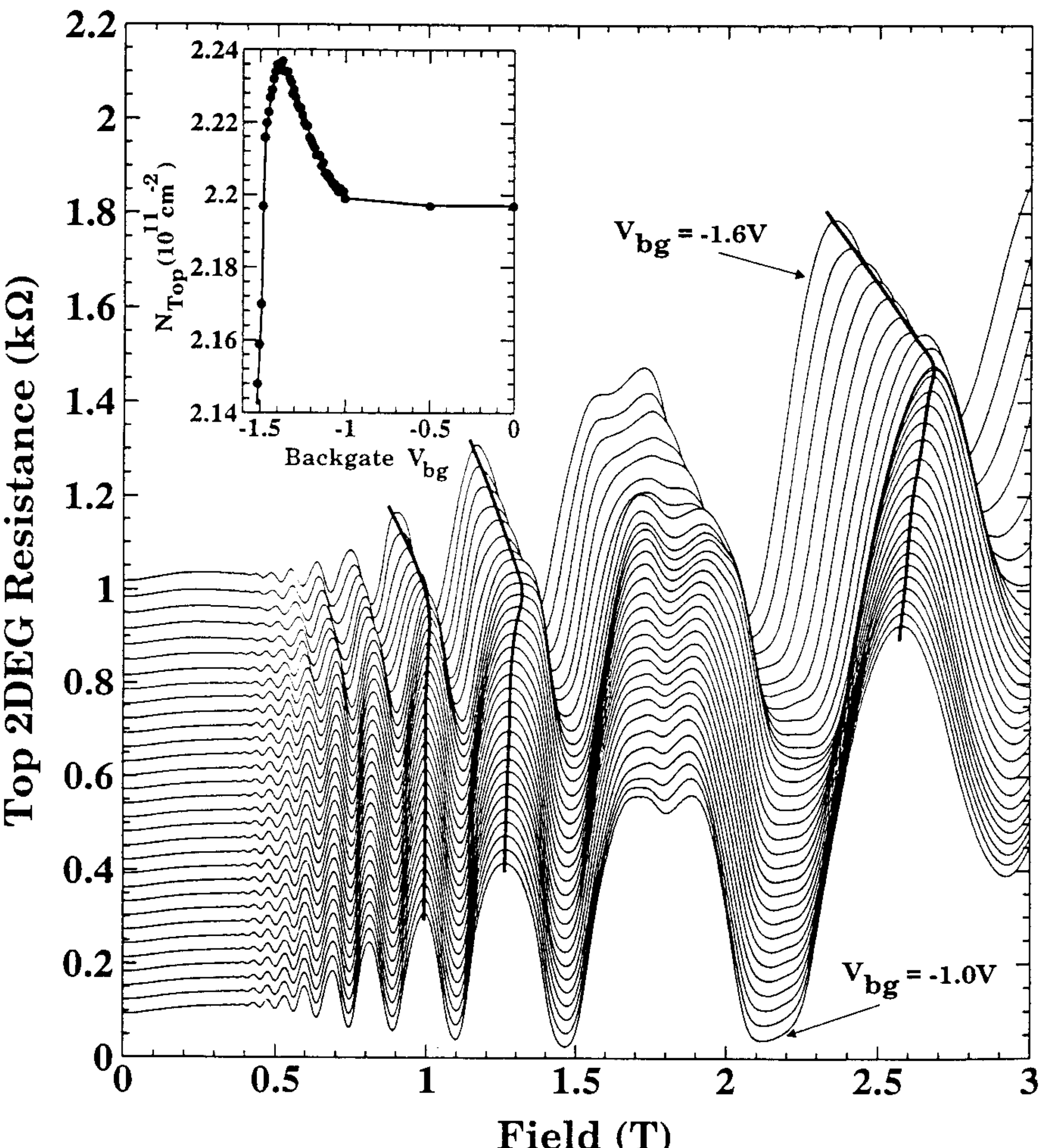


Fig. 2

$$V_{xc}(z) = -[1 + 0.0368\, r_s \ln(1 + 21/r_s)] \frac{2}{\pi \alpha r_s} R_y, \qquad (1)$$

where $\alpha = (4/9\pi)^{1/3}$, $r_s = r_s(z) = [4\pi a^3 N(z)/3]^{-1/3}$, a = Bohr radius and $R_y$ = Rydberg constant. This additional term is self-consistently included into the simulation by using the electronic wavefunction to determine the carrier density N (z) and calculate the exchange and correlation potential $V_{xc}(z)$ through the device. We should add that the above formulation for the exchange and correlation assumes that the electron density changes slowly on the scale of the Fermi wavelength. This is not strictly true for the narrow QWs; however, as we shall see later, good agreement with experiments can be obtained using this model.

In Fig. 4, the calculated carrier densities of the top and middle 2DEGs are plotted as a function of the front gate voltage, (a) when exchange and correlation are omitted and (b) when exchange and correlation are included. In both cases the top 2DEG is always depleted and so can be ignored. Without exchange and correlation, both the top and middle 2DEG carrier densities are reduced by decreasing the front gate potential. The inclusion of the exchange and correlation has a dramatic effect, resulting in the bottom 2DEG gaining carriers as the middle 2DEG is depleted. This is now in good agreement with the experimental data, which is also plotted in Fig. 4 (b). Note that the data has only been fitted at the highest gate voltage at which point the carrier densities of the experiment and simulation were matched. Deviations can, however, be seen at low carrier densities, which are related to an increase in the disorder, which at present is not included in the model.

In order to understand the physical origin of the charge increase, let us first address the situation when exchange and correlation are not included into the model. The front gate voltage alters the electric field $\Delta E$, which controls the carrier density in the middle 2DEG. In addition, if the screening provided by the middle 2DEG is not perfect, a field $\delta E$ will penetrate through to the bottom 2DEG. A change in the carrier density in the middle 2DEG will thus be accompanied by a smaller change in the bottom 2DEG density, as predicted in the simulation. This ability to screen the electric field can be described in terms of the compressibility of the 2DEG layer, which is directly related to the density of states[12]. Alternatively, we can consider the same situation in terms of the band potentials. The lowering of the gate potential by $\Delta V_c$, as in the inset, increases the carrier density in the middle 2DEG. Since the Fermi energy is constant, this forces the conduction band potential at the middle QW down by an amount $\delta V_c$. This smaller change in the potential of the middle QW produces a correspondingly smaller carrier density change in the bottom 2DEG. In

this way, the effect can be described by assigning a quantum capacitance to the 2DEG which relates the charge change to the potential energy change[13]. From both viewpoints, the chemical potential change is directly related to the density of states and is given by:

$$\frac{\delta\mu_1}{\delta N} = \frac{\pi\hbar^2}{m^*}. \qquad (2)$$

If the exchange and correlation is now included into the model, this will reduce the total energy of the system. This adds a second contribution to the chemical potential, which now becomes:

$$\frac{\delta\mu_1}{\delta N} = \frac{\pi\hbar^2}{m^*} + \frac{\delta V_{xc}(N)}{\delta N}. \qquad (3)$$

The first term on the right hand side, as already described, is related to the density of states and so remains constant. The second term due to exchange and correlation, however, depends on the carrier density and becomes larger at low carrier densities. In addition, this term is negative and hence the rate at which the chemical potential changes with carrier density can also become negative. This change in sign is the origin of the unusual charge increases observed both in the simulation and the experimental data.

In summary, we have used independent contacts to the three 2DEGs in a triple quantum well structure to investigate the effects of screening. This screening is determined by measuring the carrier density in an adjacent 2DEG, which acts as an sensitive detector. As the carrier density in the screening 2DEG is decreased, the carrier density in the detector 2DEG was found to increase. This feature arises from the effect of the exchange and correlation in the screening layer which was modelled by simulations of the structure. Since the charge in one 2DEG is increasing whilst that in the other 2DEG is reducing, this process can be considered as an exchange and correlation driven charge transfer.

*any* of the three 2DEG layers. This has enabled us to measure all three 2DEGs separately and study the interlayer coupling between the different 2DEGs.

Devices were grown by MBE, with the layer sequence shown in Figure 1 (b). After growth of the $n^+$ GaAs layer, the wafer was transferred under ultrahigh vacuum conditions to a separate chamber for ion implantation. Here a 30 keV Ga focused ion beam was used to pattern selectively the $n^+$ GaAs layer, rendering the exposed areas insulating [13]. Separate conducting regions can thus be defined which are used as back gates ($B_g$) to control the carrier density under the mesa or as back depleting gates ($B_{dg}$) which lie under the arms of the voltage probes and are used to achieve independent contacting. The various regions of the back gate are shown in the plan and cross sectional diagrams of the device shown in Figure 1.

After implantation the wafer was returned to the growth chamber where the subsequent layers were grown. These consisted of three quantum wells in which modulation doping above and below was used to form high mobility 2DEGs. The particular design of the TQW structure was chosen to ensure that all three QWs would be populated with carriers. In order to determine the type of structure needed, initial test data was obtained using a one-dimensional self-consistent Poisson and Schrodinger simulation. The results indicated that for equal sized QWs, and modulation doping on either side of the outer wells, the middle QW would be unpopulated. This is a result of the band bending introduced by the electrons that occupy the outer QWs; this causes a lowering of the Fermi energy in the middle QW to below the ground state energy. If the middle QW is, however, made thicker than the outer QWs, the ground state energy of the middle 2DEG can be lowered with respect to the outer QWs, and the middle QW can then be populated. The outer QWs were therefore made 11 nm thick, which is sufficiently wide that interface scattering, which becomes significant for QWs less than 10 nm, would not degrade the 2DEG mobility. A middle QW of 20 nm then allows all three QWs to be populated.

The width of the barriers separating the QWs were chosen on the basis of two requirements. The barriers have to be wide enough to allow independent contacts to be attainable. If the barriers are made too small, then the non-resonant tunnelling becomes large and independent contacting becomes unfeasible. The barrier also has to be sufficiently thin that significant resonant tunnelling can still be observed. This led to the choice of 14 nm barriers separating the QWs, for which the calculated symmetric - antisymmetric energy splitting $\Delta_{SAS}$ is of the order 0.5 μeV. This is within the range where wavefunction coupling effects are minimal but resonant tunnelling should still be significant [15].

After growth, conventional optical lithography was performed to define a mesa and produce AuGeNi ohmic contacts. These contacts penetrate deep into the sample and therefore would contact all three 2DEGs simultaneously. To prevent these contacts shorting to the back gate, they are formed over regions where the $n^+$ back gate layer has been ion damaged (see Figure 1(b)). The back gate regions were also contacted with AuGeNi ohmic contacts, but in this case the contacts were formed off the mesa and so would connect to the $n^+$ layer only and not effect the 2DEGs. Using this technique of in-situ focused ion beam lithography, the back gate could be placed close to the conducting layers and still operate reliably at low temperatures with negligible leakage current over a wide range of voltages. For the TQW structure, the back gate is located 350 nm from the bottom conducting layer, and voltages in excess of -2.5 V can be applied with the leakage remaining below the 1 nA level. This voltage range is found to be sufficient to deplete all the conducting layers of the TQW structure.

Schottky gates of NiCr (20 nm) followed by Au (100 nm) were patterned on the surface. These are used to control the carrier density in the mesa region ($F_g$) and produce depleting gates ($F_{dg}$) which lie on top of the arms of all the voltage probes (see Figure 1(a)). Each voltage probe, therefore, has a front and back depleting gate that can be used to pinch-off the conduction in the different layers of the TQW. The front depleting gate can be used to deplete the top and middle 2DEGs to produce an independent contact to the bottom 2DEG. Similarly, the back depleting gate can be used to deplete the bottom and middle 2DEGs to enable independent contacting of the top 2DEG. Finally, depletion of the top 2DEG with the front gate and bottom 2DEG with the back gate allows contact to the middle 2DEG alone. In this manner, *any* of the voltage probes can be used to probe *any* of the three 2DEGs by merely altering the associated depleting gate voltages. Using this method for producing independent contacts, the magnetoresistance of the three individual layers could be measured separately, as shown in Figure 2. The graphs show the characteristic Shubnikov-de Haas effect for a four-terminal constant current measurement. The traces show no signs of a low field positive magnetoresistance or beating in the period of the oscillations, which are seen when two or more layers are measured in parallel [14]. Instead, a single oscillation is observed, the period of which can be used to determine the carrier density in the 2DEG. The individual carrier densities, and the calculated mobilities of the three different 2DEGs, are marked on the traces in Figure 2.

The degree of coupling between the layers was measured by performing lateral transport measurements of the independently contacted middle 2DEG. The resistance

of the middle 2DEG is plotted as a function of the back gate in Figure 3 (a) and as a function of the front gate voltage in Figure 3 (b). As the back gate voltage is altered, the number of carriers in the bottom well changes approximately linearly with voltage, as can be determined from magnetoresistance characterisation of the device. The effect on the number of carriers in the middle layer, though, is small due to the screening of the electric field produced by the charge in the bottom 2DEG. The middle 2DEG carrier concentration therefore remains approximately constant as the gate voltage is altered. A large dip in the measured middle 2DEG resistance occurs, however, when the number of carriers in the bottom 2DEG matches that in the middle 2DEG. This decrease has been seen before in DQW structures [5] and is associated with tunnelling between the two 2DEGs. This is a resonant process since the electrons must conserve both energy and momentum, a condition that is only satisfied when the carrier densities in the two layers are matched. The onset of tunnelling provides an extra current path that results in a decrease in the total resistance that is measured. As the back gate voltage is made even more negative, the bottom layer has a lower carrier concentration than the middle and the resonant tunnelling drops, resulting in a rise of the resistance. Similarly, when the front gate voltage is varied, a resonance between the middle 2DEG and the top 2DEG can be probed as seen in Figure 3 (b). The size of the resistance change is similar in the two cases which reflects the fact that the top and bottom 2DEGs are of similar mobility.

The resistance of the independently contacted middle 2DEG can therefore be used as a direct probe of the degree of coupling between the 2DEGs. This can be used to map out the coupling between all three layers. Figure 4 is a three-dimensional plot in which the resistance of the middle 2DEG is plotted as a function of the front and back gate voltages. The data shows minima in the resistance when the carrier density in the middle 2DEG is matched with that in the top *or* bottom 2DEGs. An even stronger resonance can be observed when all three QWs have matched carrier densities. This corresponds to the large minimum in the centre of the plot. In this case, the current injected into the middle 2DEG can flow through two extra current paths; hence the current is divided between all three 2DEGs and the resistance is greatly reduced. In this way, the current flow through the top can be controlled with the front gate and the current through the bottom 2DEG with the back gate.

We have demonstrated, for the first time, the ability to contact independently all three 2DEGs of a TQW structure. Each layer can be probed separately and the carrier concentrations in the top and bottom 2DEGs can be changed independently. This provides a very versatile device for studying electron interaction effects. In particular, we have been able to observe resonant coupling between each of the

2DEGs which causes large resistance changes. This effect can be enhanced by having all three 2DEGs on resonance. Although we have concentrated in this letter on the lateral transport through this structure, other measurements can readily be performed. These include direct tunnelling between the layers, Coulomb drag induced between the layers and studies of incompressibility. The added degree of freedom provided by the inclusion of an extra 2DEG, provides new method for investigating fundamental electron interactions, as well as for designing new quantum effect devices.

This work was supported by the EPSRC. One of the authors (DAR) would like to acknowledge support from Toshiba Cambridge Research Centre. The authors would also like to thank Ian Castleton for helpful discussions on device design.

## References

[1] Palevski A, Beltram F, Capasso F, Pfeiffer L and West K W 1990 *Phys. Rev. Lett.* **65** 1929

[2] Kurobe A, Castleton I M, Linfield E H, Grimshaw M P, Brown K M , Ritchie D A, Pepper M and G. A. C. Jones G A C 1994 *Phys. Rev.* B **50** 8024

[3] Kurobe A, Castleton I M, Linfield E H, Grimshaw M P, Brown K M, Ritchie D A, Pepper M and Jones G A C 1994 *Phys. Rev.* B **50** 4889

[4] Boebinger G S, Jiang H W, Pfeiffer L N and West K W 1990 *Phys. Rev. Lett.* **64**, 1793

[5] Patel N K, Linfield E H, Brown K M, Grimshaw M P, Ritchie D A, Jones G A C and Pepper M 1994 *Appl. Phys. Lett.* **64** 3018

[6] Brown K M, Linfield E H, Ritchie D A, Jones G A C, Grimshaw M P and Pepper M 1994 *Appl. Phys. Lett.* **64** 1827

[7] Eisenstein J P, Pfeiffer L N and West K W 1993 *Phys. Rev. Lett.* **69**, 3804

[8] Brown K M, Turner N, Nicholls J T, Linfield E H, Pepper M, Ritchie D A and Jones G A C 1994 *Phys. Rev.* B **50** 15465

[9] Gramila T J, Eisenstein J P, MacDonald A H, Pfeiffer L N and West K W 1991 *Phys. Rev. Lett.* **66** 1216

[10] Eisenstein J P, Pfeiffer L N and West K W 1992 *Phys. Rev. Lett.* **68** 674

[11] Ohno Y, Tsuchiya M and Sakaki H 1993 *Electronics Letters* **29** 375

[12] Jo J, Suen Y W, Engel L W, Santos M B and Shayegan M 1992 *Phys. Rev.* B **46** 9776

[13] Linfield E H, Jones G A C, Ritchie D A and Thompson J H 1993 Semicond. Sci. Technol. **8**, 415

[14] Kane M J, Apsley N, Anderson D A, Taylor L L and Kerr T 1985 *J. Phys. C* 18 5629

[15] Patel N K, Kurobe A, Castleton I M, Linfield E H, Brown K M, Grimshaw M P, Ritchie D A, Jones G A C and Pepper M, submitted to *Phys. Rev.* B.

## Figure Captions

**Figure 1.** The plan (a) and cross sectional (b) diagrams of the TQW structure are drawn. The diagram shows six voltage probes (labelled 1 to 6) each of which has an associated front ($F_{dg}$) and back depleting gate ($B_{dg}$). There is also a full front ($F_g$) and back gate ($B_g$) to control the carrier densities in the active area. The ohmic contacts are made to all three 2DEGs, but are not shorted to the $n^+$ back gates as these areas have been ion implanted and thereby rendered highly resistive.

**Figure 2.** The longitudinal magnetoresistance is measured at 1.6 K for the three 2DEGs separately. The characteristic periodic magneto-oscillations are observed from which the carrier density can be directly calculated, the results of which are shown for each 2DEG. The mobility of each layer has also been calculated and the outer QWs are found to have a similar mobility and carrier concentration. The middle 2DEG has a much lower carrier density but still has a higher mobility indicating that this is the highest quality layer.

**Figure 3.** The device resistance as measured when independent contacts are made to the middle 2DEG. In (a) the resistance is plotted as a function of the back gate voltage with the minimum occurring when the carrier densities in the middle and bottom 2DEGs are matched. Similarly, in (b) the front gate voltage is altered, and the minimum resistance is now measured when the carrier densities in the middle and top 2DEGs are equal.

**Figure 4.** The dependence of the resistance of the middle 2DEG is plotted as a function of both the front gate ($V_{fg}$) and the back gate voltage ($V_{bg}$). The resistance is decreased by the coupling to the other 2DEGs and hence the resistance data shown in the figure can be used to directly map out the strength of the coupling.

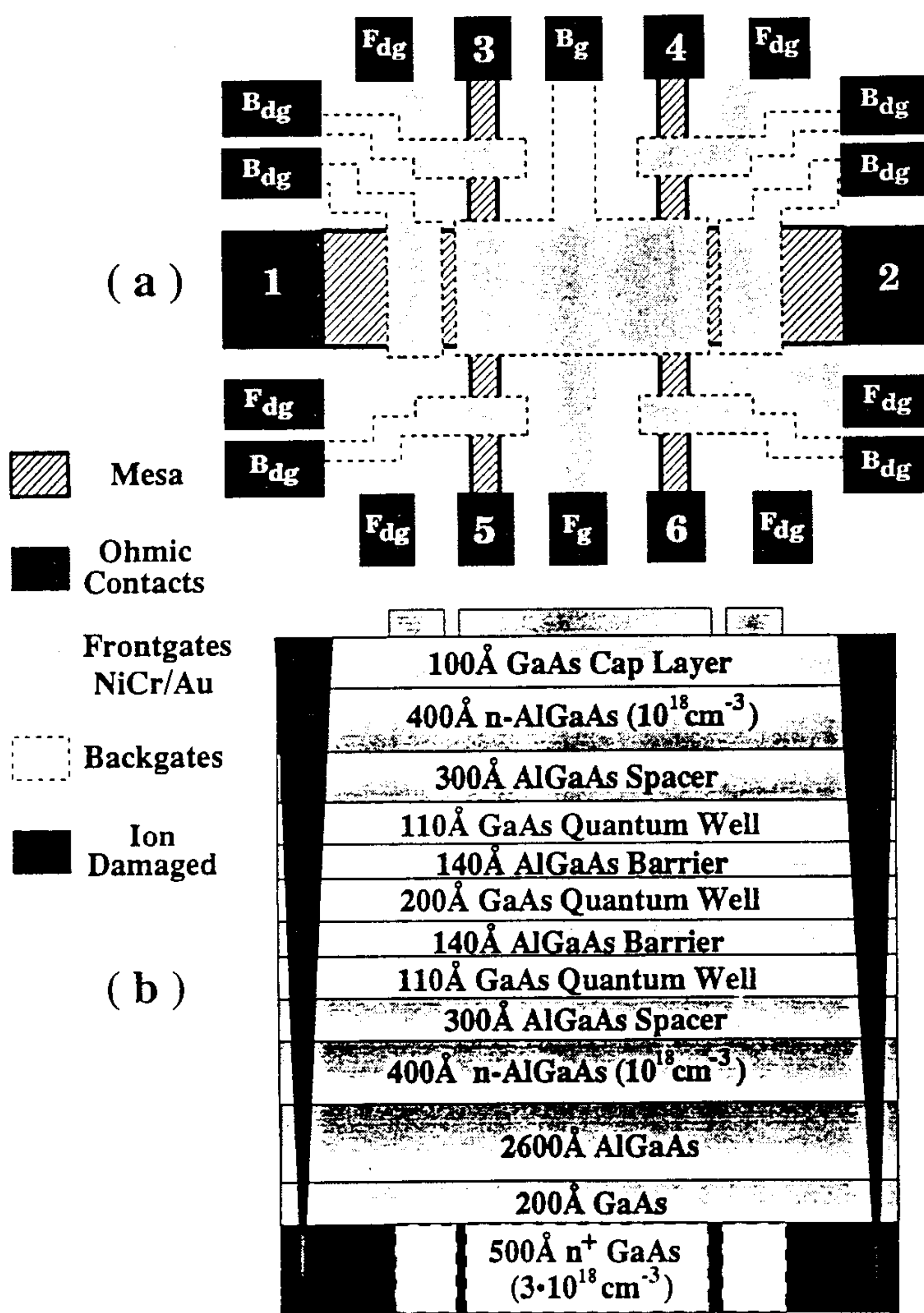

(a)
Fdg
3
Bg
4
Fdg
Bdg
Bdg
Bdg
Bdg
1
2
Fdg
Fdg
Bdg
Bdg
Fdg
5
Fg
6
Fdg
Mesa
Ohmic Contacts
Frontgates NiCr/Au
Backgates
Ion Damaged
(b)
100Å GaAs Cap Layer
400Å n-AlGaAs (10^18 cm^-3)
300Å AlGaAs Spacer
110Å GaAs Quantum Well
140Å AlGaAs Barrier
200Å GaAs Quantum Well
140Å AlGaAs Barrier
110Å GaAs Quantum Well
300Å AlGaAs Spacer
400Å n-AlGaAs (10^18 cm^-3)
2600Å AlGaAs
200Å GaAs
500Å n+ GaAs (3•10^18 cm^-3)

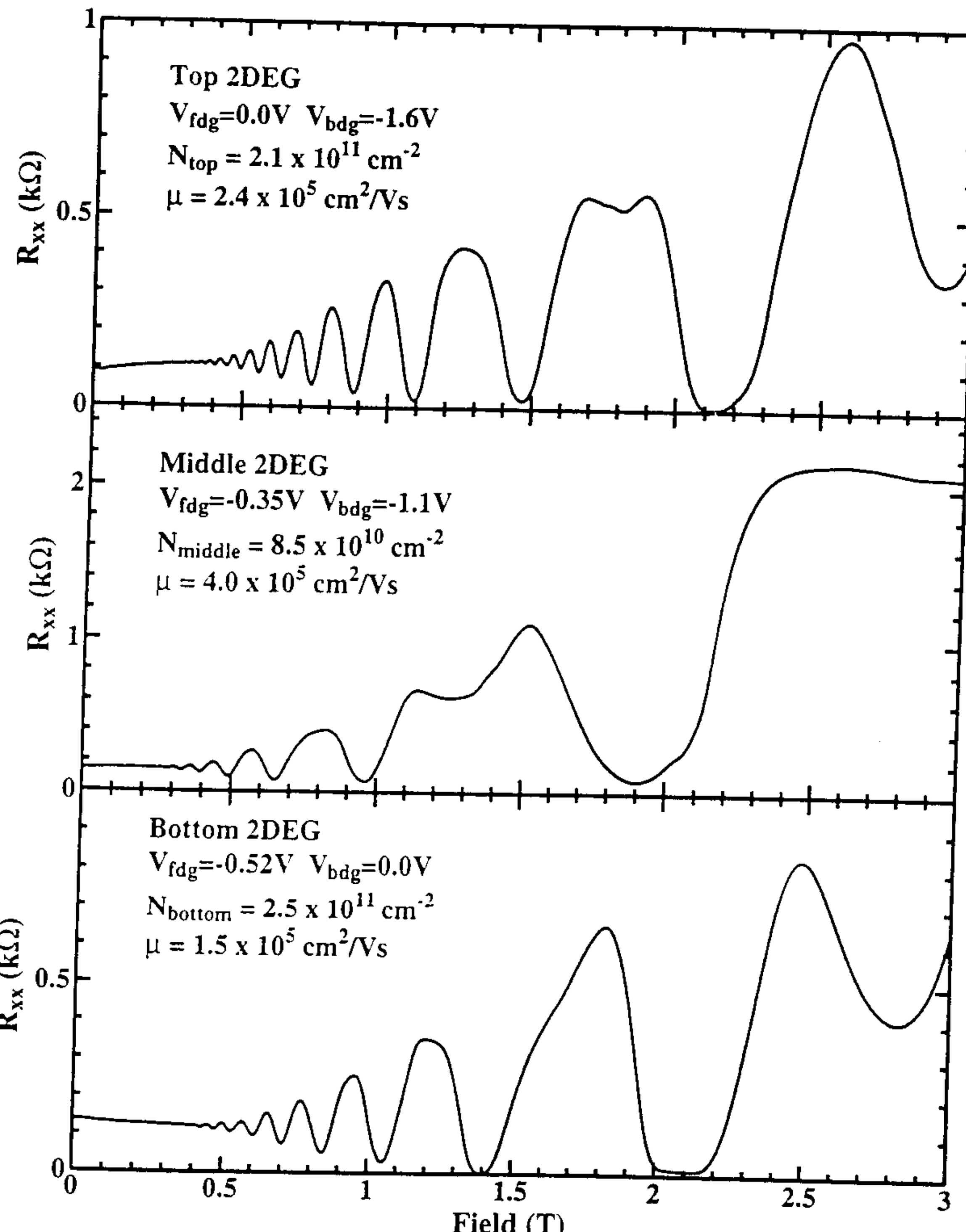


Figure 2

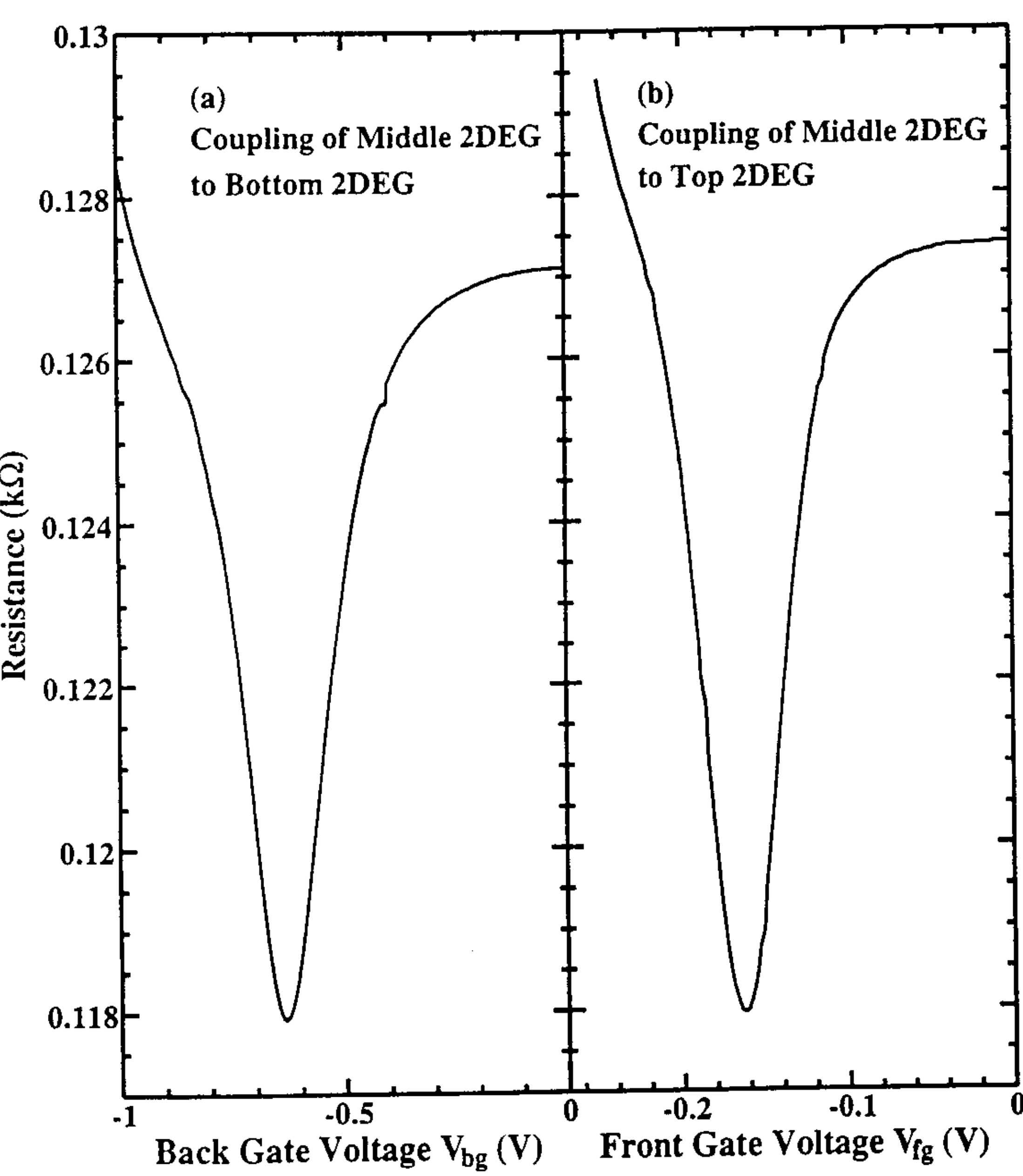


Figure 8

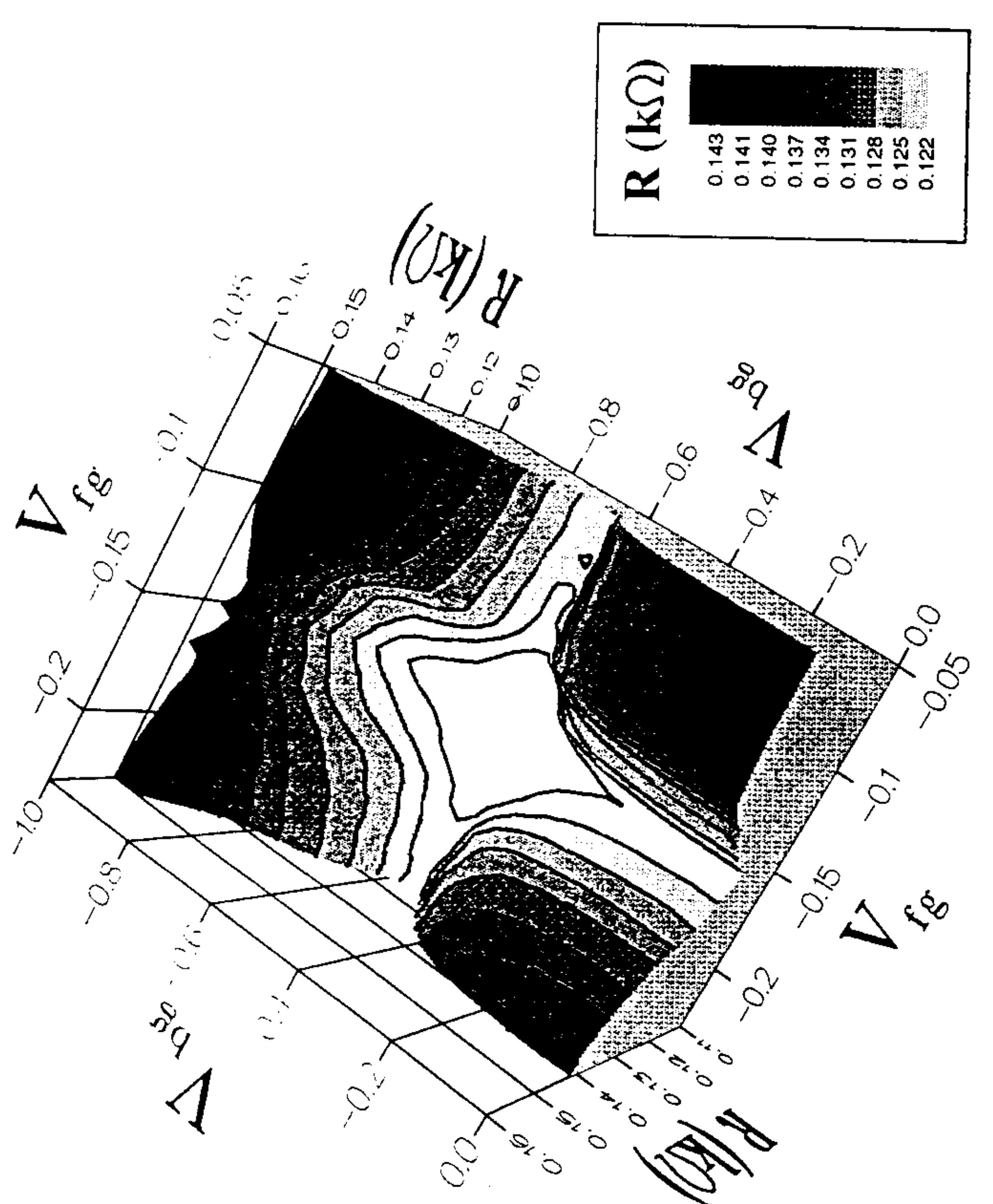


Figure 4

# Exchange and Correlation Induced "Charge Transfer" Observed in Independently Contacted Triple Quantum Well Structures

N. K. Patel
Toshiba Cambridge Research Centre, 260 Cambridge Science Park, Cambridge CB4 4WE, United Kingdom

I. S. Millard, E. H. Linfield, P. D. Rose, M. P. Grimshaw, D. A. Ritchie and G. A. C. Jones
Cavendish Laboratory, University of Cambridge, Cambridge CB3 0HE, United Kingdom

M. Pepper
Toshiba Cambridge Research Centre, 260 Cambridge Science Park, Cambridge CB4 4WE, United Kingdom and Cavendish Laboratory, University of Cambridge, Cambridge CB3 0HE, United Kingdom

**Abstract** The screening properties of two-dimensional electron gases (2DEGs) have been investigated in triple quantum well structures. By forming independent contacts to each of the three 2DEGs, an accurate determination of the carrier densities in the Quantum Wells (QWs) was obtained. Thus the screening properties of one 2DEG could be detected by carrier density changes in a second adjacent 2DEG. This led to the unusual situation where the carrier density change in the detection layer was opposite to that in the screening layer, and so charge is effectively transferred between the 2DEGs. Modelling of the structure provided good agreement with the experiments and revealed that such charge changes are a direct response to the exchange and correlation effects in a 2DEG.

PACS:- 71.70.Gm, 73.20.Dx, 72.80.Ey

Electron-electron interactions play an important role in the optical and electronic properties of two-dimensional electron gas (2DEG) systems. They directly cause the band gap renormalisation observed in quantum well structures[1] and the many varied phenomena observed in the integer and fractional quantum Hall effect regimes[2]. More recently, this work has been expanded to study the electronic properties of electrons confined to multi-quantum well structures. Interactions between the quantum wells have led to the appearance of new quantum hall states[3] and the development of a coulomb gap in high magnetic fields[4]. The latter has been seen in tunnelling measurements which have been performed on double quantum well structures where the two 2DEGs are independently contacted. In this rapid communication, measurements are reported on an independently contacted triple 2DEG structure. The exchange and correlation effects in a single 2DEG are found to be important and these can be detected by accurate measurements of the carrier density in an adjacent 2DEG. The ability of a 2DEG to screen an electric field is modified, and the situation arises where as the carrier density in one layer is increased the carrier density in the adjacent layer is decreased. This form of charge transfer[5] may be important in determining the role of exchange and correlation effects as well as for designing velocity modulation based devices[6].

The GaAs/AlGaAs structures used for our work were grown by molecular beam epitaxy on an *in-situ* focused ion beam patterned $n^+$ epilayer. The ion implanted regions were rendered insulating and hence the $n^+$ layer formed a patterned back gate for the overlying structure[7]. Devices were then fabricated by making separate ohmic contacts to the 2DEGs and back gate regions, and depositing surface Schottky front gates. The front and back gates controlled carrier densities in the devices and were used to form independent contacts to the different 2DEG layers [8]. The modulation doped triple quantum well structures had a 40 nm $n^+$ doped AlGaAs supply layer set back 30 nm above the top QW and a similar 40 nm $n^+$ doped layer 30 nm below the bottom QW. The two outer QWs were 11 nm wide with the middle QW 20 nm wide. The middle QW was made sufficiently wide to ensure that all three layers were populated with carriers. The resulting structure contained $2.1 \times 10^{11}$ cm$^{-2}$ carriers in the top 2DEG, $8.5 \times 10^{10}$ cm$^{-2}$ in the middle 2DEG and $2.5 \times 10^{11}$ cm$^{-2}$ in the bottom 2DEG. The mobilities of the layers were $2.4 \times 10^5$ cm$^2$ V$^{-1}$s$^{-1}$, $4.0 \times 10^5$ cm$^2$ V$^{-1}$s$^{-1}$ and $1.5 \times 10^5$ cm$^2$ V$^{-1}$s$^{-1}$ respectively. The barriers between the QWs were 14 nm; this corresponds to a symmetric - anti-symmetric splitting energy $\Delta_{SAS} \approx 0.5$ $\mu$eV between the top and middle and also between the middle and bottom QWs. For this coupling energy, independent contacts can be achieved to the different layers. The coupling is also large enough that inter-layer tunnelling between the layers is significant when the carrier densities of the 2DEGs are matched. Details of the

independent contacting to the three layers and measurements of the coupling for this device are documented elsewhere[9].

The tunnelling between the top and middle 2DEGs of the TQW structure was measured by forming independent contacts to the two 2DEGs. Fig. 1 shows the tunnel conductance as a function of the front gate voltage, recorded for various back gate voltages. For 2D (two-dimensional) to 2D tunnelling, the requirement for conservation of energy and momentum restricts the tunnelling to occur only when the carrier densities in the 2DEGs are equal. The tunnel peak, observed in each of the traces, thus corresponds to the point at which the carrier densities in the top and middle 2DEGs are matched. This result is confirmed by magneto-transport measurements of each 2DEG separately, from which the carrier densities can be accurately obtained[9]. The effect of altering the back gate voltage is to change the carrier density in the bottom 2DEG. If we assume that the bottom 2DEG acts as a perfect conductor, then it is able to screen the effect of the changing back gate potential from the upper 2DEGs, and the tunnelling between the middle and top 2DEGs should be unaffected. The position of the tunnel resonance, however, is found to be sensitive to the back gate voltage. Since the tunnelling resonance occurs when the top 2DEG carrier density is matched to the middle, the shifts in the resonance position indicate that the carrier density in the middle 2DEG is changing. This carrier density change is calculated from a parallel plate capacitor formula and is plotted in the inset to Fig. 1 as a function of the back gate voltage. Here, we have assumed that the top 2DEG is not significantly effected by the back gate potential. which is a good approximation as it is screened by both the bottom and middle 2DEGs. It can be seen that as the back gate voltage is reduced, and the bottom 2DEG is depleted, the carrier density in the middle 2DEG is found to increase. This process continues until the bottom 2DEG is depleted, after which the middle 2DEG is directly depleted of carriers by the back gate. In practice, due to disorder, the screening is reduced before the bottom 2DEG is completely depleted. The maximum increase in the carrier density of the middle 2DEG is $3 \times 10^9$ cm$^{-2}$ which is a relatively small change. However, since we are measuring the peak position of the tunnelling, which can be accurately determined, we are able to measure such changes in density to within 10 %.

Analysis of the magnetoresistance of the separate 2DEGs can be used to provide a more direct method for determining carrier density changes in the TQW. In Fig. 2, the Shubnikov-de Haas oscillations for the top 2DEG are shown for varying values of the back gate voltage. The periodicity of the Shubnikov-de Haas oscillations can be used to determine the carrier density of the top 2DEG, which is plotted as a function

of back gate voltage in the inset to Fig. 2. The carrier densities could also be calculated from the position of the individual minima in the longitudinal resistance. This was found to give identical results, which confirms that the carrier density changes are not significantly altered by the magnetic field that is applied in the experiments. The data presented in Fig. 2 show that whilst the bottom 2DEG is populated, little change is observed in the top 2DEG carrier density. As the middle 2DEG is depopulated, however, the carrier density in the top 2DEG increases by up to $(3\pm0.3) \times 10^9$ $cm^{-2}$. This increase is similar to that seen in Fig. 1 when the middle 2DEG was monitored via zero field tunnelling. Magneto-transport measurements performed on the middle 2DEG, as the bottom 2DEG is depleted, also resulted in the same charge increase to within experimental accuracy. This change in carrier density is thus independent of the 2DEG that is probed and also of the technique used to measure the effect.

The two-terminal conductances of the different layers were also measured and are shown in Fig. 3, as a function of back gate voltage. The conductance of the middle and top 2DEGs measured together, Fig. 3(a) trace (1), remains almost constant until the bottom 2DEG is depleted at -1.0 V, after which the conductance drops. An extra feature can be seen at -0.60 V which occurs when the middle and bottom 2DEGs have equal carrier densities. Enhanced tunnelling of electrons to the bottom 2DEG then occurs, increasing the total conductance of the device[10]. Measurements of the middle 2DEG conductance show similar features, with the conductance dropping to zero when the middle 2DEG is depleted. The top 2DEG conductance, however, remains relatively constant until the bottom and the middle 2DEGs are depleted. A closer inspection, see the magnified trace in Fig. 3(b), reveals that the top 2DEG conductance starts to increase after the bottom 2DEG is depleted. This increase in conductance has a magnitude which is consistent with the charge increase which has been observed in the previous data. A peak in the carrier density in the top 2DEG is thus produced which occurs before depletion of the middle 2DEG.

Simulations have been performed to model the properties of the triple quantum well structure under investigation. A one-dimensional model is used where the Poisson and Schrödinger equations are solved in a self-consistent manner. This program is used to determine the carrier densities in each QW for given front and back gate potentials. In the simulation an analytic expression for the exchange and correlation term has been used, following from calculations performed by Hedin and Lundqvist[11] based on the Local Density Approximation:

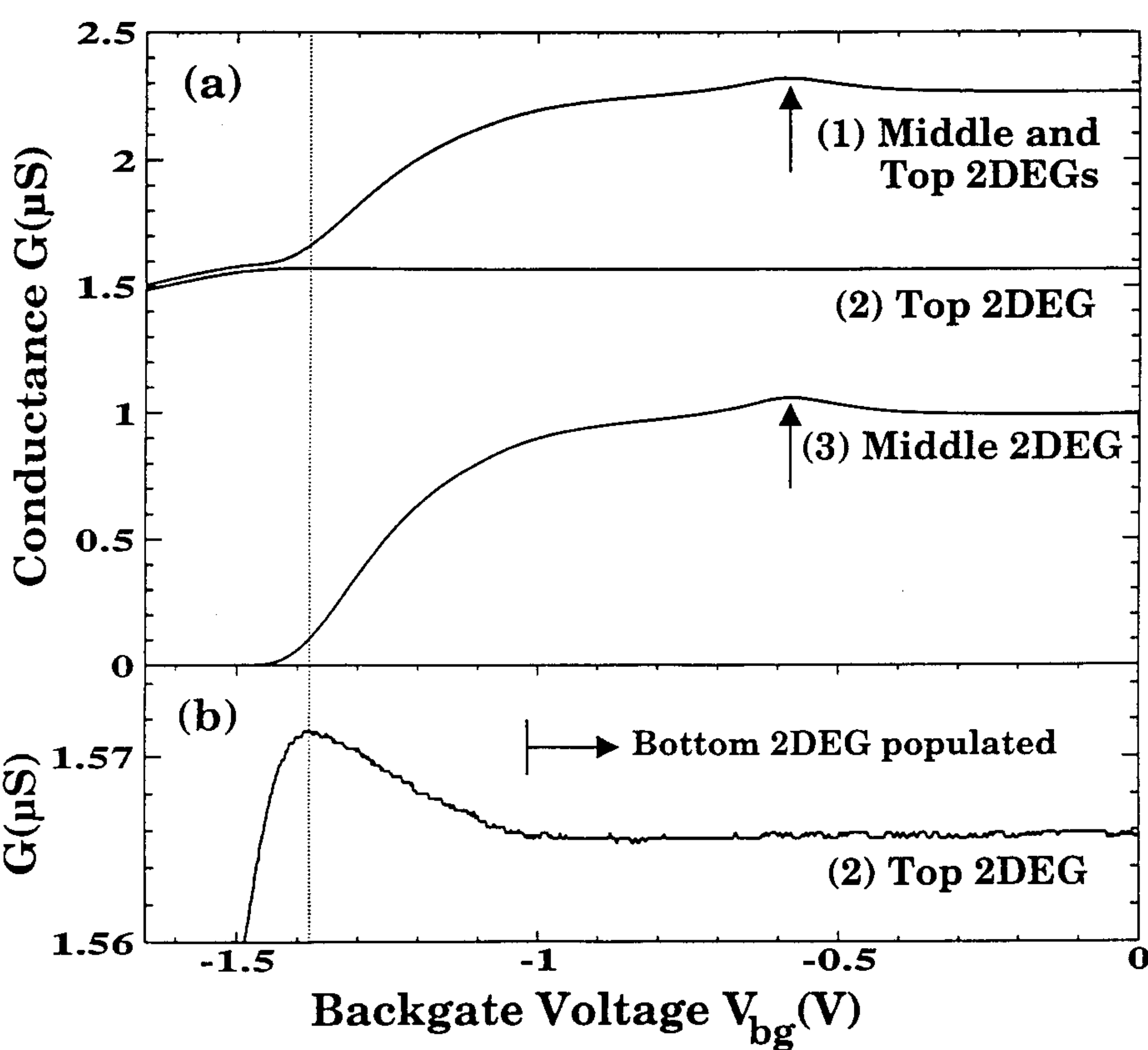

(a)
(1) Middle and
Top 2DEGs
(2) Top 2DEG
(3) Middle 2DEG
Conductance G(μS)
2.5
2
1.5
1
0.5
0
(b)
Bottom 2DEG populated
(2) Top 2DEG
G(μS)
1.57
1.56
-1.5
-1
-0.5
0
Backgate Voltage $V_{bg}$(V)

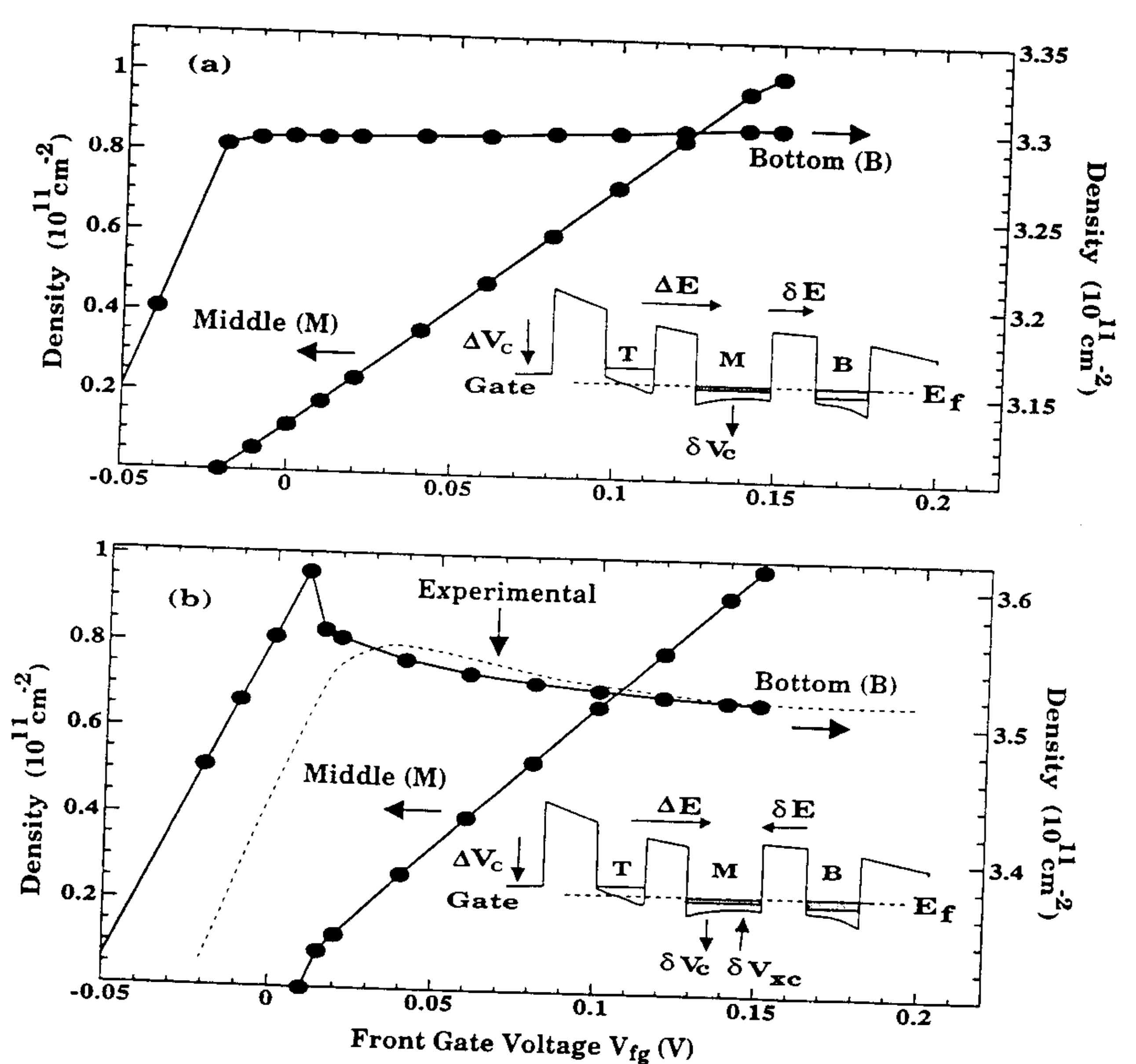


Fig4

accepted for publication in Semicond. Sci. Technol

# Study of the carrier density dependence of the frictional drag between closely spaced two-dimensional electron gases

H Rubel[#], E H Linfield[1], D A Ritchie, K M Brown, M Pepper and G A C Jones

University of Cambridge, Cavendish Laboratory, Madingley Road, Cambridge, CB3 0HE, United Kingdom.

[#] now at: Max-Planck-Institut für Festkörperforschung, Heisenbergstrasse 1, 70569 Stuttgart, Germany

**Short Title:** Carrier dependence of the drag between two 2DEGs

**PACS classification:**

| | |
|---|---|
| 72.20.Fr | Low field transport and mobility; piezoresistance *[Conductivity phenomena in semiconductors and insulators]* |
| 71.38.+i | Polarons and electron-phonon interactions |
| 73.40.Kp | III-V semiconductor-to-semiconductor contacts, p-n junctions, and heterojunctions *[Electronic transport in interface structures]* |

[1] Author to whom all correspondence should be addressed.

## Abstract

We have studied electron transport in two closely spaced, but electrically isolated, two-dimensional electron gases (2DEGs) formed in GaAs/AlGaAs double quantum wells. A frictional drag voltage is found to be induced in one layer when a current is passed through the other. This voltage represents a direct measure of the interlayer electron-electron interactions, since it is determined by the momentum transfer due to scattering events between electrons in the different layers. We present new experimental data, based on a detailed carrier-density dependence of these electron-electron interactions. Our results strongly support a recent theory proposing an interaction via virtual acoustic phonons. We have shown, in particular, that the "phonon part" of the interlayer scattering rate is a function of the relative electron densities in the layers, with a maximum scattering rate when the densities are matched.

## Introduction

Double-layer two-dimensional electron gas (2DEG) systems, where electrons are confined to nearby parallel planes, are expected to exhibit many interesting phenomena due to interlayer electron-electron interactions. These electron-electron interactions can be studied directly by measuring the "drag" voltage induced in one layer when a current is passed through the other. This voltage is generated by momentum transfer from the electrons in the drive layer, which undergo electron-electron scattering events with electrons in the "dragged" layer.

The frictional drag between barrier-separated 2DEGs was first proposed theoretically by Pogrebinskii [1] in 1977 and later discussed by Price [2] in 1983. Difficulties, however, in making independent contacts to the separate layers meant that no experimental data was published before the measurements of Gramila *et al* [3,4] and Solomon and Laikhtman [5] in 1991. Gramila *et al* [3,4] mainly investigated the temperature and barrier-separation dependence of the drag interaction. From this, they concluded that simple Coulomb scattering alone could not, especially for larger layer separations of d>200Å, explain the observed strength of the interlayer scattering (for a detailed calculation of the Coulomb interaction see ref. [6]). In further theoretical [7] and experimental [4] work, it was shown that a second mechanism, based on a virtual acoustic phonon interaction, could explain these electron-electron interactions. Gramila *et al* [4] were not, though, able to change the carrier density in both layers independently in their experiments. This is now possible in our devices, which incorporate an $n^+$ GaAs back-gate that is patterned *in situ* using Ga focussed ion beam lithography. We have thus been able to investigate the carrier dependence of the interlayer scattering rate, gaining important new information about the nature of the electron-electron interactions in double 2DEG systems.

## Experiment

Results are presented from a wafer which consists of two 200Å modulation doped quantum wells separated by a 300Å $Al_{0.33}Ga_{0.67}As$ barrier (see Figure 1). This barrier width was chosen to be sufficiently large that resonant tunnelling between the two layers [8] is negligible. The upper 2DEG has an as-grown carrier density of $3.3x10^{11}$ $cm^{-2}$ and a mobility of $9x10^5$ $cm^2V^{-1}s^{-1}$, the corresponding values for the lower layer being $2.2x10^{11}cm^{-2}$ and $1.3x10^5$ $cm^2V^{-1}s^{-1}$ respectively. The wafer also includes a buried $n^+$ GaAs back-gate layer which was patterned during growth using *in situ* Ga focused ion beam lithography, the details of which have been discussed elsewhere [8-10]. This back-gate layer is situated 3500Å below the lower 2DEG. After growth, optical lithography was used to pattern devices into a Hall bar mesa and to form AuGeNi ohmic contacts to the 2DEGs and back-gate. It was also used to deposit NiCr:Au Schottky gates onto the surface of the wafer. The carrier densities of the upper and lower 2DEGs could then be controlled independently by applying voltages to the full front and back-gates respectively.

The device was put into an independent contact configuration using a selective depletion scheme [10,11] in which negative voltages were applied to the appropriate side front and back-gates (see Figure 1). Before breakdown, a d.c. bias of up to 40mV could then be applied between the two layers with leakage currents of <0.1nA being observed. This showed that the two layers were electrically separated by a barrier resistance of more than 400MΩ and that tunnelling of electrons through the barrier did not occur.

Measurements were carried out using standard lock-in techniques with ac drive currents ($I_{drive}$) in the range 200nA-1μA at a typical frequency of 17.5Hz. This low frequency was used to minimise side effects arising from capacitive coupling between the layers. While passing a drive current through one electron gas, the drag voltage ($V_{drag}$) developed in the other was measured in an open circuit configuration in which

no macroscopic currents passed through the dragged gas. Earth loops can be problematical in this type of measurement, but these were avoided by used a floating current in the drive well, which was generated via an isolating transformer. Only one earthed point was therefore defined in the system and this was located at one of the drive well contacts.

## Results and Discussion

In drag experiments, a current is driven along one well thereby inducing a current or, when no charge is allowed to flow, a voltage in the other. The induced voltage is thus developed from the accumulation of charges swept along the direction of the drive current due to the transfer of electron momentum. As a result, $V_{drag}$ is in the opposite direction to the resistive voltage drop in the drive well and can be related to the interlayer scattering rate $1/\tau_D$ by [6]:

$$\frac{1}{\tau_D} = \frac{e^2}{m}\left(\frac{W}{L}\right)\frac{n_{drive}}{I_{drive}} V_{drag}, \qquad (1)$$

where e is the electron charge, m is the effective mass of the electron, (W/L) is the width to length ratio of the Hall bar and $n_{drive}$ is the carrier density in the drive well. Note that $\tau_D >> \tau_e$, where $\tau_e$ is the elastic scattering time.

The interlayer interactions have been shown [3,4] to be dominated, for small barrier widths, by direct Coulomb scattering between electrons in the two 2DEGs. At low temperatures such that $T << T_F$, where $T_F$ is the Fermi temperature, the Coulomb part of the interlayer scattering rate [6,12] is then:

$$\frac{1}{\tau_D} = \frac{\zeta(3) m \pi^2}{4h^3 (q_0)^2} \frac{1}{d^4} \frac{1}{(n_{drag})^{3/2}} \frac{1}{(n_{drive})^{1/2}} (k_B T)^2, \qquad (2)$$

where $\zeta(3) = 1.202...$, h is Planck's constant, $k_B$ is the Boltzmann constant, $q_0$ is the Thomas-Fermi screening length, T is the temperature and $n_{drag}$ is the carrier density in the dragged electron gas.

Recently, however, the exchange of virtual phonons was shown to be a candidate for a second coupling mechanism [4,7] and the strength of this effect was estimated to depend more weakly on the well separation. Furthermore, Tso *et al* [7] found that the low temperature interlayer scattering rate is primarily dependent on the relative electron densities in the two wells. This is because of phase restrictions on the electron-phonon interaction together with the need for energy and momentum conservation in the separate layers. Emission and adsorption of acoustic phonons with an in-plane wavevector $q_{//}$ was shown to be dominated by transitions with $q_{//} = 2k_F$ ("back-scattering"). As a result, the Fermi wavevectors of the two electron gases must be equal in order to have a strong interaction. In order to see this effect, low temperatures are required so that the broadening of the Fermi surface is sufficiently small that only electrons near the Fermi surface can take part in scattering events.

One method to probe the carrier density dependence of the drag voltage is to vary the density in the upper 2DEG with the front-gate, whilst the density in the lower 2DEG is kept at a constant value, which is determined by the back-gate. The result of one such measurement at 4.2K is shown in the inset to Figure 2. Also shown is the expected behaviour for a pure Coulomb interaction, as calculated from equation (2). Two basic features can be extracted from this graph and these have turned out to be typical for all our measurements. Firstly, we can confirm that the measured scattering rate is higher than would be expected for the Coulomb interaction alone, suggesting that a second mechanism is involved. Secondly, we can observe a clear peak in the scattering rate when the carrier densities in the two quantum wells are matched. This is characteristic of an interaction mediated by virtual acoustic phonons.

This result is further investigated in Figure 2, where the "phonon part" of the scattering rate is plotted as a function of the upper carrier density for different values of lower carrier density. The "phonon part" is defined by subtracting the calculated Coulomb interaction (equation 2) from the measured (total) interlayer scattering rate. From Figure 2, it can be seen that the peak in scattering rate always occurs when the carrier densities are matched. In contrast, when there is a considerable difference in the carrier densities, the "phonon part" of the scattering tends to zero. This is in excellent agreement with theories based on an electron-electron interaction via virtual acoustic phonons.

The carrier densities in the quantum wells can be matched in two other ways. Firstly, the back-gate can be used to vary the lower 2DEG carrier density, whilst the upper 2DEG carrier density is fixed. Secondly, an interlayer bias can be applied between the 2DEGs. The latter shifts the energies of the quantum wells relative to each other. Further, as in a simple plate capacitor, carriers are transferred from one well to the other, thereby increasing the charge in the more negatively biased well. With both techniques, the interlayer scattering rate has again been found to be maximised when the 2DEG carrier densities are matched. These results, together with those presented earlier, are summarised in Figure 3, where the scattering rate at the maximum in the "phonon part" of the interlayer scattering rate is plotted as a function of the (matched) carrier density. It can be seen that the peak scattering rate increases linearly with carrier density, similar to the behaviour observed in earlier experiments [13,14] on electron-phonon interactions.

The effect of different temperatures on the "phonon part" of the interlayer scattering rate is shown in Figure 4. It can be seen that, at temperatures above 4.2K, a maximum is still visible in the scattering rate, again occurring at matched carrier densities. At temperatures above 10K, there is, however, a substantial scattering rate even when there is a large mismatch in the carrier densities. This is not due to the

onset of plasmon interactions [15] between the two 2DEGs since the temperature is still too low for this. Instead, it arises from thermal broadening of the Fermi surfaces of the two interacting electron gases becoming more and more significant, thereby relaxing the conditions for scattering between the 2DEGs to occur.

## Conclusions

New experimental data has been presented on the carrier density dependence of interlayer electron-electron scattering rates in double 2DEG systems. We have shown, in particular, that the "phonon part" of the interlayer scattering rate is a strong function of the relative electron densities in the layers, with a maximum value at matched carrier densities. Further, this maximum scattering rate was observed to increase linearly with carrier density. Our experimental data gives important additional information to that presented in previous research, which concentrated on the temperature and barrier-separation dependence of the scattering rate. In addition, our results strongly support recent theories which suggest that the interlayer scattering between two 2DEGs is determined not only by a pure Coulomb interaction, but also by a virtual phonon scattering mechanism.

## Acknowledgements

We would like to thank Dr C H W Barnes and Dr A R Hamilton for many interesting discussions on this work and P Rose for technical assistance. H Rubel and Dr D A Ritchie acknowledge support from the Konrad-Adenauer-Foundation (Germany) and the Toshiba Cambridge Research Centre respectively. This work was supported by the Engineering and Physical Sciences Research Council (UK).

## References


[1] Pogrebinskii M B 1977 *Sov. Phys. Semicond.* **11** 372.

[2] Price P J 1983 *Physica B* **117** 750.

[3] Gramila T J, Eisenstein J P, MacDonald A H, Pfeiffer L N and West K W 1991 *Phys. Rev. Lett.* **66** 1216; Gramila T J, Eisenstein J P, MacDonald A H, Pfeiffer L N and West K W 1992 *Surf. Sci.* **263** 446.

[4] Gramila T J, Eisenstein J P, MacDonald A H, Pfeiffer L N and West K W 1993 *Phys. Rev. B* **47** 12957.

[5] Solomon P M and Laikhtman B 1991 *Superlatt. Microstruct.* **10** 89.

[6] Jauho A-P and Smith H 1993 *Phys. Rev. B* **47** 4420.

[7] Tso H C, Vasilopoulos P and Peeters F M 1992 *Phys. Rev. Lett.* **68** 2516.

[8] Brown K M, Linfield E H, Ritchie D A, Jones G A C, Grimshaw M P and Pepper M 1994 *Appl. Phys. Lett.* **64** 1827.

[9] Linfield E H, Jones G A C, Ritchie D A and Thompson J H 1993 *Semicond. Sci. Technol.* **8** 415.

[10] Brown K M, Linfield E H, Ritchie D A, Jones G A C, Grimshaw M P and Churchill A C 1994 *J. Vac. Sci. Technol. B* **12** 1293.

[11] Eisenstein J P, Pfeiffer L N and West K W 1990 *Appl. Phys. Lett.* **57** 2324.

[12] Zheng L and MacDonald A H 1993 *Phys. Rev. B* **48** 8203.

[13] Hensel J C, Dynes R C and Tsui D C 1983 *Phys. Rev. B* **28** 1124; Hensel J C, Halperin B I and Dynes R C 1983 *Phys. Rev. Lett.* **51** 2302.

[14] Rothenfusser M, Köster L and Dietsche W 1986 *Phys. Rev. B* **34** 5518.

[15] Flensberg K and Hu B Y-K 1994 *Phys. Rev. Lett.* **73** 3572.

## Figure Captions

**Figure 1** Cross-sectional and plan diagrams of the device. The initial growth consisted of a 50nm $n^+$ GaAs layer which was selectively implanted *in situ* with 30 keV Ga ions. The heterostructure was then completed by growth of two modulation doped 20nm quantum wells, separated by a 30nm AlGaAs barrier The diagrams also show how a "selective depletion" scheme can be used to contact the 2DEGs independently by applying negative voltages to the appropriate front and back defining gates.

**Figure 2** The "phonon part" of the scattering rate as a function of the upper 2DEG carrier density. Separate curves are shown for different values of the lower 2DEG carrier density, each curve being offset by $1/\tau_D = 5\times10^6 s^{-1}$. The solid lines through the sets of data points are intended only as a guide to the eye. The arrows indicate the points at which the carrier denisties in the two wells are equal. The inset shows the measured total scattering rate, together with the calculated Coulomb contribution, as a function of the upper 2DEG carrier density for a lower 2DEG carrier density of $3.35 \times10^{11}$ $cm^{-2}$.

**Figure 3** The peak height of the "phonon part" of the scattering rate as a function of the (matched) carrier density, as obtained with differing measurement configurations. The squares correspond to data from Figure 2, whilst the triangles represent measurements in which the lower carrier density was continuously varied at fixed values of the upper 2DEG carrier density. Results obtained by applying an interlayer bias between the 2DEGs are represented by circles. The solid line in the figure is a linear fit to all of the data shown.

**Figure 4** The "phonon part" of the scattering rate as a function of carrier density for different measurement temperatures. No vertical offset is used in this figure.

Figure 1

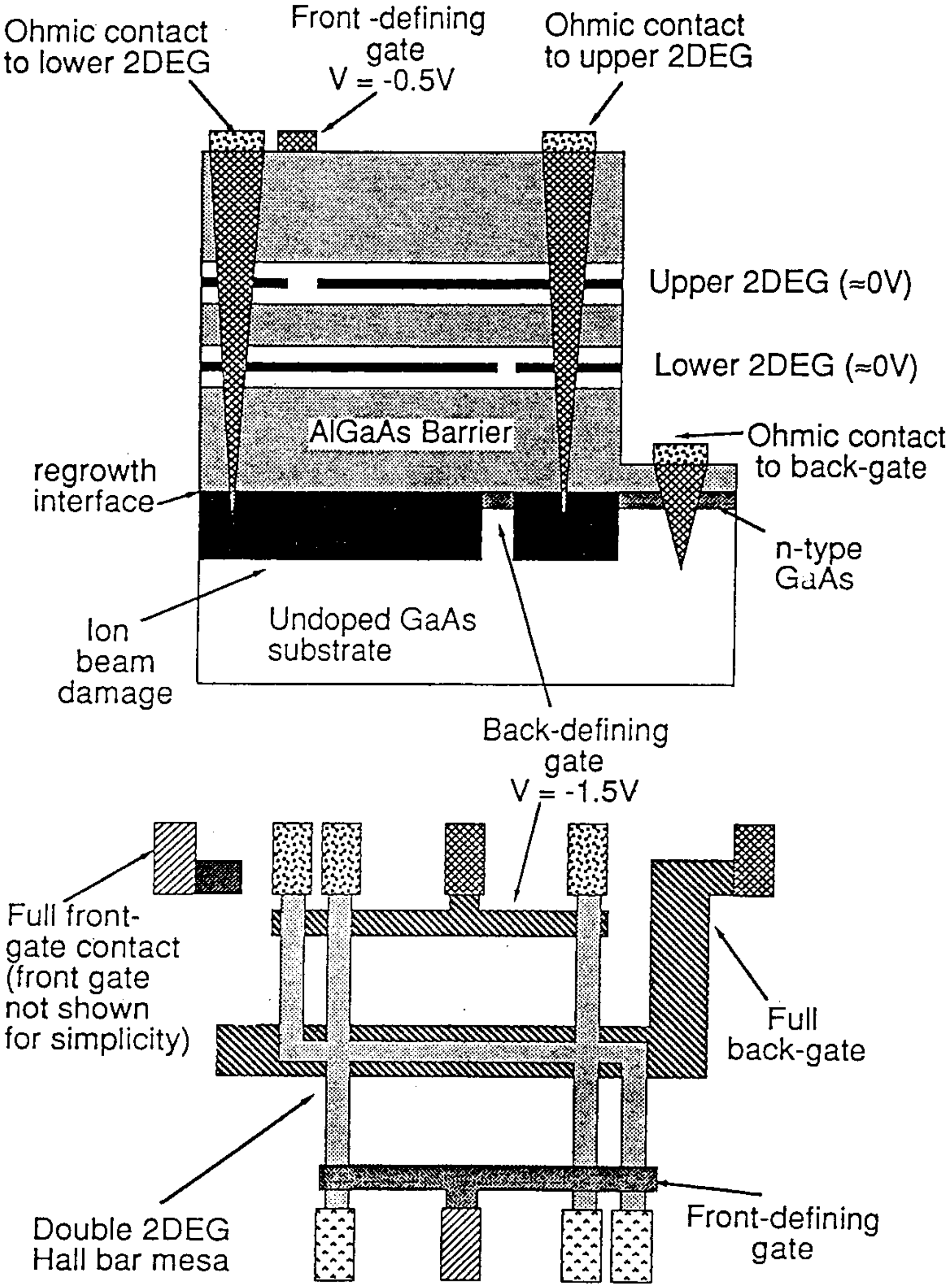

Figure 2

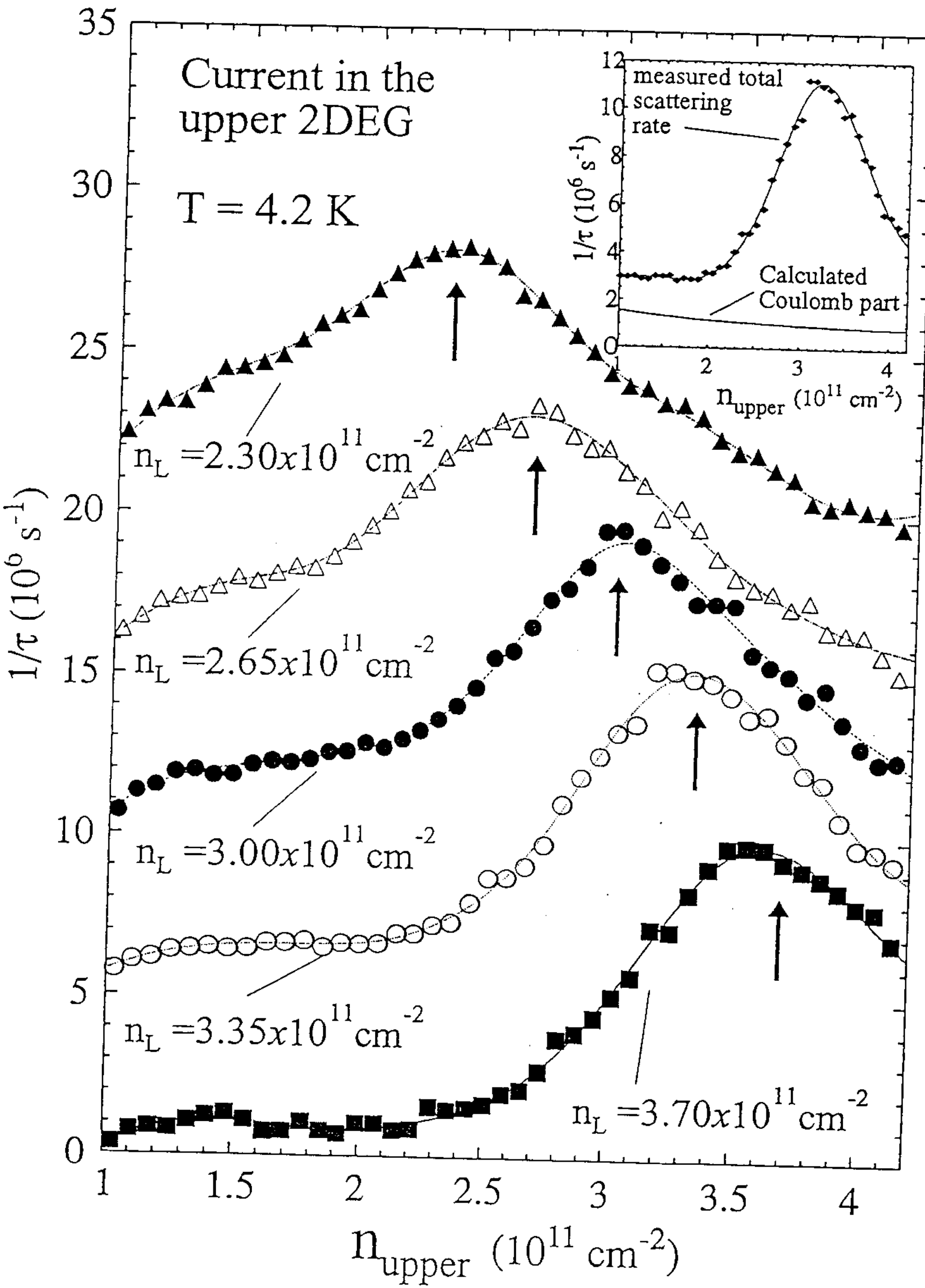

Figure 3

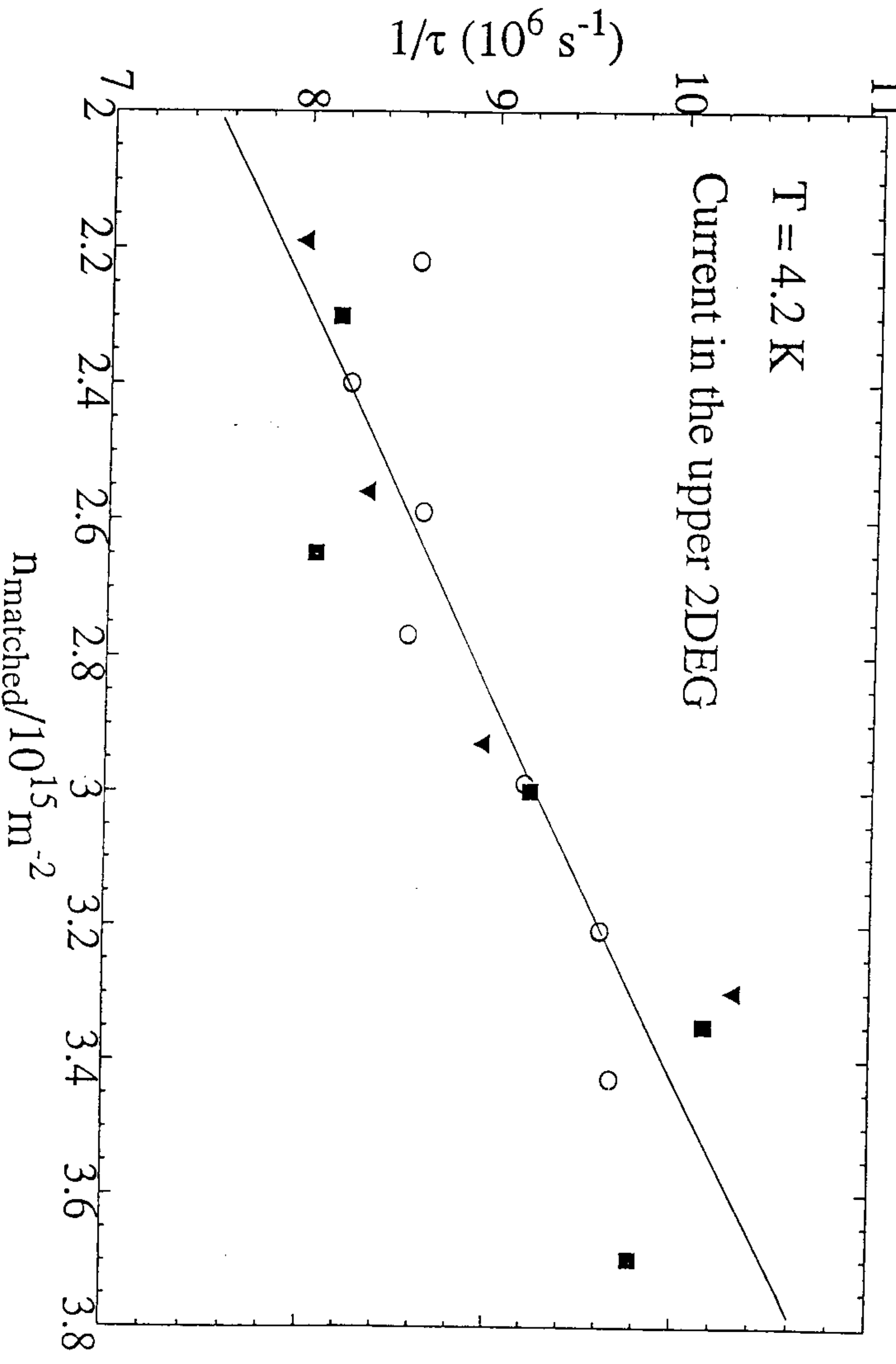

Figure 4

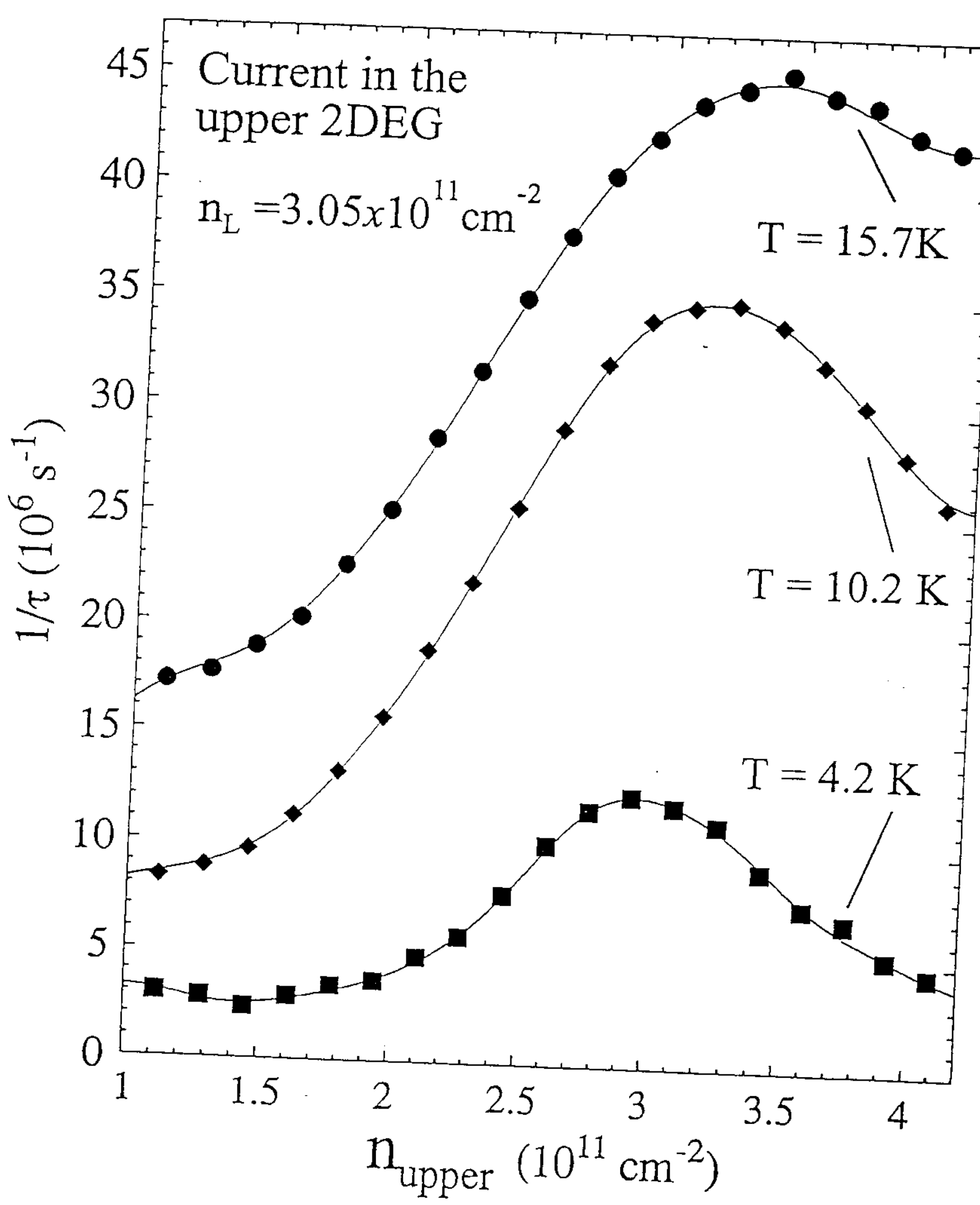

and submitted to "Surface Science"

# Coulomb Blockade as a Non - Invasive Probe in Double Layer 2DEG Systems

M. Field, C.G. Smith, M. Pepper, K.M. Brown, E.H. Linfield,
M.P. Grimshaw, D.A. Ritchie and G.A.C. Jones
*Cavendish Laboratory, Madingley Road, Cambridge CB3 0HE, United Kingdom*

We have used a double two dimensional electron gas (double 2DEG) sample to measure the density of states in one of the 2DEGs over a submicron area. The lower 2DEG screens the electric field between the plates of a mesoscopic capacitor made up of a quantum dot in the upper 2DEG and a backgate behind both 2DEGs. The capacitance is measured by observing the Coulomb blockade period of the dot as function of backgate voltage. The density of states is inferred from the screening, the technique is sensitive to both localised and extended electronic states.

Direct transport measurements disrupt the system being measured and only reveal information about the diffusivity of electrons in states contributing to conduction. The use of a "non-invasive" technique in which the local conditions in one circuit affect a nearby measuring circuit allows the system to remain undisturbed and measures properties over the small length scale in which the two circuits are brought close enough together to interact [1]. One such class of non-invasive measurement is the determination of the screening ability of a sample by capacitance techniques. In this paper we use a two dimensional electron gas (2DEG) to screen a perpendicular electric field between the plates of a mesoscopic capacitor, allowing the compressibility of the screening layer to be measured over a microscopic area.

Measuring the density of states experimentally requires a technique which measures a thermodynamic property of the 2DEG, such as specific heat [2,3], magnetisation [4] or magnetocapacitance [5,6,7]. Using samples with two separate, independently contacted, 2DEG's [8] together with a back gate behind both 2DEGs allows the capacitance between the upper 2DEG and the backgate to be measured [7]. The back 2DEG screening can then be inferred over a large area, from which the compressibility and the density of states are deduced.

A double 2DEG sample was grown with two 200 Å quantum wells a distance of 200 Å apart, and a backgate 3300 Å beneath the lower 2DEG. The mobility of the upper layer was $7 \times 10^5$ $cm^2/Vs$ at a carrier concentration $N_t = 4.5 \times 10^{11}$ $cm^{-2}$, while the lower layer had a low mobility of $3 \times 10^4$ $cm^2/Vs$ at the same carrier concentration, $N_b = N_t$. The carrier concentration in the lower layer was controllable via the backgate, complete depletion occurring at approximately -1.4 V.

The sample was patterned into a thin Hall bar shape (0.6 μm wide by 2 μm long) by low energy gallium ion beam damage [8]. Two independent surface Schottky gates of width approximately 500 Å cross the Hall bar a distance of 0.4 μm apart. Using these surface gates a quantum box can be induced in the upper 2DEG. The completed device is shown schematically in figure 1. Measurements were made in a dilution refrigerator with a base temperature of less than 50 mK. The conductance of both the top and bottom 2DEG were measured simultaneously by ac phase sensitive detection using an excitation

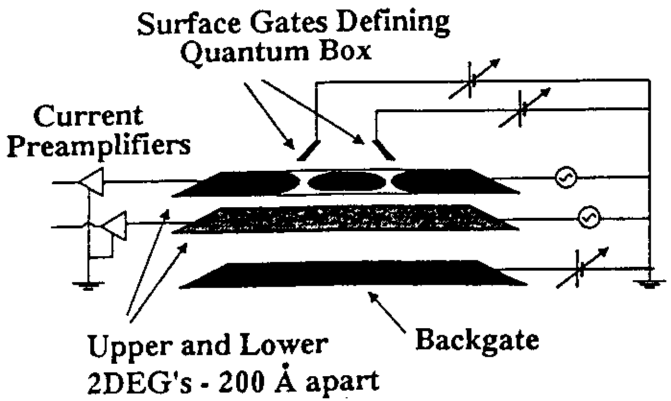


Figure 1: A schematic diagram of the double 2DEG device.

voltage of 10 $\mu$V.

We measure the screening non-invasively over a small area using the quantum box in the upper 2DEG layer. This small island of charge exhibits Coulomb blockade (CB) effects [9]. The conductance of the upper layer oscillates on changing the potential of a nearby gate; the period of oscillation being inversely proportional to the capacitance between the gate and the dot. Using the back gate to induce CB oscillations in the quantum box allows the capacitance to be measured directly, including any screening effects of the back 2DEG. By making the backgate voltage extremely negative, the carriers in the back 2DEG can be depleted out and the direct capacitance between the back gate and the quantum box measured in the absence of screening. Similarly applying a voltage directly to the back 2DEG allows it to be used as a gate, the capacitance between the back 2DEG and the dot can be measured as well as the active area, A = 0.51 x 0.51 $\mu m^2$, of the dot. In the quantum Hall regime, the dot exhibits Aharonov - Bohm oscillations as the magnetic field is swept [10]. The area extracted from this measurement agrees with that obtained from the Coulomb blockade measurement above.

The total capacitance seen by the backgate can be modelled by the equivalent circuit proposed by Luryi [11] which has an extra capacitance $C_Q$ in parallel with the geometric capacitance's due to the extra energy required to place electrons in the quantum well due to the finite density of states. This quantum capacitance was first measured by Smith [5] and calculated explicitly by Büttiker [12], who also derived the full 3x3 capacitance matrix for this system. Effects due to electron-electron interactions or the non-zero extent of the wavefunction perpendicular to the 2DEG were considered explicitly by Eisenstein [7].

The equivalent circuit gives the total capacitance as seen by the backgate. The CB period allows the capacitance from the backgate to the dot to be measured, from which the quantum capacitance and hence the density of states can be extracted.

$$\frac{1}{C_Q} = \frac{1}{e^2}\left(\frac{1}{dN_b/dE}\right) \qquad (1)$$

Applying the above theory, the density of states can be extracted from the observed period of CB oscillations as the backgate voltage is swept with the back 2DEG grounded.

The model introduced above will be used for small voltage swings (± 0.075 V) around $V_{bg} = 0$. In this region there is little variation of CB period with backgate voltage and the constant density of states model can be applied. The corrections due to the exchange and correlation energies, together with effects due to charge movement perpendicular to the 2DEG within the confines of the well, will tend to reduce the capacitance [5,7]. We have introduced a numerical factor $\gamma$ ($\gamma = 0.725$, compared with the numerical constant of 0.7 found by Smith [5]) to the quantum capacitance $C_Q$ which brings the predicted CB period in to line with the observed period at $V_{bg} = 0$. Using this value the deduced density of states is computed to be the same as the theoretical value of $m^*/\pi\hbar^2$.

On changing the magnetic field the period of CB oscillations without the back 2DEG is not substantially affected, whereas the screening component oscillates with inverse magnetic field. At zero back gate voltage the oscillation period is 16.2 mV in zero magnetic field and the lower 2DEG carrier concentration measured by Shubnikov - de Haas ~ 2.7 x $10^{11}$ $cm^{-2}$. The upper trace (a) in figure 2 shows both the CB period as a function of the inverse magnetic field (right hand axis), and the derived density of states of the back 2DEG (left hand axis). The screening oscillates with a period in 1/B of 0.135 Tesla $^{-1}$, giving a carrier concentration of 3.5 x $10^{11}$ $cm^{-2}$ compared with a measured lower layer concentration of 2.7 x $10^{11}$ $cm^{-2}$.

The carrier concentration in the lower layer immediately under the dot may well be higher than the carrier concentration at the most constricted part of the Hall bar. There is some evidence that the dot is not aligned with the narrowest portion of the ion beam defined channel.

The lower trace, figure 2(b), is the measured $R_{xx}$ of the back 2DEG showing Shubnikov - de Haas oscillations. This was taken at a more positive backgate voltage such that the measured carrier density (determined by the density at the most constricted point along the channel) is the same as that found under the dot from the change in density of states. The low field Shubnikov - de Haas oscillations follow the modulation of the density of states. At higher fields $R_{xx}$ drops to zero in the minima as the Fermi energy sits in localised states, the peak width is noticeably narrower. The density of states however continues to oscillate with the same peak width. Unlike the transport measurements the screening technique is sensitive to localised as well as extended states.

The dot is detecting densities of states of order 1 - 5 x $10^{13}$ $cm^{-2}$ $eV^{-1}$, with a resolution of ± 5 x $10^{12}$ $cm^{-2}$ $eV^{-1}$. Since the area and the energy scales are both known, the actual number of electron states can be deduced ( a carrier density of $N_b$ = 3.5 x $10^{11}$ $cm^{-2}$ implies a Fermi energy $E_F$ = 12.5 meV, the majority of screening occurs in the area of equal size directly below the dot). The system is thus measuring the screening varying by 330 - 1700 electron states, with a sensitivity of ± 170 electron states.

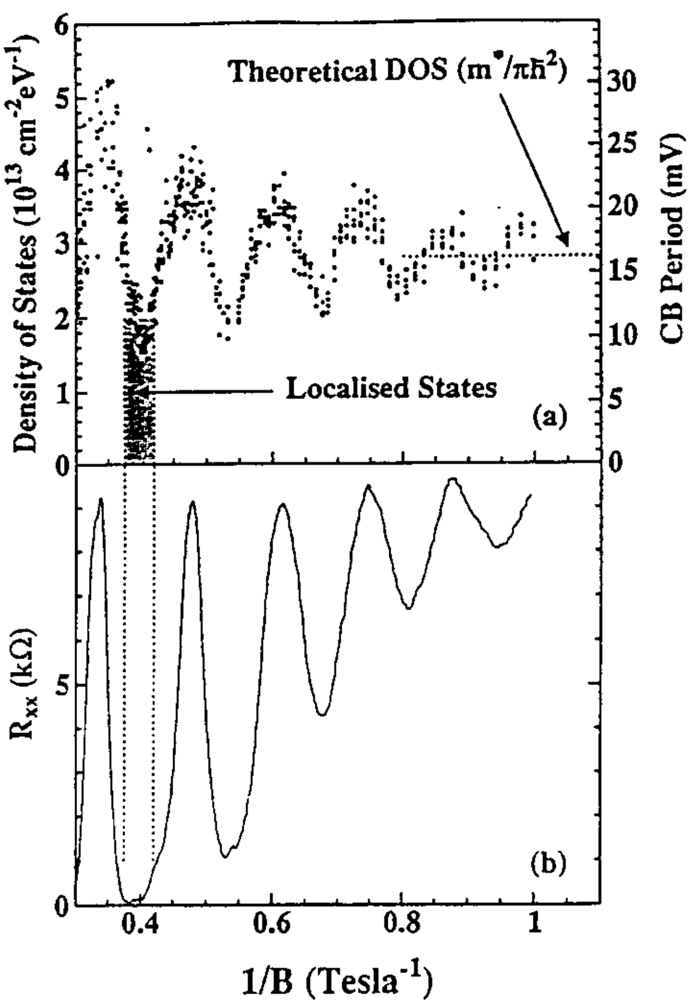


Figure 2: (a) The Coulomb blockade period as a function of inverse magnetic field (right hand axis) and the deduced density of states at the Fermi energy (left hand axis). (b) $R_{xx}$ of the back 2DEG showing Shubnikov - de Haas oscillations, taken at a more positive backgate voltage such that the measured carrier density is the same as that found under the dot. The density of states measurement is sensitive to both the extended and localised electronic states.

At zero magnetic field the period of CB oscillations is seen to change dramatically at a backgate voltage of -1.42 V (figure 3) from 7 mV to 2 mV as the screening layer is depleted. The conductance of the back 2DEG dropped below the sensitivity of the measurement at a more positive gate voltage (-1.3 V), the point of complete depletion can only be observed in the screening. As the back 2DEG depletes out it may undergo an Anderson transition, screening then occurs by thermal activation to the mobility edge or by variable range hopping. The carrier density in the lower 2DEG at the transition point is estimated by extrapolating the known dependence at higher backgate voltages at $N_b$ = 1.2 x $10^{11}$ $cm^{-2}$, $E_F$ = 4.4 meV.

The product $N_b^{1/2}a_H = 0.35$ ($a_H$ being the Bohr radius corrected for dielectric constant and effective mass) is close to the predicted value for an Anderson transition of 0.27 [13]. Increasing the temperature moves the point of depletion to more negative gate voltages and flattens out the transition. The backgate voltage can be recalibrated in terms of back 2DEG Fermi energy giving an estimate of the mobility edge at $E_c = 4.4$ meV. The actual pinch off underneath the quantum dot may well occur at different back gate voltages to the observed turn on of the back 2DEG conductivity. The screening will depend on whether the states underneath the dot are localised, and if not whether they can reach the ohmic contacts which define the ground potential.

In conclusion we have measured the density of states in a submicron area of a 2DEG using a non-invasive capacitance technique. The technique is sensitive to both the extended and localised electronic states.

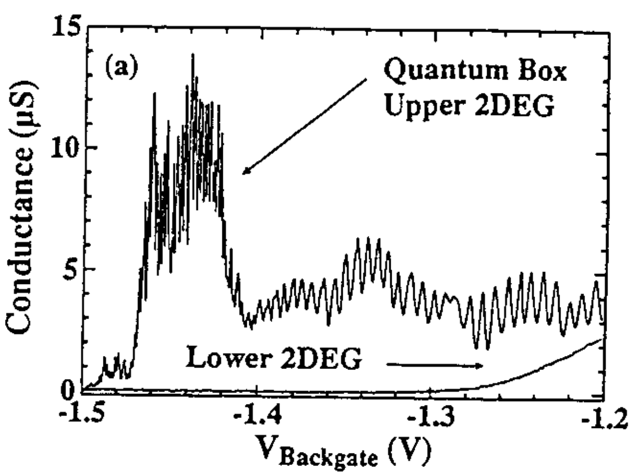


Figure 3: Coulomb blockade oscillations which change period suddenly when the lower 2DEG is fully depleted and can no longer screen. The conductance of the lower 2DEG falls below the minimum sensitivity of the equipment before the 2DEG is completely depleted.

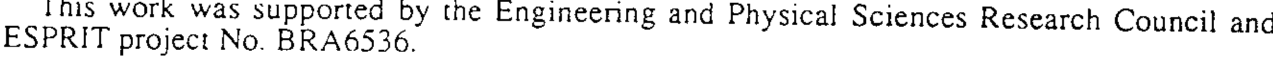

This work was supported by the Engineering and Physical Sciences Research Council and ESPRIT project No. BRA6536.

[1] M. Field, C.G. Smith, M. Pepper, D.A. Ritchie, J.E.F. Frost, G.A.C. Jones and D.G. Hasko; Phys. Rev. Lett. **70**, 1311 (1993)

[2] E. Gornik, R. Lassnig, G. Strasser, H.L. Störmer, A.C. Gossard and W. Wiegmann; Phys. Rev. Lett. **54**, 1820 (1985)

[3] J.K. Wang, J.H. Campell, D.C. Tsui and A.Y. Cho; Phys. Rev. B **38**, 6174 (1988)

[4] T. Haavasoja, H.L. Störmer, D.J. Bishop, V. Narayanamurti, A.C. Gossard and W.Wiegmann; Surface Science **142**, 294 (1984)

[5] T.P. Smith, B.B. Goldberg, P.J. Stiles and M. Heiblum; Phys. Rev. B **32**, 2696 (1985)

[6] R.C. Ashoori and R.H. Silsbee; Solid State Communications **81**, 821 (1992)

[7] J.P. Eisenstein, L.N. Pfeiffer and K.W. West; Phys. Rev. B **50**, 1760 (1994)

[8] K.M. Brown, E.H. Linfield, D.A. Ritchie, G.A.C. Jones, M.P. Grimshaw and A.C. Churchill; J. Vac. Sci. Tech. B **12**, 1293 (1994)

[9] For a review of Coulomb blockade effects see H. Grabert and M.H. Devoret, eds. "Single Charge Tunnelling". Vol. **B294** NATO ASI Series B; New York, Plenum Press (1992)

[10] R.J. Brown, C.G. Smith, M. Pepper, M.J. Kelly, R. Newbury, H. Ahmed, D.G. Hasko, J.E.F. Frost, D.C. Peacock and G.A.C. Jones; J. Phys.: Cond. Matter **1**, 6291 (1989)

[11] S. Luryi; Appl. Phys. Lett. **52** (6), 501 (1988)

[12] M. Büttiker, H. Thomas and A. Prêtre; Phys. Lett. A **180**, 364 (1993)
M. Büttiker; J. Phys.: Cond. Matter **5**, 9361 (1993)

# Tunnelling between 2D and 1D electron gases in devices fabricated by in-situ focused ion beam lithography

B.Kardynał, E.H.Linfield, D.A.Ritchie, K.M.Brown, G.A.C.Jones, M.Pepper
University of Cambridge, Cavendish Laboratory, Madingley Road, Cambridge,
CB3 0HE, UK

## Abstract

Tunnelling between one dimensional (1D) and two dimensional (2D) electron gases has been studied as the energy of the tunnelling electron was varied by the voltage applied to an in-built back gate. The tunnelling differential conductance, measured between the 2D electron gas source and the 1D electron gas drain, reflects the electron density and wavefunctions of the 1D electron gas.

One dimensional (1D) electron structures have been extensively investigated both theoretically and experimentally over the past decade. The development of the split gate[1] and discovery of conductance quantisation in semiconductor ballistic point contacts[2] initiated great interest in this field. Since then several methods have been employed to study electronic states in 1D structures independently from the lateral transport properties. These include capacitance, optical spectroscopy and tunnelling experiments. Capacitance measurements have shown a modulation of the density of states in superlattices of wires as the 1D energy levels were swept through the Fermi level.[3] This modulation was also reflected in the tunnelling current from a leaky waveguide to a 2DEG, as the 1D channels became gradually depopulated.[4] Optical spectroscopy has been used successfully to determine the electron energy levels in 1D wires.[5] The drawback of this method is that the shift of the energy levels towards higher values, due to the polarisation effect, prevents a direct comparison with transport measurements. Resonant tunnelling through 1D states has been investigated in double barrier resonant tunnelling diodes (DBRTDs) by a number of groups.[6,7] Further, tunnelling between 1D wires and a two dimensional electron gas (2DEG) through a single AlGaAs barrier has provided another way of probing 1D states,[8] as it is sensitive to the density of states and the electronic wavefunctions in a similar manner to the tunnelling in DBRTDs.[7,9] Tunnelling experiments have shown that the tunnelling current in mesoscopic RTDs is very sensitive to the presence of impurities. In all of the above tunnelling experiments the tunnelling current was measured with a DC bias applied between the emitter and the collector of the device. In DBRTDs a change of DC bias affected the confinement in the emitter of the device and therefore the tunnelling current. It was not a problem in the tunnelling through a single barrier, but in both types of tunnelling experiment the DC bias limited the sensitivity of the measurements. It is due to the fact, that the electron states are probed in the energy band set by DC bias and the phonon assisted tunnelling takes place at higher biases.

In this letter we present our work on resonant tunnelling between a superlattice of 1D wires and a 2DEG through a single AlGaAs barrier. We have studied samples in

which only a few 1D subbands and one 2D subband contribute to the tunnelling current. Moreover we have been able to control the occupancy of both systems with front and back-gates. An important aspect here has been our ability to measure the tunnelling in equilibrium, i.e. with no DC bias applied between the layers. This has allowed us to measure for the first time the tunnelling currents as a function of electron energy.

For these experiments, we used double quantum wells (Figure 1) fabricated by molecular beam epitaxy regrowth on in-situ Ga focused ion beam implanted back-gate structures.[10] We thereby achieved very effective back gating, high mobility 2DEGs and very good reproducibility. The back-gate, a 50nm $n^+$ GaAs layer, was in-situ ion implanted in order to damage selective areas and hence achieve regions of conducting back-gates which were electrically insulated from each other. After the back-gates were patterned, a double modulation doped quantum well structure was regrown, separated from the back-gate layer by a 200nm undoped $Al_{0.33}Ga_{0.67}As$ barrier. Each 2DEG occupied the lowest subband of a 20nm GaAs quantum well, with a 12.5nm undoped $Al_{0.33}Ga_{0.67}As$ barrier being used to separate the wells. The modulation doping layers deposited above and below the double quantum wells created 2DEGs with densities of $3.3 \cdot 10^{15} m^{-2}$ and $2.0 \cdot 10^{15} m^{-2}$ in the upper and lower layers respectively. The low temperature mobilities were $50 m^2 V^{-1} s^{-1}$ and $20 m^2 V^{-1} s^{-1}$.

Optical and electron beam lithography processes were subsequently used to fabricate the samples, which are shown schematically in Figure 1. The mesa was patterned using an $H_2SO_4$:$H_2O_2$ based solution with standard AuGeNi ohmics being used to contact the 2DEGs and the back-gates. Both sets of contacts were fabricated in the same process, ion implantation under the contacts to the 2DEGs preventing any leakage between the 2DEGs and the back-gates.[10] The 2DEG ohmic contacts connected both 2DEGs to each other so in order to contact each of them separately, we used a selective depletion scheme.[11] In this technique there is one gate (front Schottky or the back $n^+$ GaAs) formed next to each ohmic contact to the 2DEGs. By applying an appropriate negative bias voltage to a front Schottky gate ($V_{FG1}$) the upper 2DEG may

be depleted, leaving only the lower one conducting. Similarly a back-gate voltage ($V_{BG1}$) can be used to deplete the lower 2DEG while leaving the upper one unaffected. This allows the measurements of both layers together, each 2DEG individually or the tunnelling between them.

The properties of the lower and the upper 2DEGs in the tunnelling region were controlled with a back-gate underneath and a front Schottky gate on top of the sample respectively. Application of a voltage to the full back-gate ($V_{BG}$) below the tunnelling region allowed the carrier concentration to be changed in the lower 2DEG from zero up to $3.5 \cdot 10^{15}$ m$^{-2}$. The front Schottky gate was patterned by the electron lithography into a superlattice of 200nm wide gates. This introduced a modulation of the confining potential in the upper 2DEG and for this work three samples were measured with superlattice periods of 700nm, 600nm and 350nm. By applying a bias to this front gate, the potential in the top well could be varied from zero to that required to form 1D channels. The relatively weak coupling between the two quantum wells meant that the lower 2DEG was not affected. Care was taken to align the front and back-gates in order to minimise the effect of tunnelling from unpatterned regions of the device.

Samples were measured in the dark at 300mK. There was no leakage current between pairs of gates, or the gates and the quantum wells, over the whole range of gate bias voltages used in the experiment. The tunnelling differential conductance was measured in a two terminal, constant voltage mode with a 100μV ac excitation voltage at a frequency of 79Hz. The measured current, due to tunnelling, was detected using a lock-in technique with the in-phase part of the response signal being monitored.

Figure 2 shows the tunnelling differential conductance of the device with a 700nm superlattice period, measured as a function of the back-gate voltage, but with the front gate voltage fixed. The back-gate voltage changes the carrier concentration in the lower 2DEG and hence the Fermi energy of the tunnelling electrons. The graph therefore effectively represents the tunnelling differential conductance as a function of energy of the tunnelling electrons. The uppermost curve in this figure was obtained with the front gate earthed and is a typical characteristic of 2D-2D tunnelling.[12] The

tunnelling current is very small over the whole range of the back-gate voltages except for $V_{BG}$=0.8V (peak A in the figure) when the carrier concentrations in both 2DEGs are matched. The condition of total energy and the in-plane momentum conservation is then fulfilled and for the resonant tunnelling between the two 2DEGs occurs.

When a bias voltage was applied to the front gate, the tunnelling signal changed. The differential conductance is shown in Figure 2 for $V_{FG}$=-0.2V and $V_{FG}$=-0.45V. In the former case, the 2DEG in the top well is modulated but separate 1D wires are not yet formed; in the latter, the modulation is strong enough to separate the wires from each other. Full formation of the 1D wires is seen by the disappearance of the 2D-2D tunnelling signal from regions underneath the gates. The differential conductance of the tunnelling between the modulated and the plain 2DEGs (for $V_{FG}$=-0.2V) shows two large peaks. One of them (B in the figure) is due to the 2D-2D tunnelling from regions not covered with the front gate and the second (C in the figure) is due to the 2D-2D tunnelling from the regions under the front gate, where the carrier concentration is reduced. The additional small structure between these two peaks is due to the periodic modulation of the potential in the 2DEG, that changes the dispersion relation in the direction of confinement and hence the position of peaks.[13]

Once the wires are formed ($V_{FG}$=-0.45V), the tunnelling characteristics change completely. The peak at $V_{BG}$=0.8V disappears and a peak (D in the figure) which is much smaller in amplitude and broader replaces it together with several smaller peaks at more negative back-gate voltages. This structure is superimposed on a background conductance of 1μS, which is larger than for 2D-2D tunnelling, where the tunnelling signal away from the resonance was less than 0.1μS. The tunnelling structure observed in this 2D-1D experiment does not however directly reflect the 1D density of states. The main difference between the 2D-2D tunnelling and 2D-1D tunnelling is that in the latter case the conservation rules are relaxed: the component of the wavevector of the tunnelling electron in the confinement direction does not have to be conserved.[7,9] This means that provided the energy of the electron in the 2DEG is lower than the energy of the bottom of the 1D subband, the tunnelling between these two subbands is

allowed. This means if there are n 1D subbands with energy higher than the Fermi energy in the 2DEG, then these n 1D subbands will all contribute to the tunnelling. The probability of an electron tunnelling between the 2D subband and the 1D subband is proportional to the Fourier transform of the wavefunction of the 1D subband, as is found by considering the overlap integral between electron wavefunctions in the initial and final states.[7,9] The tunnelling current, calculated from conservation rules and from the tunnelling probability, has a number of maxima which depends on the index of the subband. One of these maxima is much higher than the rest. Its position does not coincide with the position of the 1D subband energy, but is shifted towards higher energies. In the case of a weak confinement, as obtained in our samples when a bias voltage is applied to the front Schottky gate, the tunnelling current maxima from all 1D subbands occur at almost the same electron energies (i.e. back gate voltages). This explains why the 2D-1D tunnelling signal, as seen in Figure 2, has one broad and smooth peak with several smaller ones.

In Figure 3 we compare the tunnelling signal from 1D wires for three devices with different superlattice periods (700nm, 600nm, 350nm), but measured at the same front gate bias voltage ($V_{FG}$=-0.5V). The 350nm period superlattice sample was slightly misaligned and as a result, the measured tunnelling current in this sample was superimposed on a background, which is independent of the front Schottky gate voltage. As the width of the wires decreases, the main broad tunnelling peak moves to more negative back-gate voltages and its amplitude decreases. The former effect may be due to both: stronger capacitive coupling between gates and electron gas for the superlattice with smaller period, and also a shift of 1D subband energies to higher values. The amplitude decrease reflects the fact that there are less 1D subbands contributing to the tunnelling in narrower wires. More notably, the main tunnelling peak (C in the figure) from the narrowest wire has a shoulder on top of it (arrowed in the figure). This is because there are at most six 1D subbands in a channel of this width, so the tunnelling signal from the higher subbands does not smear out the signals from the lowest ones. In this case we can recognise the contribution of the lowest

subbands to the tunnelling differential conductance. In the experiment with 700nm or 600nm period superlattice samples, where the channels support more than ten 1D subbands, it is impossible to recognise the contribution of single subbands to the main tunnelling peak (A and B in the figure).

In conclusion, we have observed equilibrium resonant tunnelling between a one dimensional and a two dimensional electron gas. The tunnelling experiments revealed a drastic change of tunnelling differential conductance as the dimensionality of the electron gas in the upper quantum well was altered. This demonstrates the importance of the contribution of the overlap integral of the electron wavefunctions to the resonant tunnelling current between 1D and 2D electron gases.

B.K. acknowledges the financial support for the Trinity College, University of Cambridge and the Committee of Vice-Chancellors and Principals of the Universities of the UK. D.A.R acknowledges support from TCRC. This work was funded by the EPSRC.

References

[1]T.J.Thorton, M.Pepper, H.Ahmed, D.Andrews and G.J.Davies, Phys.Rev.Lett. **56**, 1198 (1986)

[2]D.A.Wharam, T.J.Thornton, R.Newbury, M.Pepper, H.Ahmed, J.E.F.Frost, D.G.Hasko, D.C.Peacock, D.A.Ritchie and G.A.C.Jones, J.Phys.C**21** L209 (1988); B.J.van Wees, H.van Houten, C.W.J.Beenakker, J.G.Williamson, L.P.Kouvenhaven, D.van der Marel and C.T.Foxon, Phys.Rev.Lett.**60**, 848 (1988)

[3]T.P.Smith,III, H.Arnot, J.M.Hong, C.M.Knoedler, S.E.Laux and H.Schmid, Phys.Pev.Lett.**59**, 2802 (1987)

[4]C.C.Eugster, J.A.del Alamo, M.R.Melloch, M.J.Rooks, Phys.Rev.B **48**, 15057 (1993)

[5]W.Hansen, M.Horst, J.P.Kotthaus, V.Merkt, Ch.Sikorski and K.Ploog, Phys.Rev.Lett.**58**, 2586 (1987)

[6]M.M.Dignam, R.C.Ashoori, H.L.Stromer, L.N.Pfeiffer, K.W.Baldwin and K.W.West, Phys.Rev.B **49**, 2269 (1994)

[7]J.Wang, P.H.Beton, N.Mori, L.Eaves, H.Buhmann, L.Mansouri, P.C.Mori, T.J.Foster and M.Henini, Phys.Rev.Lett.**73**, 1146 (1994)

[8]J.Smoliner, F.Hirler, E.Gornik, G.Weimann, M.Hauser and W.Schlapp, Semicond.Sci.Technol. **6**, 389 (1991)

[9]W.Demmerle, J.Smoliner, E.Gornik, G.Bohm and G.Weimann, Phys.Rev.B **47**, 13574 (1993)

[10]E.H.Linfield, G.A.C.Jones, D.A.Ritchie and J.H.Thompson, Semicond.Sci.Tech.**8**, 415 (1993)

[11]J.P.Eisenstein, L.N.Pfeiffer and K.W.West, Appl.Phys.Lett.**57**, 2324 (1990); K.M.Brown, E.H.Linfield, D.A.Ritchie, G.A.C.Jones, M.P.Grimshaw and M.Pepper, Appl.Phys.Lett.**64**, 1827 (1994)

[12]J.P.Eisenstein, L.N.Pfeiffer and K.W.West, Phys.Rev.Lett.**58**, 1497(1991); K.M.Brown, E.H.Linfield, D.A.Ritchie, G.A.C.Jones, M.P.Grimshaw and A.C.Churchill, J.Vac.Sci.Technol.B **12**, 1293 (1994)

[13]to be published

## Figure Captions

Figure 1) Cross sectional and plan diagrams of the device structure. The selective depletion technique used to separately contact each 2DEG is shown schematically in the cross sectional diagram and independent contacts to the 2DEGs and to the back-gates are shown in the plan diagram.

Figure 2) Tunnelling differential conductance of the device with a 700nm wide superlattice plotted as a function of back gate voltage. Different degrees of the potential modulation are induced in the upper 2DEG by application of different front Schottky gate voltages, (V). Symbols are inserted for clarity.

Figure 3) Tunnelling differential conductance of three devices with d'fferent superlattice periods plotted as a function of back gate voltage. The devices had periods of 700nm, 600nm, 350nm and were all measured with the same bias voltage ( $V_{FG}$=-0.5V) applied to the front Schottky gate. Symbols are inserted for clarity.

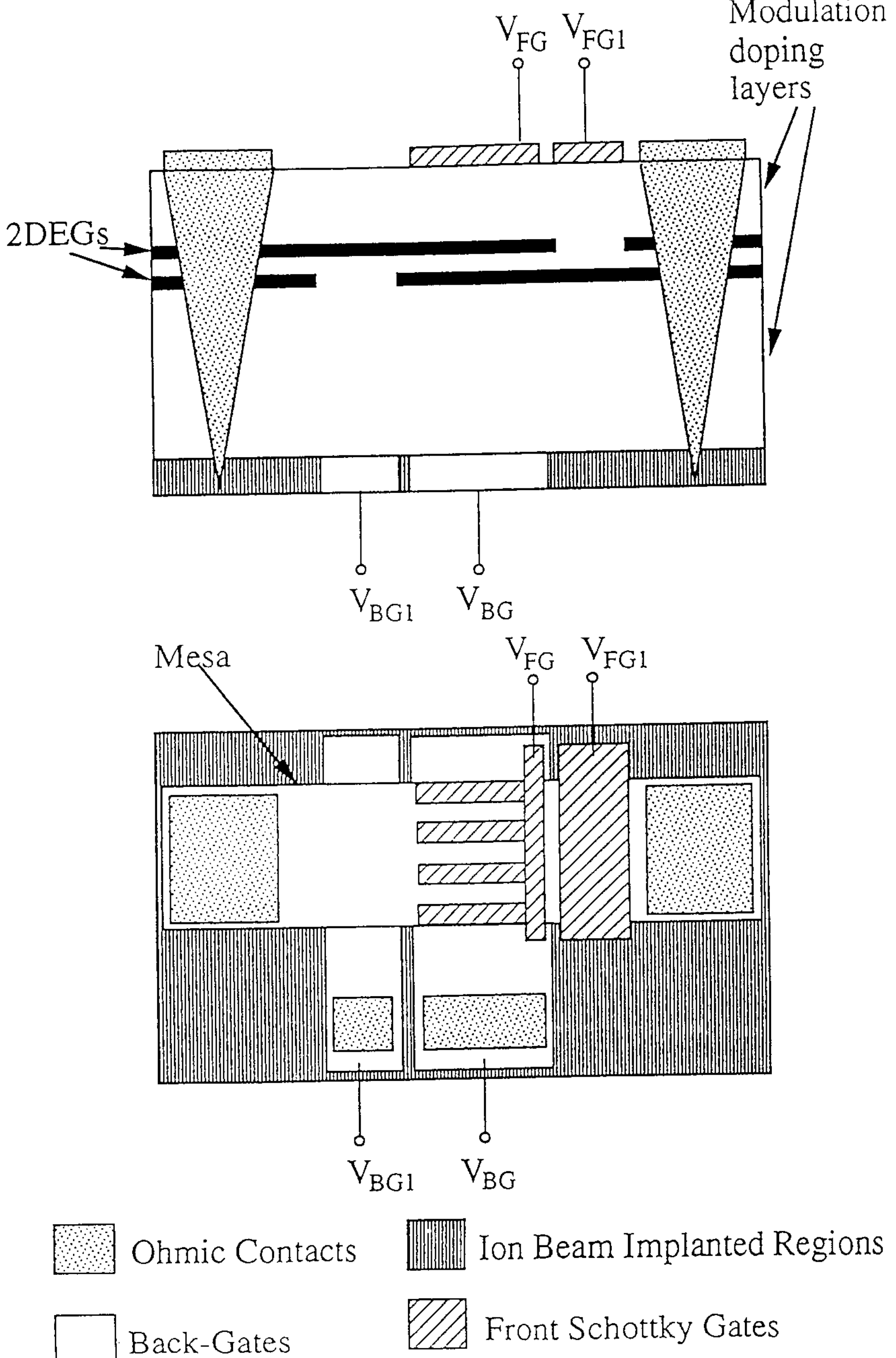

$V_{FG}$
$V_{FG1}$
Modulation doping layers
2DEGs
$V_{BG1}$
$V_{BG}$
Mesa
$V_{FG}$
$V_{FG1}$
$V_{BG1}$
$V_{BG}$
Ohmic Contacts
Ion Beam Implanted Regions
Back-Gates
Front Schottky Gates

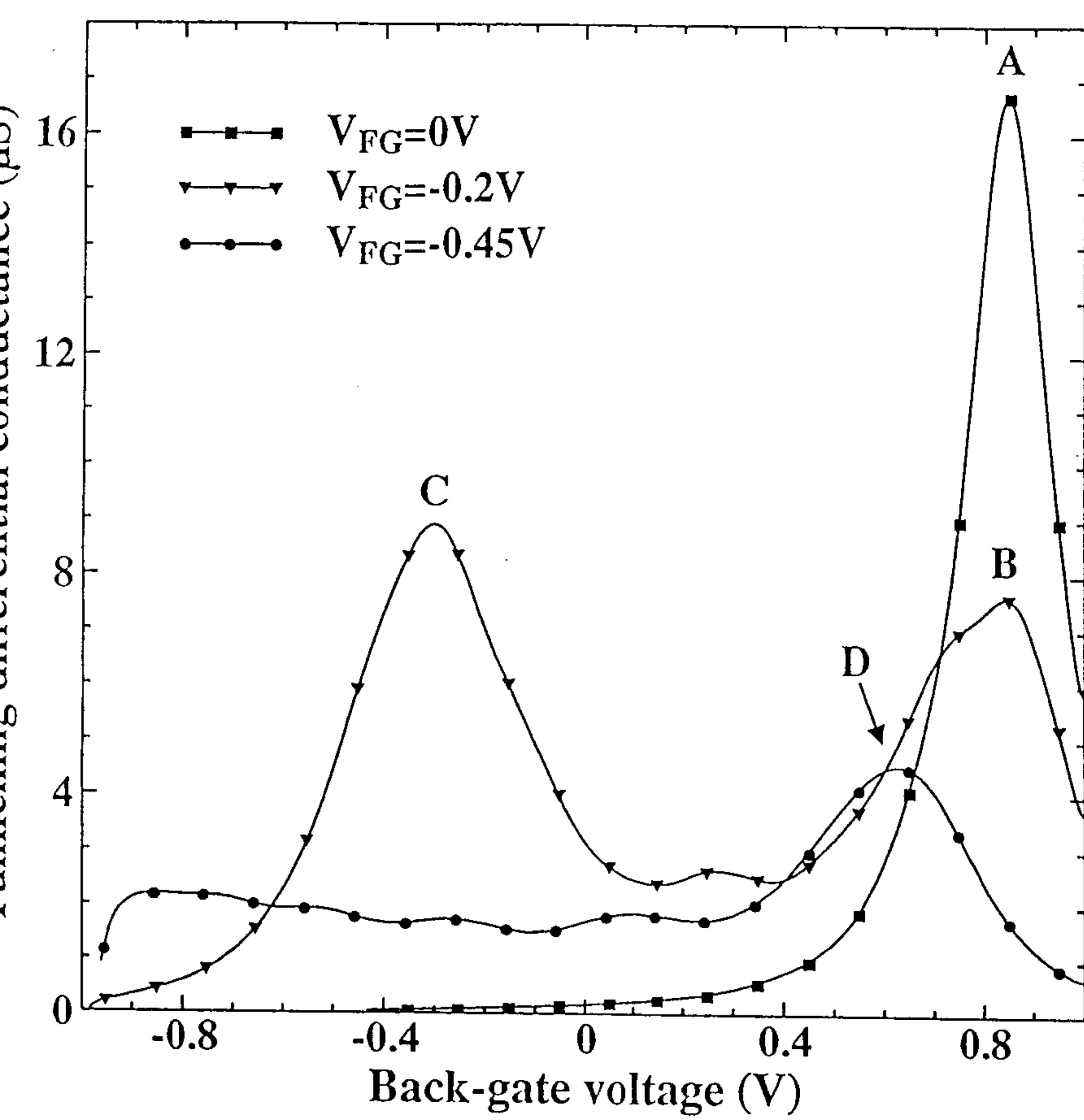


18

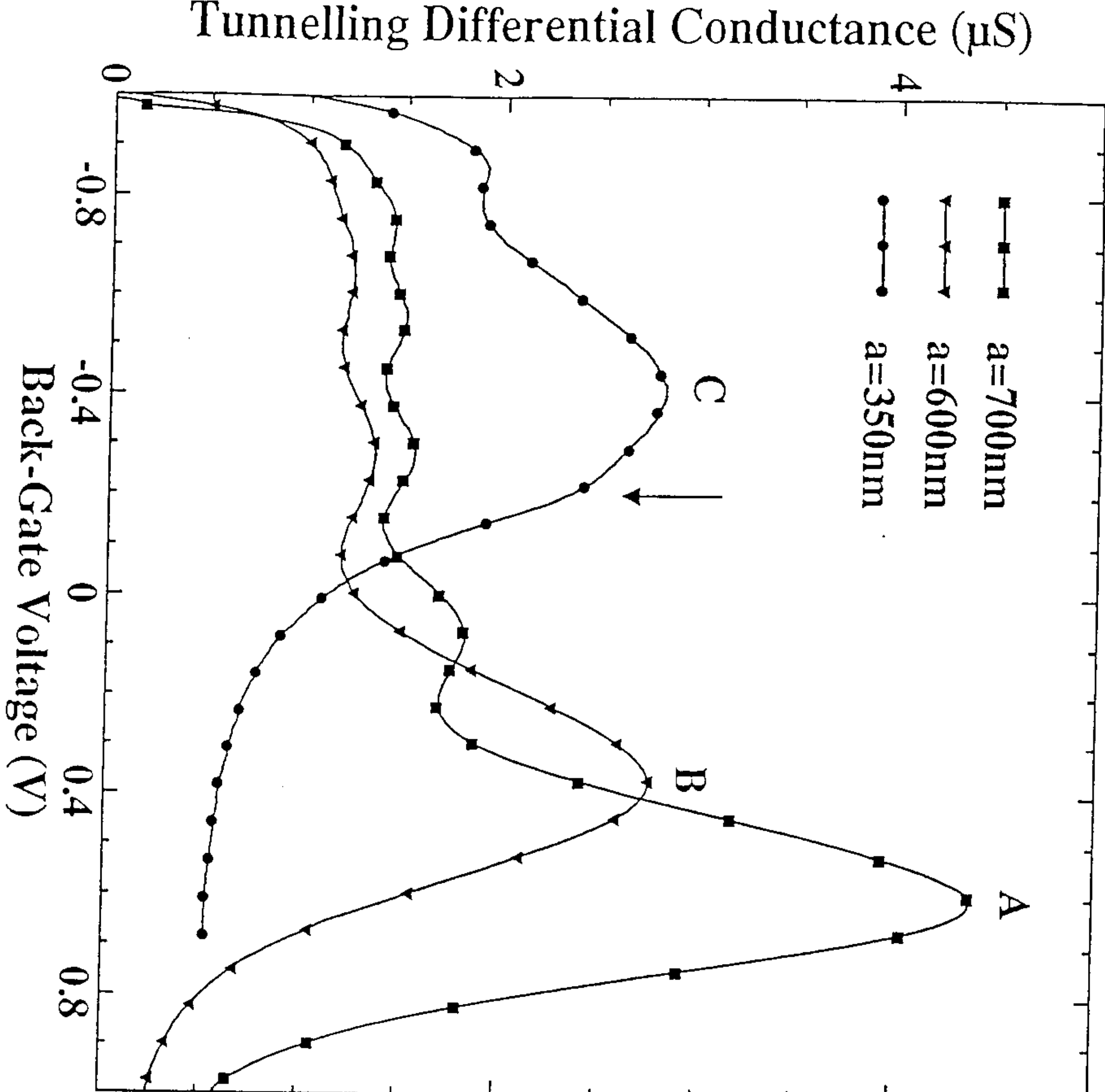
Tunnelling Differential Conductance (µS)
0
2
4
-0.8
-0.4
0
0.4
0.8
Back-Gate Voltage (V)
a=700nm
a=600nm
a=350nm
A
B
C

# Devices Fabricated by *In Situ* Focussed Ion Beam Lithography

## *List of Publications*


1) E H Linfield, D A Ritchie, G A C Jones, J E F Frost and D C Peacock, "The effect of low energy Ga ions on GaAs/AlGaAs heterostructures", *Semicond. Sci. Technol.* **5** 385-390 (1990).

2) E H Linfield, D A Ritchie, G A C Jones, J E F Frost, D C Peacock and M Pepper, "The fabrication of submicron gated wires on GaAs/AlGaAs heterostructures using low energy Ga ion beam damage", *Microcircuit Engineering* **11** (Elsevier Science Publishers B. V.) 19-22 (1990).

3) G A C Jones, D A Ritchie, E H Linfield, J H Thompson, A P. Hamilton and K Brown, "UHV *in situ* fabrication of three-dimensional semiconductor structures using a combination of particle beams", *J. Vac. Sci. Technol.* **B10** 2834-2837 (1992).

4) E H Linfield, G A C Jones, D A Ritchie and J H Thompson, "The fabrication of a back-gated high electron mobility transistor - a novel approach using MBE regrowth on an *in situ* ion beam patterned epilayer", *Semicond. Sci. Technol.* **8** 415-422 (1993).

5) E H Linfield, G A C Jones, D A Ritchie A R Hamilton and N Iredale, "The fabrication of a back-gated high electron mobility transistor - a novel approach using MBE regrowth on an *in situ* ion beam patterned epilayer", *J. Crystal Growth* **127** 41-45 (1993).

6) E H Linfield, N Iredale, D A Ritchie, G A C Jones and A R Hamilton, "The transport properties of a 2DEG closely separated from an underlying $n^+$ GaAs layer - the fabrication of independent ohmic contacts using MBE regrowth and *in situ* focussed ion beams", *J. Vac. Sci. Technol.* **B11** 982-984 (1993).

7) K M Brown, E H Linfield, G A C Jones, D A Ritchie and J H Thompson, "Fabrication of a novel split-back-gate transistor by *in situ* focussed ion beam lithography and MBE regrowth", *J. Vac. Sci. Technol.* **B11** 2493-2496 (1993).

8) K M Brown, E H Linfield, D A Ritchie, G A C Jones, M P Grimshaw and A C Churchill, "The fabrication of independent contacts to two closely spaced 2DEGs using MBE regrowth and *in situ* focussed ion beam lithography", *J. Vac. Sci. Technol.* **B12** 1293-1295 (1994).

9) K M Brown, E H Linfield, D A Ritchie, G A C Jones, M P Grimshaw and M Pepper, "Resonant tunnelling between parallel 2DEGs: A new approach to device fabrication using *in situ* ion beam lithography and MBE growth.", *Appl. Phys. Lett.* **64** 1827-1829 (1994).

10) N K Patel, E H Linfield, K M Brown, M P Grimshaw, D A Ritchie, G A C Jones and M Pepper, "Large Transconductances Observed in an Independently Contacted Coupled Double Quantum Well", *Appl. Phys. Lett.* **64** 3018-3020 (1994).

11) A Kurobe, I M Castleton, E H Linfield, M P Grimshaw, K M Brown, D A Ritchie, M Pepper and G A C Jones, "Wave Functions and Fermi Surfaces of Strongly Coupled Two Dimensional Electron Gases Investigated by In-Plane Magnetoresistance", *Phys. Rev. B* **50** 4889-4892 (1994).

12) A Kurobe, I M Castleton, E H Linfield, M P Grimshaw, K M Brown, D A Ritchie, M Pepper and G A C Jones, "Resonant resistance enhancement in double-quantum-well GaAs/AlGaAs heterostructures", *Phys Rev* **B50** 8024-8027 (1994).

13) A Kurobe, I M Castleton, E H Linfield, M P Grimshaw, K M Brown, D A Ritchie, M Pepper and G A C Jones, "Transport properties of a wide-quantum-well velocity modulated transistor structure", *Semicond. Sci. Technol.* **9** 1744-1777 (1994).

14) K M Brown, N Turner, J T Nicholls, E H Linfield, M Pepper, D A Ritchie and G A C Jones, "Tunnelling Between Two-Dimensional Electron Gases in a Strong Magnetic Field", *Phys. Rev.* **B50** 15465-8 (1994).

15) K M Brown, J T Nicholls, B Tieke, S A J Wiegers, P J M van Bentum, E H Linfield, M Pepper, D A Ritchie and G A C Jones, "Tunnelling Between Two-Dimensional Gases up to 25T", presented at the 1994 European High Magnetic Field Conference, Nijmegan and published in the proceedings.

16) K M Brown, N Turner, J T Nicholls, E H Linfield, M Pepper, D A Ritchie and G A C Jones, "Tunnelling Between Parallel Two-Dimensional Electron Gases", presented at the 1994 International Conference on the Physics of Semiconductors, Vancouver and published in the proceedings (World Scientific).

17) A Kurobe, I M Castleton, E H Linfield, M P Grimshaw, K M Brown, D A Ritchie, M Pepper and G A C Jones, "Electron transport in strongly coupled double quantum well structures investigated by application of in-plane magnetic field", presented at the 1994 International Conference on the Physics of Semiconductors, Vancouver and published in the proceedings (World Scientific).

18) S G Ingram, E H Linfield, K M Brown, G A C Jones, D A Ritchie and M J Kelly, "Performance of Double Heterostructure Unipolar Transistors in High Frequency Power applications", presented at the 1994 IEEE topical conference on electronic devices, Japan and published in the proceedings.

19) S G Ingram, E H Linfield, K M Brown, G A C Jones, D A Ritchie and M J Kelly, "2DEG Base Hot Electron Transistor fabricated using MBE and *in situ* ion beam lithography", *IEEE Transactions on Electron Devices* **42** 1065-1069 (1995).

20) A R Hamilton, E H Linfield, M J Kelly, D A Ritchie, G A C Jones and M Pepper, "The transition from one to two subband occupancy in the 2DEG of back-gated modulation doped GaAs-AlGaAs heterostructures", *Phys. Rev.* **B51** 17600-17604 (1995).

21) H Rubel, E H Linfield, D A Ritchie, K M Brown, M Pepper and G A C Jones, "Study of the frictional drag between closely spaced two-dimensional electron gases", accepted for publication in *Semicond. Sci. Technol.*

22) B Kardynal, E H Linfield, D A Ritchie, K M Brown, G A C Jones and M Pepper, "Tunnelling between 2D and 1D electron gases in devices fabricated using in-situ focused ion beam lithography", submitted to *Appl. Phys. Lett.*

23) N K Patel, A Kurobe, E H Linfield, I M Castleton, D A Ritchie, M Pepper and G A C Jones, "Lateral Transport Studies of Coupled Electron Gases", submitted for publication.

24) N K Patel, I S Millard, E H Linfield, P D Rose, D A Ritchie, G A C Jones and M Pepper, "Resonant coupling effects observed in independently contacted triple quantum well structures", submitted to Appl. Phys. Lett.

25) N K Patel, I S Millard, E H Linfield, P D Rose, M P Grimshaw, D A Ritchie, G A C Jones and M Pepper, "Exchange and Correlation Induced "Charge Transfer" Observed in Independently Contacted Triple Quantum Well Structures", submitted to *Phys Rev* **B** *(Rapid Commun.)*

26) N Turner, J T Nicholls, E H Linfield, K M Brown, M Pepper, D A Ritchie and G A C Jones, "Temperature Studies of the Tunnelling Between Parallel Two-Dimensional Electron Gases", presented at MSS7 (Madrid) and to be published in the proceedings.

27) M Field, C G Smith, M Pepper, K M Brown, E H Linfield, M P Grimshaw, D A Ritchie and G A C Jones, "Coulomb Blockade as a Non-Invasive Probe in Double Layer Systems", accepted for EP2DS (Nottingham) and to be submitted to *Surface Science*.

28) H Rubel, E H Linfield, N P R Hill, J T Nicholls, D A Ritchie, K M Brown, M Pepper and G A C Jones, "Study of the frictional drag between closely spaced two-dimensional electron gases", accepted for EP2DS (Nottingham) and to be submitted to *Surface Science*.